BIODIESEL PRODUCTION THROUGH ESTERIFICATION APPLYING IONIC LIQUIDS AS CATALYSTS

FERNANDA FONTANA ROMAN

Dissertation presented to Escola Superior de Tecnologia e Gestão do Instituto Politécnico de Bragança for the Master Degree in Chemical Engineering

Supervised by

Professor Ana Maria Alves Queiroz da Silva

Professor António Manuel Esteves Ribeiro

Professor Paulo Miguel Pereira de Brito

Co-supervised by

Professor Giane Gonçalves Lenzi

BRAGANÇA

May 2018

ACKNOWLEDGEMENTS

I acknowledge and express thanks to both the Universidade Tecnológica Federal do Paraná – campus Ponta Grossa and the Instituto Politécnico de Bragança for the opportunity provided. I appreciate all the effort made by these two institutions and the people who represent them that allowed me to be here today. I also appreciate all the help provided by my supervisors. Prof. Dr. Paulo Brito, Prof. Dr. Ana Queiroz and Prof. Dr. António Ribeiro, here in Portugal, and Prof. Dr. Giane Gonçalves, in Brazil.

I would also like to acknowledge Prof. Dr. Eduardo Chaves for the help in the beginning of this work and Dr. Isabel Patrícia Fernandes, for the support provided in the FT-IR analysis.

Finally, I express thanks to all my family and friends, who have somehow supported me throughout this year.

RESUMO

O biodiesel é um combustível líquido obtido a partir de fontes renováveis através da reação de transesterificação de triglicerídeos. O interesse por este combustível está relacionado com uma nova tendência: a procura de alternativas às fontes de energia baseadas em petróleo. A sua utilização está associada a vários benefícios ambientais, como a redução da emissão de poluentes. No entanto, devido ao elevado custo associado à sua matéria-prima usual, como os óleos vegetais comestíveis, o biodiesel não é no momento atual economicamente viável. Portanto, há uma necessidade de reduzir o preço final deste combustível. Uma das formas de reduzir os custos será a de se utilizarem matérias-primas mais baratas no processo de produção, como óleos usados ou não comestíveis. A principal característica dessas matérias-primas mais baratas é a baixa qualidade quando comparada com os óleos comestíveis. Esta baixa qualidade está normalmente associada a um alto teor em ácidos gordos livres (AGL) e/ou água. Os AGLs presentes na matéria-prima devem ser convertidos em biodiesel, também conhecido por ésteres metílicos de ácidos gordos (*Fatty Acid Methyl Esters*: FAME), por uma reação de esterificação. A reação de esterificação não pode ser promovida por catalisadores alcalinos, geralmente aplicados na transesterificação, como o NaOH ou o KOH. Os catalisadores alcalinos na presença de AGLs levam à formação de sabão, consumindo o catalisador, diminuindo a sua atividade catalítica e tornando a separação dos produtos finais mais complexa. Apenas os catalisadores ácidos são capazes de promover a reação de esterificação de AGLs. Os catalisadores ácidos são capazes de catalisar ambas as reações, no entanto, a velocidade da reação de transesterificação é cerca de 4000 vezes mais lenta do que quando se utilizam catalisadores alcalinos [1,2], levando a longos tempos de reação e, consequentemente, custos elevados de produção. Desta forma, existe uma crescente necessidade de encontrar catalisadores alternativos que promovam tanto a reação de transesterificação quanto a reação de esterificação em condições mais favoráveis. Atualmente, os líquidos iónicos têm sido utilizados como uma alternativa

aos catalisadores convencionais. Os líquidos iónicos são sais fundidos compostos por um catião orgânico e um anião orgânico ou inorgânico. No presente estudo avalia-se a utilização do catalisador *hidrogenossulfato de 1-metilimidazólio* ([HMIM][HSO_4]) na produção de biodiesel através da reação de esterificação do ácido oleico. A influência dos principais parâmetros (tempo, temperatura, razão molar metanol/ácido oleico e quantidade de catalisador) foi estudada através de uma metodologia de superfície de resposta conhecida por Box-Behnken Design (BBD), avaliando duas repostas: a conversão de ácido oleico e o conteúdo de FAMEs. Concluiu-se que os parâmetros mais relevantes para ambas as respostas foram a razão molar entre os reagentes e a quantidade de catalisador. As condições ótimas para a conversão foram determinadas como sendo 8 h, 110°C, 15:1 relação molar metanol/ácido oleico e uma quantidade de catalisador de 15% em massa, resultando numa conversão de 95% e para o conteúdo de FAMEs foram 8 h, 110 °C, uma razão molar de 14:1 e uma dosagem de catalisador de 13,5% em peso, conduzindo a um conteúdo de ésteres metílicos de ácidos gordos de 90%. Foram também determinados os parâmetros cinéticos da reação. A energia de ativação foi estimada em 6.8 kJ/mol e o fator pré-exponencial em 0.0765 $L^2.mol^{-2}.min^{-1}$.

Palavras-chave: Produção de biodiesel; Esterificação; Líquidos iónicos; Metodologia de Superfície de Resposta.

ABSTRACT

Biodiesel is a liquid fuel obtained from several renewable sources by transesterification reaction of triglycerides. Its development is related to a new tendency: the search for alternatives to petroleum-based energy sources. Its utilization is associated with several environmental benefits, such as a reduction in pollutants emissions. However, due to the high cost associated to its usual feedstock, such as edible vegetable oils, biodiesel is not economically viable. Therefore, there's a requisite to decrease the final price of this fuel. The logical way is by introducing cheaper feedstock into the industrial production, such as non-edible feedstock or waste cooking oil. The main characteristic of cheaper feedstock is the high content of free fatty acids (FFAs) and/or water when compared to edible feedstock. FFAs present on the feedstock must be converted into biodiesel, also referred to as fatty acid methyl esters (FAMEs), by an esterification reaction. The esterification reaction cannot be catalyzed by alkali catalyst, usually applied in the transesterification such as NaOH or KOH. Alkali catalysts in the presence of FFAs lead to the formation of soap, consuming the catalyst, decreasing its catalytic activity and turning the separation of the final products much more complex. Hence, only acidic catalysts are able to promote the esterification reaction of FFAs. Those acidic catalysts are able to catalyze both reactions, however, the rate of the transesterification reaction is about 4000 times slower than for the reactions promoted by alkali catalysts [1,2], leading to long reaction times and, again, high costs. In this way, there is an increasing need to find alternative catalysts that promote both the transesterification and the esterification reaction under adequate conditions. Thus, ionic liquids emerge as an alternative to conventional catalysts. Ionic liquids are molten salts composed of an organic or inorganic anion and an organic cation. The present study evaluated the use of the catalyst 1-methylimidazolium hydrogen sulfate ([HMIM][HSO_4]) in the production of biodiesel through the esterification reaction of oleic acid. The influence of the main parameters (time, temperature, molar ratio methanol/oleic acid and catalyst dosage) on two responses (conversion of oleic acid and FAME content of the

biodiesel samples) were studied through a response surface methodology (RSM) known as Box-Behnken Design (BBD). It was concluded that the most relevant parameters for both responses were the molar ratio between the reactants and the catalyst dosage. The optimum conditions for the conversion were determined as being 8 h, 110 °C, 15:1 molar ratio methanol/oleic acid and a catalyst dosage of 15 wt%, resulting in a 95% conversion and for the FAME content were 8 h, 110 °C, 14:1 molar ratio and a catalysts dosage of 13.5 wt%, leading to a content of 90%. The kinetics of the reaction were also studied. The activation energy was estimated as 6.8 kJ/mol and the pre-exponential factor as 0.0765 $L^2.mol^{-2}.min^{-1}$.

Keywords: Biodiesel production; Esterification; Ionic liquids*;* Response Surface Methodology.

TABLE OF CONTENTS

LIST OF FIGURES

LIST OF TABLES

NOMENCLATURE

A	Variable time in the experimental design (h)
a	Order of the reaction related to the oleic acid
A_{FAME}	Area of FAMEs
A_{IS}	Area of internal standard
ANN – GA	Artificial Neural Network – Generic Algorithm
ANOVA	Analysis of variance
AV	Acid Value (mg KOH/g of sample)
B	Variable temperature in the experimental design (°C)
b	Order of the reaction related to methanol
BBD	Box-Behnken Design
β_0	Intercept coefficient
βi	Coefficient for linear terms
βii	Coefficient for quadratic terms
βij	Coefficient for interaction terms
$[BHSO_3MIM][HSO_4]$	1-sulfobutyl-3-methylimidazolium hydrogen sulfate
$[BMIM][CH_3SO_4]$	1-butyl-3-methylimidazolium methanesulfonate
$[BMIM][FeCl_4]$	1-butyl – 3-methylimidazolium tetrachloroferrite
$[BMIM][HSO_4]$	1-butyl – 3-methylimidazolium hydrogen sulfate
[BMIM][OH]	1-butyl – 3-methylimidazolium hydroxide
$[BMIM][MeSO_4]$	1-butyl – 3-methylimidazolium methyl sulfate

[BSMBIM][CF_3SO_3]	3-methyl-1-(4-sulfobutyl)-benzimidazolium trifluoromethanesulfonate
C	Variable molar ratio between methanol and oleic acid in the experimental design (mol/mol)
c	Order of the reaction related to the oleic acid methyl ester (biodiesel)
Cat.	Catalyst
$C_{18}H_{34}O_2$	Oleic acid
$C_{19}H_{36}O_2$	Oleic acid methyl ester (biodiesel)
C_{OA}	Concentration of oleic acid (mol/L)
$C_{OA;0}$	Initial concentration of oleic acid (mol/L)
CH_3OH	Methanol
CH_3SO_2OH	Methanesulfonic acid
C_{KOH}	Concentration of KOH solution (mol/L)
CO_2	Carbon dioxide
D	Variable catalyst dosage in the experimental design (wt%)
d	Order of the reaction related to the water
df	Degrees of freedom
DG	Diglyceride
Ea	Activation energy (kJ/mol)
ESTiG	Escola Superior de Tecnologia e Gestão
EtOH	Ethanol
FAME	Fatty acid methyl ester (biodiesel)
FFA	Free fatty acid

FID	Flame ionization detector
FT-IR	Fourier transform infrared spectroscopy
F-value	Value calculated to be compared in the Fisher's test
GC	Gas chromatography
GC-FID	Gas chromatograph with flame ionization detector
GL	Glycerol
HCl	Hydrochloric acid
[HO_3S-PMIM][HSO_4]	1-(3-sulfonic acid)-propyl-3-methylimidazolium hydrogen sulfate
H_2SO_4	Sulfuric acid
[HMIM][HSO_4]	1-methylimizadolium hydrogen sulfate
ID	Identification
k_0	Pre-exponential factor
k_1	Reaction rate constant of the direct reaction ($mol^{1-n}.L^{n-1}.min^{-1}$)
k_{-1}	Reaction rate constant of the inverse reaction ($mol^{1-n}.L^{n-1}.min^{-1}$)
k'_1	Reaction rate constant of the direct reaction including the concentration of methanol ($mol^{1-n}.L^{n-1}.min^{-1}$)
IL	Ionic liquid
KOH	Potassium hydroxide
m	Mass (g)
MeOH	Methanol
MG	Monoglyceride
MS	Media of the square

MS_{model}	Media of square of the regression
$MS_{residual}$	Media of square of the residuals
MW	Molar weight (g/mol)
n	Global reaction order
NaOH	Sodium hydroxide
OA	Oleic acid
OAME	Oleic acid methyl ester (biodiesel)
p-value	Value calculated from the F-value
R	Ideal gas constant (8.314 $J.mol^{-1}. K^{-1}$)
R^2	Coefficient of determination
$-r_{OA}$	Reaction rate related to oleic acid (mol. $L^{-1}.min^{-1}$
RSM	Response Surface Methodology
SS	Sum of squares
SS_{lof}	Sum of squares due to lack of fit
SS_{model}	Sum of square due to the model
SS_{pe}	Sum of squares due to pure error
$SS_{residuals}$	Sum of squares due to the residuals
SS_{TOTAL}	Total sum of squares
T	Temperature (°C)
t	Time (h or min)
[TBMA][$MeSO_4$]	Tributylmethylammonium methyl sulfate

TGL	Triglycerides
TSIL	Task specific ionic liquid
V	Volume (mL)
X	Conversion (%)
WCO	Waste cooking oil

1. BACKGROUND AND OBJECTIVES

1.1 Background

Since the industrial revolution in the early 19th century, the demand for energy has increased considerably. According to the International Energy Agency (2017) report, from 1971 to 2015, the total final consumption of energy doubled, with the transportation sector being one of the major responsible for this boost, with a consumption share that increased from 23% in 1971 to 29% in 2015. Furthermore, the projection presented by the U.S. Energy Information Administration (2016) in the last report affirms that, for the period of 2012 - 2040, the diesel consumption will show the largest growth, comparing to all other transportation fuels [3,4].

The rising demand for fuels, mainly for the transportation sector, allied with an increasing concern for the environment, has been leading several researchers to look for alternatives to petroleum-based energy sources. Hence, a new term emerges: Biofuels. A biofuel is defined as a liquid or gaseous fuel derived from biomass sources, such as wood, vegetation, organic residues, vegetable oils, amongst others [5,6].

Biofuels have several advantages over traditional fuels obtained from other sources. They are obtained from renewable energy sources and have lower impact on the environment. Amongst the available biofuels, such as bioethanol, biogas and syngas, biodiesel is a good alternative as energy source. Biodiesel has been greatly explored in the past decades, but the production process currently applied has several drawbacks related to cost issues, environmental concerns, food competition, amongst others.

Hereof, searching for alternative routes to produce biodiesel is a contemporary concern. Most of the focus is invested in finding new catalysts that allow overcoming the disadvantages of the traditional production process. In this way, ionic liquids

appear as possible substitutes, due to its characteristics that promote a greener process.

1.2 Objectives

1.2.1 Main objective

The main objective of this work is to study the biodiesel production by applying ionic liquids as catalysts to the esterification reaction between oleic acid and methanol.

1.2.2 Specific objectives

- Evaluate the effect of different ionic liquids over the conversion of the esterification reaction of oleic acid with methanol, for biodiesel production;
- Estimate the optimal reaction conditions (reaction time, reaction temperature, molar ratio between methanol and oleic acid and catalyst dosage) for the esterification reaction of oleic acid with methanol using a suitable ionic liquid, by applying a Response Surface Methodology (RSM) known as Box-Behnken Design (BBD);
- Evaluate the reaction kinetics of the esterification reaction catalyzed by the chosen ionic liquid;
- Assess the performance of the selected ionic liquid in the catalysis of the transesterification reaction between a waste cooking oil with high acidity value and methanol.

2. BIODIESEL

Among the many biofuels known, biodiesel emerges as a promising replacement for petro diesel. Biodiesel can be defined as a fuel suitable for compression ignition engines that is formed by a mixture of fatty acids alkyl esters derived from oils or fats. It can be obtained from a transesterification reaction of triglycerides or an esterification reaction of free fatty acids and it can be produced from a wide variety of raw materials [7,8].

Biodiesel has been explored in several locations, including USA, Brazil, and the European Union, among others. Globally, the production increased from 15 thousand barrels per day in 2000 to 289 thousand barrels per day in 2008. In 2011, the European Union produced 22 million tons of biodiesel, against 9.5 million in 2009. These numbers only highlight the importance of biodiesel as a fuel [7,9].

2.1 Advantages and disadvantages of biodiesel

Biodiesel presents several advantages over diesel derived from petroleum. Properties of both fuels are very similar, allowing a mixture of biodiesel and diesel in any proportions and implying that it can be employed in diesel engines without major changes, with the engine performance remaining practically unaltered. The storage and transportation of biodiesel is much safer when compared to regular diesel, due to its biodegradability, higher cetane number and higher flash point [7,10].

Biodiesel presents, in general, better characteristics than petrodiesel in combustion. The unburned hydrocarbons can be reduced by 90% when applying biodiesel and aromatic compounds emissions can be reduced by 75% to 90%. For CO_2 emissions, there is also a significant reduction, mainly when the entire life cycle of the oil is considered. Finally, particle emissions are lower and biodiesel can be obtained from

a wide range of renewable sources, such as vegetable oils, animal fats, and algae, among others [7,8,10].

However, the emissions of nitrogen oxides can be slightly higher. Also, the engine speed and power are lower and the cloud and pour point is higher, decreasing the engine power by around 5% when compared to petrodiesel. Biodiesel production is currently more expensive than petrodiesel due to the high cost associated to feedstock [10].

2.2 Raw materials for biodiesel production

Nowadays, biodiesel has a greater cost than petrodiesel due to the raw materials employed. Traditionally, most processes apply edible vegetable oils, such as soybean oil, rapeseed oil and palm oil [11]. Those oils have some advantages, mainly related to the fact that they do not require a pretreatment. On the other hand, those oils have a high cost, leading to an expensive final product. Also, the use of such oils could generate competition with the food market, leading to issues related to food supply [10].

Besides edible oils, several other materials can be exploited for biodiesel production, such as nonedible oils, for instance jatropha oil, mahua oil, castor oil and cotton seed oil [11,12]. Nonedible oils have some compounds in their structure that make them unsuitable for human consumption. There are several advantages related to using nonedible oils over edible oils, such as their reduced price, the fact that they won’t create issues related to food supply, amongst other. The downside is that they are usually rich in free fatty acids, which for the traditional biodiesel production poses issues related to yield of the reaction and purification of products [13].

Another possibility is the use of waste cooking oils (WCO), which is any oil that has been previously used for cooking or frying, and is, therefore, not suitable for consumption anymore. The advantages of applying those oils are that its price is

much lower than refined oils, and likewise, there is no competition with the food market. Again, the major disadvantage of this feedstock is the high content of free fatty acids and moisture. The quality of the raw materials cited, nonedible oils and waste cooking oil, could be increased by applying a number of pretreatments steps. If not subjected to treatment, the content of free fatty acids could lead to a saponification reaction, decreasing drastically the biodiesel yield and the downstream process would be more complex [9,10].

Another alternative to vegetable oils is the use of algae. The advantages of algae are related to their fast growth rate, the high yield of oil produced per acre of plant (up to 31 times higher than the obtained with other vegetable oils), the fact that they can be produced all year around and that they are environmentally friendly. On the other hand, production of biodiesel applying algae brings some challenges, mainly related to the upstream and downstream process, such as algae dehydration, oil extraction and purification process [10,14].

Finally, another pointed solution for biodiesel feedstock is animal fat. The main advantage of this feedstock is the availability and low price. On the other hand, the disadvantages are related to the high content of free fatty acids, which would again require pretreatment, and the fact that it results in a biodiesel that cannot be fully employed in lower temperatures, due to its higher viscosity. However there are studies investigating how to improve the quality of biodiesel derived from animal fats [9].

Table 1 presents a comparison between the distribution of fatty acids in animal fat, edible and non-edible vegetable oil and waste cooking oils. The most common fatty acid in oils originated from plants are the palmitic (hexadecanoic - C16:0), stearic (octadecanoic - C18:0), oleic (9(z)-octadecanoic - C18:1), linoleic (9(z)-12(z)-octadecanoic - C18:2) and linolenic (9(z)-12(z)-15(z)-octadecanoic - C18:3) [15].

Table 1 - Fatty acid distribution among different feedstock.

Feedstock	Type	Fatty acid distribution (wt%)					
		C14:0	C16:0	C18:0	C18:1	C18:2	C18:3
Chicken fat	Animal fat	3.1	19.82	3.06	37.62		
Tallow	Animal fat	23.3	19.3	42.4	2.9	0.9	2.9
Rapeseed oil	Edible oil	-	1 - 3	0 - 1	10 - 15	12 - 15	8 - 12
Sunflower oil	Edible oil	-	5 - 8	2 - 6	15 - 40	30 – 70	3 - 5
Soybean oil	Edible oil	-	6 - 10	2 - 5	20 - 30	50 - 60	5 - 11
Jatropha oil	Non-edible oil	14 - 15	0 - 13		34 - 45	14 - 15	0.3
Cotton seed oil	Non-edible oil		22 - 28	1	13 - 18		0.2
Yellow grease	WCO	2.43	23.24	12.96	44.32	6.97	0.67
Brown grease	WCO	1.66	22.83	12.54	42.36	12.09	0.82

Source: adapted from Ambat, Srivastava and Sillanpää. [12]

2.3 Physical properties of biodiesel

The physical properties of biodiesel are compared to those of petroleum-based diesel presented in Table 2. The most important property of biodiesel is the kinetic viscosity, since it is directly related to the fuel injection in the engine. The lower the viscosity, the better is the injection operation. According to Table 2, it is clear that the biodiesel is a viable replacement for petroleum based diesel, since the viscosity of a regular diesel fuel is in the range of 12 to 3.5 mm^2/s and the viscosity for biodiesel produced from several sources are within that range. [10].

Table 2 - Physical properties of biodiesel from several sources and diesel fuel.

Vegetable oil methyl ester	Viscosity (mm^2/s)	Cetane number	Lower heating value (MJ/ton)	Flash Point (°C)	Density (g/L)	Sulfur (wt %)
Peanut	4.9 [a]	54	33.6	176	0.883	-
Soybean	4.5 [a]	45	33.5	178	0.885	-
Babassu	3.6 [a]	63	31.8	127	0.879	-
Palm	5.7 [a]	62	33.5	164	0.880	-
Sunflower	4.6 [a]	49	33.5	183	0.860	-
Rapeseed	4.2 [b]	51-59.7	32.8	-	0.882 [d]	-
Used rapeseed	9.48	53	36.7	192	0.895	0.002
Used corn oil	6.23 [c]	63.9	42.3	166	0.884	0.0013
Diesel Fuel	12-3.5 [b]	51	35.5	-	0.830-0.840[d]	-
JIS-2D (gas oil)	2.8 [c]	58	42.7	59	0.833	0.05

[a] at 37.8°C; [b] at 40°C; [c] at 30°C; [d] at 15°C; Source: Fukuda, Kond, and Noda [8]

The cetane number is a measurement of the ignition quality of the fuel. The higher it is, the shorter the ignition delay, implying that a higher cetane number leads to a fuel with better quality. For biodiesel, as it can be seen on Table 2, the cetane number is slightly higher than for diesel due to the higher oxygen content of biodiesel. Usually, the longer the fatty acid chain is, the higher cetane number of the resulting biodiesel will be [16].

Other relevant properties are the cloud point and the pour point. Those properties are related to the applicability of the fluid in low temperatures. Biodiesel displays higher cloud point and pour point, which means that biodiesel is more difficult to be employed in low temperatures than diesel [10]. Finally, biodiesel shows great combustion efficiency, due to its oxygen content. Furthermore, biodiesel can extend the life of diesel engine, due to its lubricating properties [10].

2.4 Methods for biodiesel production

Vegetable oils rich in triglycerides are a promising replacement to petroleum-based diesel. The main issue with applying those oils as fuel is the high viscosity exhibited by them, which would require major changes in the regular diesel engine. Therefore, the main objective for biodiesel production is to lower the viscosity of the employed oils. The differences in the viscosities of oils and biodiesel can be easily observed in Table 3, where the properties of several vegetable oils are compared to the properties of diesel fuel. By comparing the values of viscosity displayed on Table 3 to those displayed on Table 2, it is very clear that the objective of lowering the viscosity of the oils is reached.

There are several methods to approximate the properties of triglycerides-based fuels to diesel properties, such as pyrolysis, microemulsion, dilution and transesterification [8,16].

Table 3 - Properties of diesel D2 and other vegetable oils.

Fuel type	Heating value (MJ/kg)	Density (kg/m^3)	Viscosity at 300k (mm^2/s)	Cetane number
Diesel D2	43.4	815	4.3	47.0
Sunflower oil	39.5	918	58.5	37.1
Cottonseed oil	39.6	912	50.1	48.1
Soybean oil	39.6	914	65.4	38.0
Corn oil	37.8	915	46.3	37.6
Opium poppy oil	38.9	921	56.1	-
Rapeseed oil	37.6	914	39.2	37.6

Source: Demirbas (2008) [10]

Transesterification has shown to be a favorable reaction to obtain triglycerides derivatives (known as biodiesel) with properties close to those of diesel. The oils employed might contain an amount of free fatty acids, which can be converted to biodiesel through an esterification reaction. Both reactions – transesterification and esterification – are equilibrium reactions [8,17].

2.4.1 Esterification

Free fatty acids are carboxylic acids and they are converted to esters by a condensation reaction with alcohols, also known as esterification. The reaction can only be accomplished if the equilibrium is driven towards product formation, such as when there is an excess of reactants or one of the products is continuously removed from the reaction media [18]. Figure 1 shows the general scheme for an esterification reaction. Carboxylic acid **(1)** reacts with an alcohol **(2)**, giving rise to water **(3)** and an ester **(4).**

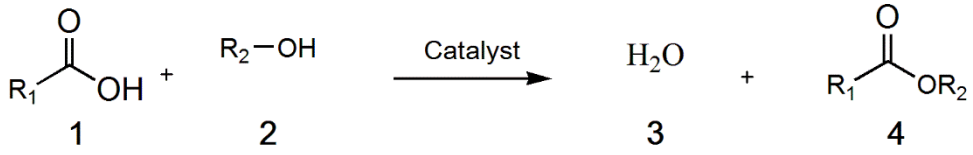

R_1 = methyl, ethyl, etc.
R_2 = methyl, ethyl, isopropyl, etc.

Figure 1 - Scheme for the esterification reaction.
Source: Andreani and Rocha (2012) [17]

The mechanism in which the esterification reaction of carboxylic acids occurs is tetrahedral. The reaction happens in five steps, as shown on Figure 2. First, the oxygen belonging to the carbonyl group of the carboxylic acid **(1)** is pronated by the acid catalyst **(2)**, making the carbonyl group a much stronger electrophile **(3)**. Then, the electrophile undergoes 1,2-addition by the alcohol **(4)**, giving origin to a tetrahedral intermediate **(5)**. The proton from the alcohol is transferred to the OH group. Then, there's a 1,2-elimination of water, which leads to a protonated ester **(6)** and water **(7)**. The protonated ester then loses the proton, regenerating the catalyst **(2)** and generating the ester **(8)** [19].

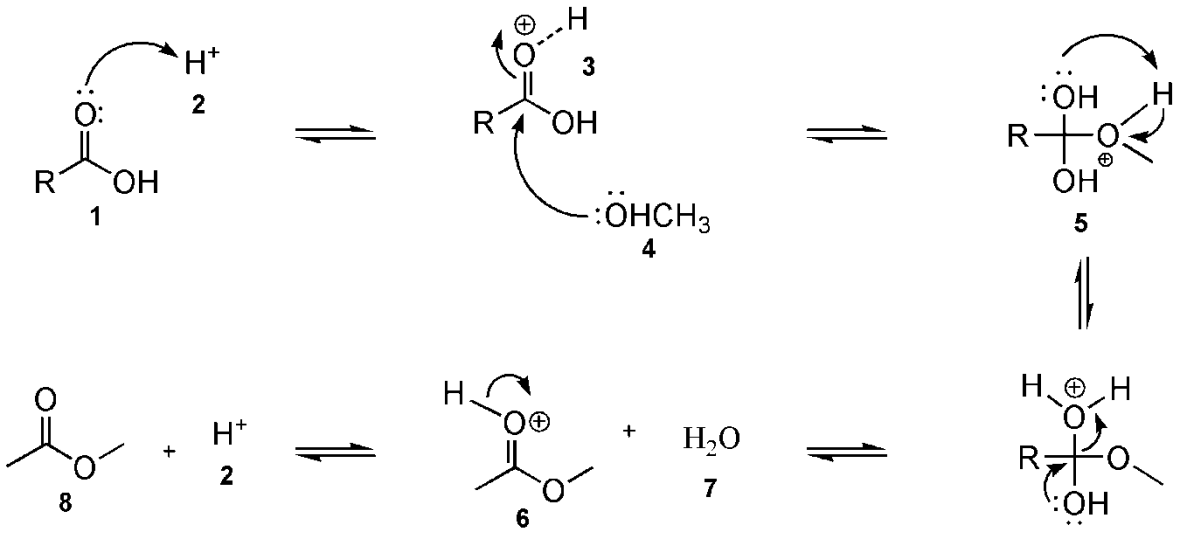

Figure 2 - Mechanism for the esterification of carboxylic acids.
Source: Adapted from Zeng et al. (2012) [19].

2.4.2 Transesterification

The transesterification reaction is performed using oils rich in triglycerides with a short chain alcohol, such as methanol or ethanol, in the presence of a catalyst. Methanol is widely used in most countries due to its low cost, although in a few countries, such as Brazil, ethanol can be applied. Biodiesel obtained from

transesterification with methanol can also be referred as Fatty Acids Methyl Esters (FAMEs) [17].

Figure 3 shows a scheme for the transesterification reaction. The stoichiometry dictates that it is necessary 3 moles of alcohol **(2)** for each triglyceride **(1)** in order to achieve a stoichiometric conversion but it is common to use much higher molar ratios in order to force the reaction in the direction of product formation. The reaction gives glycerol **(3)** as by-product and 3 moles of ester **(4)**. It is an equilibrium reaction and the reaction requires a catalyst. Usually, catalysts with an alkali character are employed. If water or carboxylic acids (free fatty acids) are present under alkali catalyzed reaction, it can lead to hydrolysis of the alcoholic ester and saponification [20].

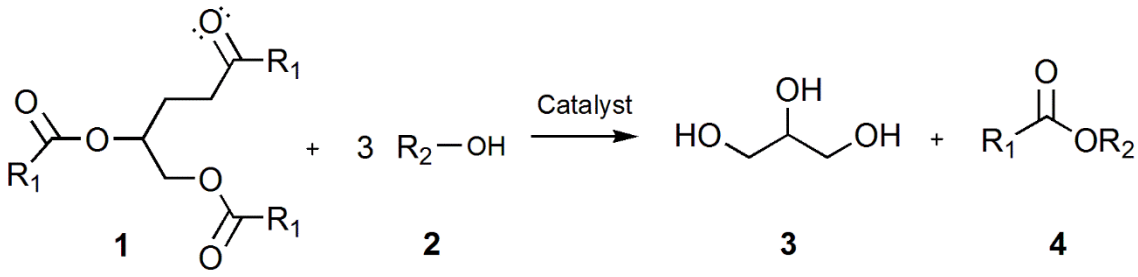

R_1 = methyl, ethyl, etc.
R_2 = methyl, ethyl, isopropyl, etc.

Figure 3 - Scheme for the transesterification reaction.
Source: Andreani and Rocha (2012) [17]

The mechanism for the transesterification reaction catalyzed by an acidic catalyst is displayed on Figure 4. This mechanism was proposed by Ishak et al. (2017). The catalyst **(2)** promotes the transesterification reaction by donating a proton to the carbonyl group of the triglyceride **(1)**, turning it into a stronger electrophile **(3)**. The electrophile **(3)** then reacts with the short chain alcohol **(4)**, through a nucleophilic substitution, forming molecules of diglyceride **(6)**, esters **(7)** and a proton, which will catalyze the next set of reactions [21]. The diglyceride will then be converted into

monoglyceride, which will then be converted into glycerol. Each step gives rise to one mole of an ester.

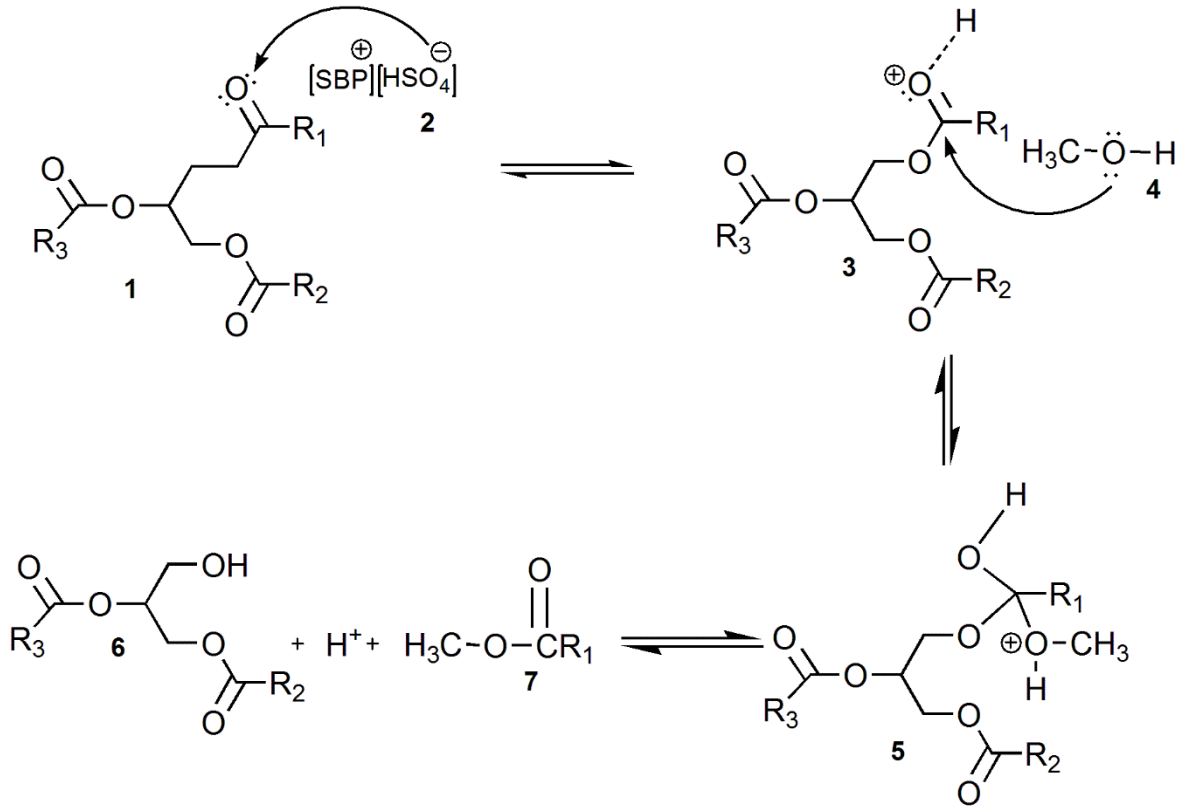

Figure 4 - Mechanism for the transesterification reaction of triglycerides.
Source: Ishak et al. (2017) [21]

2.4.3 Catalysts

Both reactions discussed in the previous section require a catalyst in order to achieve a reaction time and reaction conversions that are suitable for industrial processes. The most common processes use alkali catalysts; however, other catalysts can be applied, such as acidic catalysts and enzymes.

Alkali catalysts can only catalyze the transesterification reaction. The most applied ones are NaOH and KOH. The transesterification reaction catalyzed by a basic catalyst has the advantage of being much faster than the acid-catalyzed reaction

(about four thousand times faster), but the presence of even a small amount of water and/or free fatty acids can lead to a saponification reaction, consuming the catalyst and lowering the catalytic performance. It can also influence the downstream process, making the separation of the final product more complex. Some authors suggest that the transesterification reaction under basic catalysis must be performed with anhydrous refined oils with free fatty acids content lower than 0.5%, thus, requiring the use of edible or refined feedstock. As already mentioned, edible feedstock is expensive, leading to a final product with high prices, which is economically non-viable [7,8,21].

On the other hand, the acidic catalysts are able to promote both the esterification and transesterification reactions, thus allowing the use of cheaper feedstock with higher content of Free Fatty Acids (FFA) and water. However, the employment of acidic catalyst for the transesterification reaction has several disadvantages: it is much slower than the basic catalyzed reaction and it requires a considerable amount of alcohol to shift the equilibrium towards product formation, usually a proportion of 30-150:1 moles of methanol to moles of triglycerides, for instance. Also, catalysts that are highly acidic can lead to equipment corrosion [17,21].

Another possibility that has been studied is the enzyme-catalyzed reaction. Lipases can be used as catalysts for biodiesel production, having several advantages, for instance the high selectivity and the use under mild conditions. Also, it is easier to recover the glycerol obtained as byproduct and the FAMEs are simpler to purify. Yet, enzymes can be deactivated due to contamination of side products or even by organic solvents and they are usually expensive [22,23]. The methods discussed for biodiesel production are summarized on Table 4.

In this way, the latest research has been focused on looking for alternative synthesis, mainly focusing on designing processes that allow the use of low-cost feedstock in order to decrease biodiesel price and turn biodiesel into a competitive fuel. Ionic

liquids have been explored as an alternative to traditional catalysts, due to the fact that they may overcome some of the drawbacks of the traditional methods [24].

Table 4 - Comparison of methods for Biodiesel production.

Method	Catalyst	Advantages	Disadvantages
Alkali catalyzed	KOH, NaOH, Carbonates	It is much faster; relative short reaction time, relative mild conditions.	Leads to saponification in the presence of water, does not catalyze the esterification reaction.
Acid catalyzed	H_2SO_4	It can catalyze both the transesterification and the esterification reaction; Can be used with low quality feedstock.	Reaction time is much longer and it requires a large amount of alcohol. It can lead to corrosion.
Enzyme catalyzed	Lipase	It is selective, mild conditions can be applied.	High costs, possible enzyme deactivation.

Sources: Helwani et al. (2009) [25]; Andreani & Rocha (2012) [17]; Fukuda et al. (2001) [8]; Ramos et al. (2011) [22].

3. IONIC LIQUIDS

Ionic Liquids (ILs) can be defined as organic salts that are consisted of ions (an organic cation and an organic or inorganic anion) and, opposed to inorganic salts, remain liquid at room temperatures. The melting temperatures of those salts lay usually below 100ºC due to the presence of a delocalized charge and large ions, causing packing to be difficult [17,26,27].

There are several advantages related to the use of ionic liquids. Due to the interactions between the anion and cation, they have negligible vapor pressure, a good solubility in both organic and inorganic materials, they are non-flammable, have a high catalytic activity and can be easily manipulated in order to achieve a specific property, just by changing the anion/cation combination, and thus being referred to as Task Specific Ionic Liquid (TSIL). This variation in the anion/cation combination is also advantageous in terms of variety, since it can give origin to at least 1 million binary ionic liquids and potentially 10^{18} ternary ionic liquids, comparing to only 600 organic solvents. Besides, they are easily recyclable, can be used under mild conditions and produce less waste [13,17,27].

Ionic liquids can exhibit acidic, basic or neutral characteristics. The ability to present an acidic character (which could be depicted as Brønsted, Lewis or both) could be linked to the cation and/or the anion and their character may influence greatly their ability to catalyze a reaction. There are studies trying to connect the acidity of an ionic liquid to its catalytic activity in biodiesel production [28,29].

There is a high cost associated to ionic liquids, although, this high cost can be easily manageable due to the fact that ionic liquids can be easily recovered and recycled back to the process. Usually, due to their low vapor pressure, distillation presents a suitable option for the recovery process. However, when the system is sensitive to temperature or other non-volatile compounds are mixed, there are other options in

terms of recovery, such as extraction with solvents, adsorption, separation applying membranes, etc. [30].

In biodiesel production, ionic liquids are able to reduce the number of reactions and purifications steps, decreasing the production cost and energy consumption throughout the process. The majority of studies focus on the application of Brønsted acidic ionic liquids to biodiesel production, since they usually show high catalytic activity, although, a few publications report that basic ionic liquids require less reaction time and less temperature in biodiesel synthesis [13,27,29].

3.1 Ionic liquids applied to biodiesel production

The use of ionic liquids in biodiesel production has attracted a great attention from the scientific community, since its use allows overcoming several issues related to the traditional processes of biodiesel synthesis, such as the possibility of exploiting low-cost feedstock, reducing environmental issues and the number of downstream steps, among others [27]. There are several studies on the literature focusing on employing ionic liquids as catalyst for biodiesel production. Table 5 summarizes a few studies found on the literature.

In 2011, Elsheikh et al. [31] investigated ionic liquids containing an imidazolium ring in their cation for the transesterification reaction of crude palm oil with methanol. The ILs investigated showed a high catalytic activity and a similar trend was observed for all ionic liquids when the amount of catalyst added was varied. The best catalyst was *1-butyl-3-methylimidazolium hydrogen sulfate* [BMIM][HSO_4], with which a conversion of 91.2% was achieved, with the optimal condition being 4.4 wt% of catalyst, crude palm oil/methanol ratio of 12:1, temperature of 160ºC for 120 min reaction time.

Table 5 - Review of reaction conditions found in literature.

Oil	Ionic Liquid	Conditions				Conversion/ FAME content/yield	Ref.
		T(ºC)/ Power (W)	Time (h)	MeOH/ Oil ratio	Cat. dosage		
Oleic Acid	[$BHSO_3MIM$][HSO_4]	120[d]	4	4:1	10%wt	97.7%[a]	[32]
Crude Palm oil	[BMIM][HSO_4]	160[d]	2	12:1	4.4%wt	91.2%[a]	[31]
Castor Oil	[HMIM][HSO_4]	77[d]	4	6:1	12%wt	89.8%[b]	[33]
Oleic acid	[BMIM][HSO_4]	87[d]	5.2	9:1	0.06 mole	80.4%[a] 81.8%[c]	[34]
Waste oil	[HO_3S-PMIM][HSO_4]	120[d]	8	12:1	2g	96%[a]	[35]
Waste oil	[BMIM][HSO_4]	160[d]	1	15:1	5 wt%	95.6%[c]	[36]
Oleic acid	[HMIM][HSO_4]	-	6	4:1	3.5 mL	92.5%[a]	[37]
Palm Oil	[HSO3-BMIM][HSO_4]	168[e]	6.43	11:1	9.17 wt%	98.9%[b]	[38]

[a] Given in terms of conversion based in acidity; [b] Given in terms of FAME content; [c] ester yield in mass base; [d] Temperature; [e] Microwave power.

In 2013, Fauzi and Amin [34] performed a multi-objective optimization for the esterification reaction between oleic acid and methanol catalyzed by ionic liquid *1-butyl-3-methylimidazolium hydrogen sulfate* [BMIM][HSO_4], evaluating simultaneously the oleic acid conversion and the methyl oleate yield. An Artificial Neural Network – Generic Algorithm (ANN–GA) was applied to optimize the main reaction variables: temperature, reaction time, molar ratio between methanol and oleic acid and the catalyst dosage. They found that the optimal combination was a temperature of 87°C, reaction time of 5.2 h, molar ratio alcohol/oil of 9:1 and a catalyst loading of 0.06 moles, leading to an oleic acid conversion of 80.4% and a methyl oleate yield of 81.8%.

Also in 2013, Liu et al. [35] studied the reaction between waste cooking oil and methanol, applying ionic liquids that depicted Brønsted acidity. They tested 10 different catalysts, including sulfuric acid. The best result was obtained with the ionic liquid *1-(3-sulfonic acid)propyl-3-methylimidazole hydrogen sulfate* [HO_3SPMIM][HSO_4]. The best condition found was a reaction temperature of 120 °C, molar ratio between methanol and oil of 12:1, catalyst loading of 2 g and a reaction time of 8 h, leading to a 96% conversion. The same conditions were applied to acidic

oils, which were prepared by adding oleic acid in different proportions to the raw material, and again, the conversion was over 90%. The recyclability was also addressed, and after 6 subsequent runs, no obvious reduction in the catalytic activity of the IL was detected.

In 2014, Li et al. [32] investigated seven ionic liquids to determine their applicability and catalytic activity in biodiesel production. They studied the esterification reaction between oleic acid and methanol. Their conclusion was that the higher catalytic activity was connected to the anion's acidity, and that the stronger it is, the higher the methyl oleate yield will be. In their work, they found that *1-sulfobutyl-3-methylimidazolium hydrogen sulfate* [$BHSO_3MIM$][HSO_4] was the best catalyst and the optimal condition was 120 ºC, 4 hour reaction, methanol/oleic acid ratio 4:1 and a concentration of catalyst of 10 wt%. They also studied the recyclability of the ionic liquid, and they only noticed a slight decrease on conversion after eighth consecutive runs.

In 2015, Xu et al. [33] compared the catalytic activity of the ionic liquid *1-methylimidazolium hydrogen sulfate* ([HMIM][HSO_4]) with the catalysts *1-butyl-3-methylimidazolium hydroxide* ([BMIM][OH]), sodium hydroxide (NaOH), and concentrated sulfuric acid (H_2SO_4). Although results showed that for the transesterification reaction between castor oil and methanol, the catalyst NaOH presented the best results, the ionic liquid *1-methylimidazolium hydrogen sulfate* [HMIM][HSO_4] displayed a very similar trend, so due to its advantages compared to the traditional catalyst, this ionic liquid was chosen for further studies. They run a screening test to study out of the 4 factors (temperature, time, and molar ratio methanol/oil and catalyst dosage) which factors were significant in the reaction conversion. They found that the reaction time was not an important factor and carried out the experiments with the remainder factors to the optimal conditions for the reaction, using a response surface methodology. They concluded that the optimal conditions were molar ratio methanol/oil of 6:1, reaction time of 4 h, temperature of 77 ºC and a catalyst dosage of 12 wt%.

Also in 2015, Ullah et al. [36] studied the transesterification reaction between waste palm cooking oil with methanol in a two-step process. The first step, an esterification reaction, was catalyzed by an ionic liquid, in order to decrease the acidity of the waste oil. The second stage was the utilization of KOH to catalyze the transesterification reaction. Three ionic liquids were tested and *1-butyl-3-methylimidazolium hydrogen sulfate* [BMIM][HSO_4] displayed the best results. The best condition for the first stage was a concentration of catalyst of 5 wt%, a molar ratio between methanol and waste oil of 15:1, reaction time of 60 min and a temperature of 160°C. The final yield observed applying the determined condition for the first stage and followed by the transesterification with the KOH catalyst resulted in an overall yield of 95.7% [36].

In 2015, Sun et al. [37] studied the esterification reaction of oleic acid and methanol using the catalyst *1-methylimidazolium hydrogen sulfate* [HMIM][HSO_4]. The optimized reaction conditions were 4:1 molar ratio of methanol/oleic acid, catalyst dosage of 3.5 mL and a reaction time of 6h, leading to a conversion of 92.5%. After 9 reuse cycles, the conversion was still above 85%.

In 2018, Ding et al. [38] investigated the transesterification reaction of palm oil and methanol. Three synthesized ionic liquids were studied in order to determine their catalytic activity, followed by a single factor experiment to investigate the effect of several parameters on the reaction and then a RSM to optimize those factors. The best catalyst was the ionic liquid [HSO_3-BMIM][HSO_4] and the optimum condition was a methanol/oil ratio of 11:1, a ionic liquid dosage of 9.17 wt%, a microwave power of 168 W and a reaction time of 6.43h, leading to a yield of 98.9%.

3.2 Kinetic studies of esterification reaction

The determination of the kinetic parameters of the esterification reaction of FFAs is also interesting, as it allows a better understanding of the suitability of a determined catalyst for biodiesel production. Normally, the main studied kinetic parameter is the

activation energy (E_a), defined as the minimum energy required for the reaction to take place. Only when the reactants collide with this minimum energy is that the products are formed [39,40]. Also, the activation energy is a measure of how the reaction rate is influenced by the temperature. Reactions that have a small activation energy (below 10 kJ/mol) have a little dependency on temperature, while reactions with high activation energies (above 60 kJ/mol) have a strong dependency on temperature [39]. Therefore, the lower the activation energy, the easier it is to turn reactants into products. Using a catalyst is a practical way to decrease the activation energy, as catalysts work by providing a different pathway for the reaction to occur with lower activation energy. The catalyst has no effect on the reaction equilibrium, and therefore the equilibrium is not impacted. Also, the catalyst is always regenerated at the end of the process [39]. There are several studies on the literature that focuses on the estimation of the activation energy of both the esterification and the transesterification reactions for biodiesel production. The main studies are summarized on Table 6.

Table 6 - Review of kinetic studies regarding biodiesel production.

Feedstock	Alcohol	Order	Reaction type	Catalyst	Temperature range (K)	Activation Energy (kJ/mol)	Ref.
Oleic acid	MeOH	1st	Esterification	[BMIM][$FeCl_4$]	313 – 343	17.97	[41]
Waste plum stone	MeOH	1st	Esterification	H_2SO_4	313 - 333	13.20 - 11.55[a]	[42]
Oleic acid	EtOH	2nd	Esterification	H_2SO_4	348 – 393	36.62	[43]
Palm fatty acids	MeOH	1st	Esterification	H_2SO_4	403 - 433	6.53 – 15.05[a]	[44]
				CH_3SO_2OH		3.78 – 10.12[a]	
Palm oil	MeOH	1st	Esterification	H_2SO_4	328 - 338	75.3	[45]
		2nd	Transesterif.	KOH		1.45[b] 328[c] 89.3[d]	
Waste cooking oil	MeOH	1st	Transesterif.	[BSMBIM][CF_3SO_3]	353 - 413	19.24	[46]

[a] Variation in the catalyst dosage; [b] TGL – DG; [c] DG – MG; [d] MG – GL.

Fauzi, Amin and Mat (2014) investigated the esterification of oleic acid with methanol using the ionic liquid *1-butyl-3-methylimidazolium tetrachloroferrite* [BMIM][$FeCl_4$] as a catalyst. The conditions applied were a molar ratio methanol/oleic acid of 22:1, 3 mmol of catalyst loading and a total reaction time of 3.6 h, with sampling every 36 min. The temperature was varied from 40 to 70°C. The change in oleic acid concentration was evaluated by titration with a KOH solution. They arrived at the conclusion that the reaction follows pseudo-first order kinetics and estimated the activation energy as 17.97 kJ/mol and a pre-exponential factor as 181.62 min^{-1} [41].

Kostić et al. (2016) studied the esterification reaction of waste plum stone with methanol applying sulfuric acid as catalyst. The study was carried out under variation of catalyst loading, methanol/oil ratio, and temperature, modeling the reaction as a pseudo-first order. They concluded that the activation energy suffers a slight decrease when the catalyst dosage increases. The catalyst loading of 0.049 mol/dm^3 leads to an activation energy of 13.20 kJ/mol, whereas increasing the catalyst loading to 0.172 mol/dm^3 leads to an activation energy of 11.55 kJ/mol, that represents a very small decrease [42].

Neumann et al. (2016) examined the esterification reaction of oleic acid with ethanol using sulfuric acid as catalyst. They approached the variation of the concentration of oil by a second order reaction, arriving at an activation energy of 36.62 kJ/mol and a pre-exponential factor of 4.72 x 10^2 $m^3mol^{-1}s^{-1}$ [43].

Aranda et al. (2008) studied the esterification reaction of palm fatty acids with methanol applying several acidic catalysts. The two catalysts that presented the best results were sulfuric acid and methanesulfonic acid. The reaction promoted by both catalysts was modeled as a first order reaction related to the oil. They varied the concentration of the catalysts and the temperature, and they found out that the activation energy decreases as the catalyst loading increases. For a 0.01wt% catalyst loading, the activation energy was found as 15.05 kJ/mol for the reaction catalyzed by sulfuric acid and 10.12 kJ/mol for the reaction catalyzed by

methanesulfonic acid. Increasing the catalyst loading to 0.05 wt% led to activation energies of 6.53 kJ/mol (sulfuric acid) and 3.785 kJ/mol (methanesulfonic acid) [44].

Jansri et al. (2011) investigated the reaction of palm oil with methanol in a two-stage process: esterification reaction of the FFAs with sulfuric acid as catalyst followed by a transesterification reaction of the triglycerides with sodium hydroxide. The overall order of the esterification was assumed as being first order, while for the transesterification a second order reaction. The temperature was varied from 55 to 65°C. They arrived at the activation energy of 75.3 kJ/mol for the esterification reaction. For the transesterification reaction, they estimated the activation energies for each step of the reaction: conversion of triglycerides (TGL) into diglyceride (DG) (1.45 kJ/mol), diglyceride into monoglyceride (MG) (328 kJ/mol) and monoglyceride into glycerol (GL) (89.35 kJ/mol) [45].

Ullah et al. (2017) studied the transesterification reaction between waste cooking oil and methanol with ionic liquid *3-methyl-1-(4-sulfo-butyl)-benzimidazolium trifluoromethanesulfonate* [BSMBIM][CF_3SO_3]. They simplified the reaction by ignoring the intermediates of the transesterification reaction, modeling the reaction as a first order. The temperature range studied was from 80 to 140°C and they estimated an activation energy of 19.24 kJ/mol [46].

4. TECHNICAL DESCRIPTION AND PROCEDURES

4.1 Chemicals and raw materials

All the reagents used for biodiesel production and for quality control analysis were at least of analytical grade. Oleic acid, tech 90%, was obtained from ThermoFisher (Germany). The reagents obtained from Sigma Aldrich (Switzerland) included the 5 ionic liquids: *1-butyl-3-methylimidazolium hydrogen sulfate, 1-butyl-3-methylimidazolium methyl sulfate, 1-methylimidazolium hydrogen sulfate, 1-butyl-3-methylimidazolium methanesulfonate* and *tributylmethylammonium methyl sulfate* and the Supelco 37 FAME mixture. Methanol, n-heptane, absolute ethanol and diethyl ether, used as solvents, were obtained from Carlo Erba (France). Concentrated sulfuric acid was obtained from Pronalab (Portugal). Methyl heptadecanoate was obtained from Tokyo Chemical (Japan). A sample of waste cooking oil (WCO) was qualitatively and quantitatively characterized, and used as a raw material for the test of the transesterification reactions. All reagents were used without any further treatment. Table 7 presents the proprieties of the reactants.

Table 7 - Properties of reactants and catalyst

	Methanol	Oleic acid	[HMIM][HSO_4]
Formula	CH_4O	$C_{18}H_{34}O_2$	$C_4H_6N_2{\cdot}H_2SO_4$
Molecular weight ($g.mol^{-1}$)	32.0419	282.4614	180.18
Boiling temperature (K)	337.8	467.77	-
Melting temperature (K)	176	289.45	-
Density at 25 °C ($g.cm^{-3}$)	0.79	0.895	-

Source: NIST webbook [47] and The Merck Index [48]

4.2 Equipment

The reaction for biodiesel production was performed in an automatic heating plate (IKA, model C-MAG HP4), with a condenser to reflux the excess methanol. For biodiesel separation, a centrifuge (SIGMA, model 2-4) was utilized. The content of FAMEs was evaluated in a gas chromatograph system (VARIAN CP-3800) equipped with a FID detector and a chromatographic column Supelcowax 10 (30mx0.25mmx0.25 µm). The infrared analysis was done in ABB Inc. FT-IR, model

MB3000, in transmittance mode by using a Miracle single reflection horizontal ATR accessory from Pike Technologies.

4.3 Esterification reaction of oleic acid

In the following order, ionic liquid, oleic acid and methanol were added, in different proportions, to a 100 mL reaction vessel. The vessel was immersed in a bath with paraffin, in an automatic heating plate under determined temperature and agitation, coupled with a reflux condenser, as shown in Figure 5. When the pre- determined reaction time was achieved, the vessel was removed from the bath and it was immersed in cool water to stop the reaction. The mixture was transferred to centrifuge tubes and centrifuged for 20 minutes at 3000 rpm and then stored at 4°C until the organic and the aqueous phases were completely separated and ready to be splitted, as displayed in Figure 6. Both phases were stored in vials at 4°C waiting for further analysis, as displayed in Figure 7.

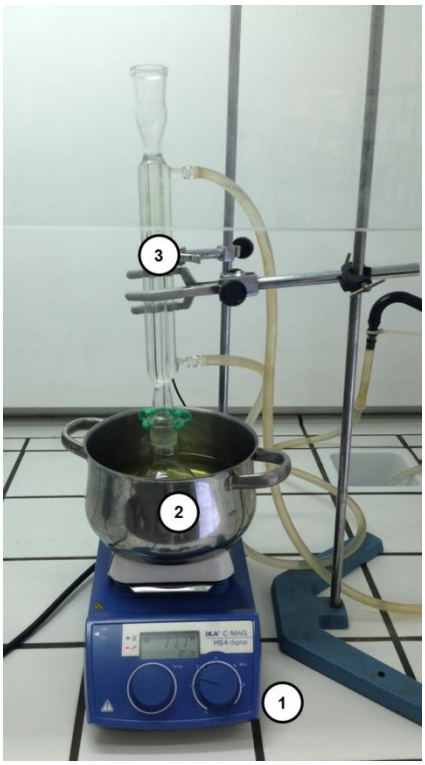

Figure 5 – Experimental set up for the esterification reaction: 1: heating plate with temperature and agitation control; 2: paraffin bath; 3: condenser for methanol reflux.

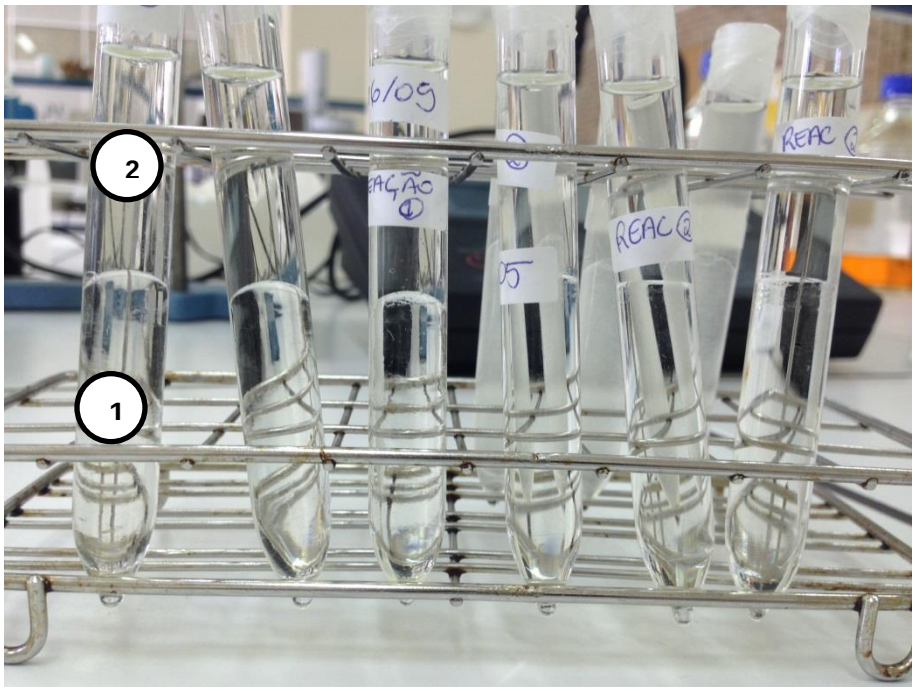

Figure 6 - Layers separated and ready to be split.1 (bottom layer): organic phase containing mainly biodiesel and unreacted oleic acid; 2 (upper layer): aqueous phase containing mainly water, unreacted methanol and ionic liquid.

Figure 7 – Visual appearance of the separated layers.

4.4 Conversion measurements

Acid value determination was performed using a methanolic standardized KOH solution, according to the EN 14104 standard procedure [49]. Half a milliliter of the oleic acid/biodiesel was transferred to an Erlenmeyer using a micropipette and weighed using an analytical balance. Then, 25 mL of diethyl ether/ethanol 1:1 (v/v) solvent mixture was added to the Erlenmeyer along with 5-6 drops of phenolphthalein. The oleic acid/biodiesel was then titrated with a standard KOH solution. The acid value is given in terms of mg of KOH/g biodiesel by equation (1)

$$Acid\ Value, AV\ \left(\frac{mg\ KOH}{g\ biodiesel}\right) = \frac{V_{KOH} * C_{KOH} * MW_{KOH}}{m_{biodiesel}} \quad (1)$$

Where V_{KOH} is the volume of the KOH solution used in the titration, in mL, C_{KOH} is the concentration of the KOH solution, in mol/L, MW_{KOH} is the molecular weight of KOH, which is 56.1 g/mol, $m_{biodiesel}$ is the oleic acid/biodiesel mass measured, in g.

The conversion was then measured by comparing the acid value of the oleic acid to the acid value of the final product, according to equation (2).

$$Conversion, X(\%) = \frac{(AV_{oleic\ acid} - AV_{biodiesel})}{AV_{oleic\ acid}} \times 100 \quad (2)$$

Where X is the conversion of the oleic acid (%); $AV_{oleic\ acid}$ is the acid value for the oleic acid and $AV_{biodiesel}$ is the acid value for the biodiesel, both in mg of KOH/g of sample.

4.5 Characterization of biodiesel

4.5.1 FAME content by Gas Chromatography

Chromatography analysis was performed to measure qualitatively and quantitatively the fatty acid methyl ester (FAME) content in the obtained biodiesel samples. This

experimental determinations was performed respecting the EN 14103 standard [50]. The samples for chromatographic analysis were prepared in the following way: around 250 mg of biodiesel were measured in an analytical balance using a micropipette and a 10 mL flask. Then, 5 mL of methyl heptadecanoate internal standard solution, with a known concentration of around 10 mg/mL, were added. The sample was dried by adding a small amount of anhydrous sodium sulfate; the solution was agitated and left standing until clarification. The volume of sample injected in the GC equipment was 1 µL.

The operation conditions used for GC analysis were a helium flow (carrier gas) of 1 mL/min and an initial oven temperature of 50^{o}C, which was held for 1 min. Then, a first ramp was done up to 200^{o}C at 25^{o}C/min rate and a second ramp up to 230^{o}C with a 3^{o}C/min rate, which was held for 23 min, leading to a total running time of 40 min. Injection temperature was 250 ^{o}C, split ratio 1:25 and detector temperature 250°C.

The identification of each FAME compound present in biodiesel samples was determined by comparison of the obtained retention times of each standard obtained by performing an analysis of a Supelco 37 component standard FAME mix, using the same GC-FID equipment under the same operation conditions. Figure 8 displays the elution order of each FAME in the mixture, as appointed by previously published work from Agilent Technologies [51]. This elution order was used to identify each FAME in the analysis performed in the equipment used. The column used for obtaining the chromatogram displayed on Figure 8 is a DB WAX column, which has a similar packing and the same dimensions as the column used in this work (a Supelcowax 10), which allows comparison of the results obtained in both. It is important to notice the similarity of the elution order for all the components. The chromatogram displayed on Figure 9 is the chromatogram obtained for the same sample in the ESTiG equipment, using the operation conditions described in the beginning of this section. Table 8 displays the retention time for each of the FAMEs, as well with the peak number used in the chromatogram, the name and the ID of the component. These retention times were used to identify the presence of each FAME

in the biodiesel samples, as exemplified on Figure 10. After the peaks were identified, the total area of the peaks identified as FAMEs was calculated.

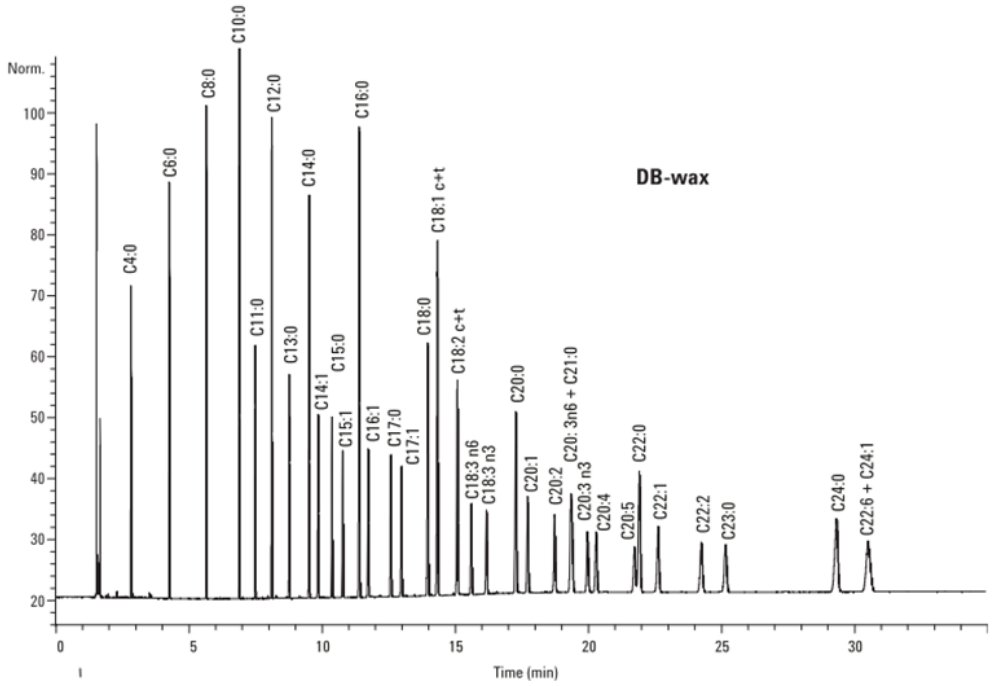

Figure 8 - Chromatogram for the 37 Component FAME mix from Supelco in a DB WAX column. Source: David, Sandra and Vickers (2005) [51].

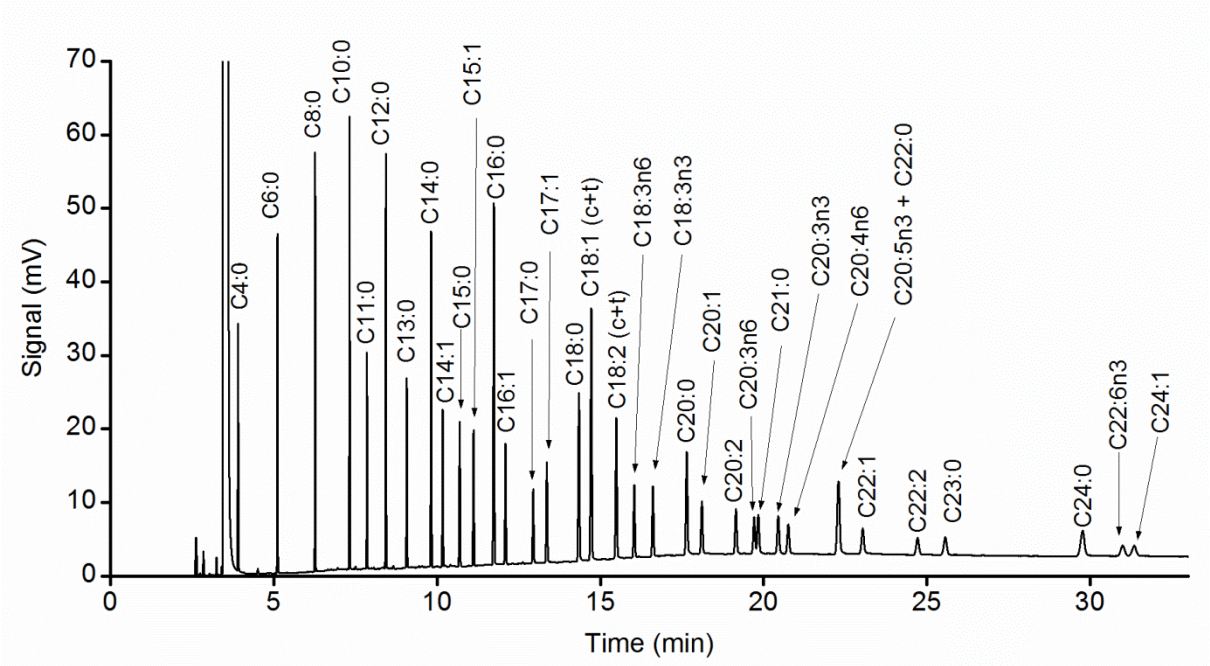

Figure 9 - Chromatogram for 37 Component FAME mix obtained in our equipment: elution order is the same as the published work from Supelco.

Table 8 - Elution order; peak name, peak ID and retention time for 37 Component FAME mix.

Peak number	Peak name	Peak ID	Retention time (min)
1	Butyric acid methyl ester	C4:0	3.904
2	Caproic acid methyl ester	C6:0	5.109
3	Caprylic acid methyl ester	C8:0	6.264
4	Capric acid methyl ester	C10:0	7.319
5	Undecanoic acid methyl ester	C11:0	7.852
6	Lauric acid methyl ester	C12:0	8.429
7	Tridecanoic acid methyl ester	C13:0	9.071
8	Myristic acid methyl ester	C14:0	9.818
9	Myristoleic acid methyl ester	C14:1	10.171
10	Pentadecanoic acid methyl ester	C15:0	10.692
11	cis-10-Pentadecanoic acid methyl ester	C15:1	11.116
12	Palmitic acid methyl ester	C16:0	11.740
13	Palmitoleic acid methyl ester	C16:1	12.095
14	Heptadecanoic acid methyl ester	C17:0	12.942
15	cis-10-Heptadecanoic acid methyl ester	C17:1	13.362
16	Stearic acid methyl ester	C18:0	14.345
17,18	Oleic acid methyl ester, Elaidic acid methyl ester	C18:1 (c+t)	14.723
19,20	Linoleic acid methyl ester, Linolelaidic acid methyl ester	C18:2 (c+t)	15.489
21	gamma-Linolenic acid methyl ester	C18:3n6	16.039
22	Linolenic acid methyl ester	C18:3n3	16.609
23	Arachidic acid methyl ester	C20:0	17.648
24	cis-11-Eicosenoic acid methyl ester	C20:1	18.110
25	cis-11,14-Eicosadienoic acid methyl ester	C20:2	19.153
26	cis-8,11,14-Eicosatrienoic acid methyl ester	C20:3n6	19.711
27	Heneicosanoic acid methyl ester	C21:0	19.838
28	cis-11,14,17-Eicosatrienoic acid methyl ester	C20:3n3	20.449
29	Arachidonic acid methyl ester	C20:4n6	20.757
30,31	cis-5,8,11,14,17-Eicosapentaenoic acid methyl ester, Behenic acid methyl ester	C20:5n3 + C22:0	22.295
32	Erucic acid methyl ester	C22:1	23.038
33	cis-13,16-Docosadienoic acid methyl ester	C22:2	24.718
34	Tricosanoic acid methyl ester	C23:0	25.566
35	Lignoceric acid methyl ester	C24:0	29.773
36	cis-4,7,10,13,16,19-Docosahexanoic acid methyl ester	C22:6n3	31.001
37	Nervonic acid methyl ester	C24:1	31.352

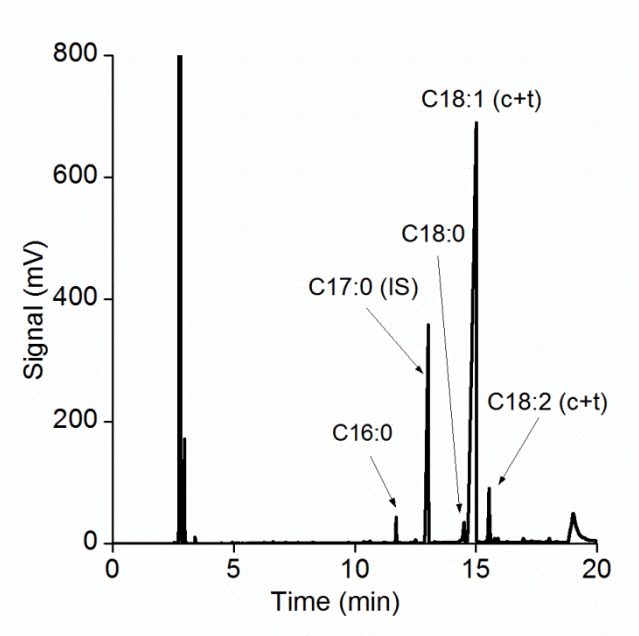

Figure 10 - GC-FID chromatogram obtained from a biodiesel sample.

The FAME content was determined according to equation (3).

$$C\ (\%) = \frac{(\sum A_{\ FAMEs} - A_{IS})}{A_{IS}} \times \frac{m_{\ IS}}{m_{biodiesel}} \qquad (3)$$

Where $\sum A_{\ FAMEs}$ is the sum of the areas of all FAMEs (from C4:0 to C22:0), A_{IS} is the area of the internal standard, $m_{\ IS}$ is the mass of the internal standard and $m_{biodiesel}$ is the mass of biodiesel.

4.5.2 Qualitative analysis using FT-IR

FT-IR was done to characterize several samples, including starting materials and products. FT-IR analysis helps to understand whether the reactants are being converted into the desired products. FTIR spectra were obtained on ABB Inc. FTIR, model MB3000, (Quebec, Canada) in transmittance mode by using a Miracle single reflection horizontal ATR accessory from Pike Technologies (Madison, WI, USA).

Spectra were recorded between 650 and 4000 cm^{-1} at a resolution of 16 cm^{-1} and cumulative 32 scans. Spectra were acquired using the software Horizon MB v.3.4.

4.6 Experimental design

To estimate the optimal conditions, 4 factors were studied. The chosen factors were reaction time (h), reaction temperature (°C), molar ratio between methanol and oleic acid (mol/mol) and the amount of catalyst added to the system (%wt), in relation to the mass of oleic acid. A response surface methodology (RSM) was employed, known as Box-Behnken Design (BBD) [52]. Table 9 describes the 4 parameters chosen, the code applied and the 3 levels used.

Table 9 - Levels chosen for Box-Behnken Design.

Parameter	Code	-1	0	+1
Time (h)	A	4	6	8
Temperature (ºC)	B	80	95	110
Molar ratio methanol/oleic acid	C	5:1	10:1	15:1
Catalyst dosage (%wt)	D	5	10	15

The methodology estimates that 27 runs are adequate to understand the influence of each factor on the response. The design matrix in coded and in real values is displayed on Table 10. Each run was carried out accordingly to the generic esterification procedure presented in section 4.3. Two responses were evaluated: the conversion of oleic acid, according to the procedure described in section 4.4, and the FAME content, according to the procedure described in section 4.5.1.

The methodology allows fitting a quadratic mathematical model that describes the relationship between the parameters and each response. The generic formula for the mathematical model is given by equation (4).

Table 10 - Experimental conditions applied for each run, in coded values and in real values.

Run	Parameters							
	Coded values				Real values			
	A	B	C	D	Time (h)	Temperature (°C)	Molar Ratio MeOH/OA	Catalyst Dosage (wt%)
1	-1	1	0	0	4	110	10	10
2	-1	0	0	-1	4	95	10	5
3	0	0	0	0	6	95	10	10
4	0	0	-1	-1	6	95	5	5
5	-1	0	-1	0	4	95	5	10
6	0	-1	1	0	6	80	15	10
7	0	1	0	1	6	110	10	15
8	1	1	0	0	8	110	10	10
9	0	1	1	0	6	110	15	10
10	0	-1	-1	0	6	80	5	10
11	1	0	-1	0	8	95	5	10
12	0	1	0	-1	6	110	10	5
13	-1	0	1	0	4	95	15	10
14	1	0	0	-1	8	95	10	5
15	0	-1	0	-1	6	80	10	5
16	0	0	1	1	6	95	15	15
17	0	0	1	-1	6	95	15	5
18	1	-1	0	0	8	80	10	10
19	0	1	-1	0	6	110	5	10
20	1	0	0	1	8	95	10	15
21	0	0	0	0	6	95	10	10
22	0	0	-1	1	6	95	5	15
23	-1	-1	0	0	4	80	10	10
24	-1	0	0	1	4	95	10	15
25	1	0	1	0	8	95	15	10
26	0	0	0	0	6	95	10	10
27	0	-1	0	1	6	80	15	15

$$Y = \beta_0 + \sum_{i=1}^{4} \beta_i X_i + \sum_{i=1}^{4} \beta_{ii} X_i^2 + \sum_{j<i} \beta_{ji} X_j X_i \quad (4)$$

Where *Y* is the response, in this case either the oleic acid conversion or the FAME content, β_0 is the intercept coefficient, β_i are the linear terms, β_{ii} the quadratic terms, $\beta_{ji}$the interaction terms and X_i and X_j are the independent factors, which are

displayed in Table 6. The values for each coefficient can be obtained by multiple linear regression and by maximizing the equation it is possible to obtain the optimal conditions for each of the responses separately.

4.7 Kinetic study

The procedure was similar to the one for the esterification reaction, presented on section 4.3. Throughout the reaction, in pre-determined times (0, 15, 30, 60, 90, 120, 180, 240, 300, 360, 420 and 480 min), 1 mL of sample was removed from the vessel using a micropipette and stored in a 2 mL flask at 4 °C, waiting for further analysis. The conversion was determined by acid value decrease, as stated on section 4.4. The kinetic study was performed for different reaction temperatures (70, 80, 90, 100 and 110°C) with the goal of establishing the activation energy.

4.8 Transesterification study

The procedure was similar to the general esterification reaction. In this specific case, the oleic acid was substituted by a mixture of oleic acid and a used vegetable oil. The mass proportion in which the oil and the acid were blended varied in each experiment. The proportions are appointed in Table 11. The factors were set up to the optimum determined for the esterification, except for the quantity of methanol added, which was added in a proportion of 20 mol of methanol/mol of triolein (it was considered that the mixture was only composed by triolein). This approach regarding the amount of methanol was chosen as it would allow a better comparison amid the results obtained in each run.

Table 11 – Experimental conditions for transesterification reaction.

Run	Amount of oleic acid (wt%)	Amount of oil (wt%)	Temperature (°C)	Catalyst dosage (wt%)	Molar ratio MeOH/triolein
T1	80	20	110	15	20
T2	60	40	110	15	20
T3	50	50	110	15	20
T4	40	60	110	15	20
T5	20	80	110	15	20

5. RESULTS AND DISCUSSION

5.1 Preliminary ionic liquid screening

The catalytic activities of five ionic liquids in the esterification reaction of oleic acid were compared. The goal was to understand the influence of the cation and the anion on the catalytic activity of the ionic liquid and then choose the most suitable one for biodiesel production. In order to do so, several experiments were carried out under the same reaction conditions. The conditions applied were chosen based on previous studies done in our research group [53] and were as follows: 6 h reaction time, reaction temperature of 90ºC, catalyst loading of 10 wt% and a methanol/oleic acid ratio of 10:1. Table 12 presents the obtained results and are displayed on Figure 11 for better interpretation.

Table 12 – Experimental results for ionic liquid screening.

Ionic Liquid	Code	Acidity (mg KOH/g)		Oleic Acid Conversion (%)
		Initial	Final	
1-butyl-3-methylimidazolium methyl sulfate [BMIM][$MeSO_4$]	1	183.74	37.75	79.45
1-methylimidazolium hydrogen sulfate [HMIM][HSO_4]	**2**	**183.74**	**21.10**	**88.52**
1-butyl-3-methylimidazolium hydrogen sulfate [BMIM][HSO_4]	3	183.74	41.03	77.66
1-butyl-3-methylimidazolium methanesulfonate [BMIM][CH_3SO_4]	4	183.74	149.98	18.38
Tributylmethylammonium methyl sulfate [TBMA][$MeSO_4$]	5	183.74	155.47	15.39

The order of catalytic activity of the ionic liquids was **2** > **1** > **3** >> **4** > **5**, under the used conditions. The ionic liquids **1**, **3** and **4** comprised the same cation (*1-butyl-3-methylimidazolium)*, and the results differed greatly from ionic liquid **4**. This may indicate that the acidity of the methanesulfonate anion is very low. On the other hand, the results obtained with catalysts **1** and **3** are very close, indicating that the catalytic activity of those two catalysts may also be similar. Comparing ionic liquids **2** and **3**, which display the same hydrogen sulfate anion but containing a different cation, the

results may indicate that the cation plays an important role on the catalytic activity, as the change in the cation resulted in a higher conversion.

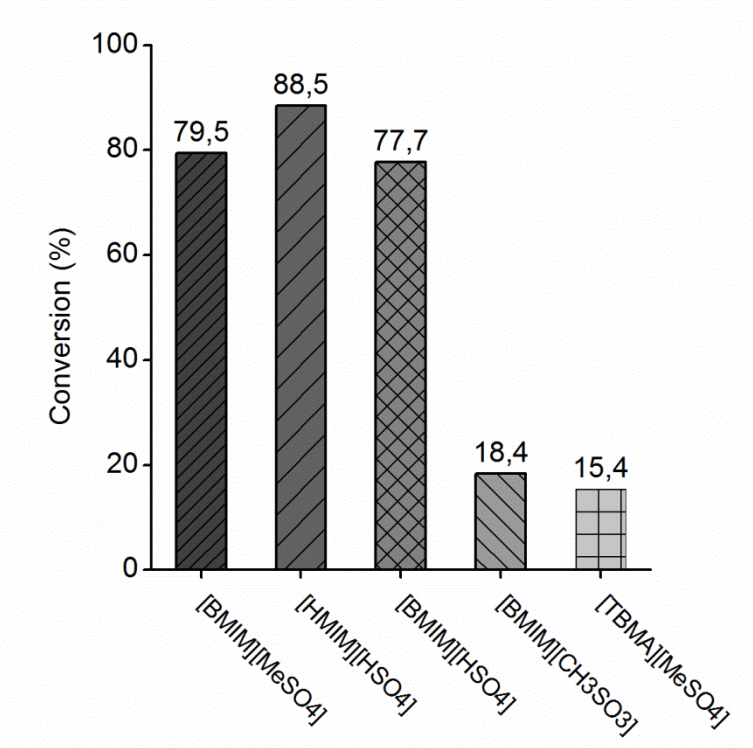

Figure 11 - Catalyst screening. Conditions: 6h, 90°C, 10:1 molar ratio and 10wt% catalyst dosage.

Finally, by comparing ionic liquids **1** and **5**, which have the same anion and a different cation, there's a huge difference in the conversion, indicating that the cation based on an imidazole ring has a stronger acidity and therefore catalytic activity. The catalyst *1-methylimidazolium hydrogen sulfate [HMIM][HSO_4]* **2** was identified, from those analyzed, as the most suitable catalyst for biodiesel production through esterification reaction. Therefore, this ionic liquid was chosen for further studies. Figure 12 presents the structure of the ionic liquid *[HMIM][HSO_4].*

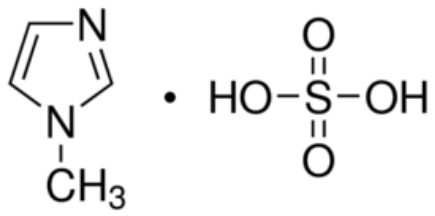

Figure 12 - Structure of ionic liquid *1-methylimidazolium hydrogen sulfate.*

5.2 Experimental design

After choosing the ionic liquid *1-methylimidazolium hydrogen sulfate [HMIM][HSO_4]*, optimization for the esterification reaction was performed based on a Response Surface Methodology (RSM). This kind of methodology is based on a set of mathematical and statistical techniques that intends to fit a non-linear equation to the experimental data, in such a way that this equation is able to describe the relationship between the studied parameters and the response and make statistical previsions [54]. Compared to one-variable-at-time methodologies, where the influence of only one factor is monitored at a time while others remain fixed, response surface methodologies have the advantage of a small number of runs, meaning that RSM is time and cost efficient [54].

Amongst the available RSM, the design chosen was the Box-Behnken Design (BBD). According to Bezerra et al (2008) [54]:

> "Box and Behnken suggested how to select points from the three-level factorial arrangement, which allows the efficient estimation of the first- and second-order coefficients of the mathematical model. These designs are, in this way, more efficient and economical then their corresponding 3k designs, mainly for a large number of variables".

The requirements of such design is that the factors must be adjusted in three levels (-1, 0 and +1), equally spaced. The experimental points are located on a hyper sphere, being equally distant from the central point. For a design with four variables and three levels, a complete factorial would require 81 runs, while for the same

situation, the Box-Behnken Design requires only 27 [54]. Replicates in the central point are necessary to estimate pure errors.

Four parameters were chosen to be studied. Those factors were chosen based on previously done investigations in our group [53] and also based on several papers found on the literature.

The parameters chosen were reaction time (A), reaction temperature (B), molar ratio between methanol and oleic acid (C) and the catalyst dosage (D) and the factors and their respective levels are summarized on Table 13. Two responses were evaluated: the conversion of oleic acid, based on acidity decrease, and the FAME content, through gas chromatography analysis.

Table 13 - Summary of factors and levels for the BBD.

Factor	Code	Levels		
		-1	0	+1
Reaction time (h)	A	4	6	8
Reaction temperature (°C)	B	80	95	110
Molar ratio MeOH/OA (mol/mol)	C	5:1	10:1	15:1
Catalyst dosage (%wt)	D	5	10	15

Table 14 describes the conditions applied in each run, both by the experimental design and the real values, and the obtained responses. As mentioned earlier, the Box-Behnken Design for four factors and three levels requires 27 runs.

The evaluation of the responses was done separately. This means that a different model was developed for each of the responses and different optimal conditions were estimated. The FAME content was determined by gas chromatography analysis according to the procedure appointed on section 4.5.1. The conversion was determined by acidity decrease, as mentioned on section 4.4.

Table 14 - Experimental design, real conditions and experimental responses.

Run	Experimental Design				Real Conditions				Experimental Responses	
	Time (h)	Temp. (°C)	Molar ratio MeOH/ AO	Cat dosage (wt%)	Time (h)	Temp. (°C)	MeOH /Oleic acid ratio	Catalyst dosage (wt%)	FAME content (%)	Conversion of oleic acid (%)
	A	B	C	D	A	B	C	D		
1	-1	1	0	0	4	110	10	10	82.8	83.8
2	-1	0	0	-1	4	95	10	5	74.2	78.5
3	0	0	0	0	6	95	10	10	85.0	88.6
4	-1	0	-1	0	4	95	5	10	65.9	73.4
5	0	-1	1	0	6	80	15	10	85.5	89.6
6	0	1	0	1	6	110	10	15	86.8	90.5
7	0	1	1	0	6	110	15	10	87.5	92.2
8	0	1	0	-1	6	110	10	5	78.0	79.5
9	0	-1	-1	0	6	80	5	10	72.6	77.2
10	1	1	0	0	8	110	10	10	88.0	90.4
11	1	0	-1	0	8	95	5	10	74.4	77.3
12	-1	0	1	0	4	95	15	10	84.6	84.6
13	0	-1	0	-1	6	80	10	5	77.7	82.8
14	0	0	1	1	6	95	15	15	87.4	92.5
15	0	0	1	-1	6	95	15	5	78.7	82.4
16	1	0	0	-1	8	95	10	5	80.4	84.3
17	1	-1	0	0	8	80	10	10	86.0	90.9
18	0	1	-1	0	6	110	5	10	68.4	74.5
19	0	0	0	0	6	95	10	10	84.6	89.2
20	-1	-1	0	0	4	80	10	10	81.4	83.5
21	0	0	0	0	6	95	10	10	85.5	88.3
22	-1	0	0	1	4	95	10	15	81.7	83.4
23	1	0	0	1	8	95	10	15	87.0	90.5
24	1	0	1	0	8	95	15	10	90.2	92.8
25	0	-1	0	1	6	80	10	15	84.5	89.3
26	0	0	-1	1	6	95	5	15	73.3	74.8
27	0	0	-1	-1	6	95	5	5	64.4	71.9

5.2.1 Analysis for the conversion of oleic acid

5.2.1.1 ANOVA table

The experimental design was evaluated using several statistical tools. The first one was the Analysis of Variance (ANOVA) table, found on Table 15. The main idea of the ANOVA is to compare the variation in the response due to treatment, which

means the change in the level of the variables, with the variation due to random errors that are inherent to the measurement of the response. With this approach, it is possible to determine whether the regression proposed is adequate while taking into consideration the experimental inaccuracies associated to the process [54].

The ANOVA table is constructed by calculating the squares of the deviations of each observation from the mean. The sum of squares for all deviations gives origin to the total sum of squares (SS_{TOTAL}), which can be dismantled in two parts: the sum of squares due to the regression (SS_{model}) and the sum of squares due to residuals ($SS_{residuals}$) generated by the model. Since replicates of the center points are made, it is possible to estimate pure errors associated to the measurement of the response and therefore to break the sum of squares of the residuals into the sum of squares due to pure error (SS_{pe}) and the sum of squares due to the lack of fit (SS_{lof}) [54]. The total sum of squares is given by equation (5). Then, each of the sums of squares should be divided by its respective degree of freedom, giving rise to the media of the square (MS).

$$SS_{TOTAL} = SS_{model} + SS_{pe} + SS_{lof} \quad (5)$$

The significance of the regression is evaluated by the ratio of the MS of the regression (MS_{model}) by the MS of the residuals ($MS_{residual}$), leading to the calculated F-value. This value must be compared to the F-value tabulated (F test) by taking into account the degrees of freedom from both the regression and the residual. If the calculated value is higher than the tabulated one, means that the regression is statistically significant and therefore, the model is well fitted to the data, with a 95% confidence level. In the current analysis, the calculated F-value for the regression is 112.74. Considering the degrees of freedom of the regression (df1 = 14) and the degrees of freedom of the residual (df2 = 12), and checking the Fisher's distribution table for the critical value of $F_{14,12,0.05}$ (α equal to 0.05), it is possible to find a

tabulated value of 2.637. The calculated value is higher than the tabulated, indicating a reliable model.

Table 15 - ANOVA table for conversion.

Source	Sum of squares (SS)	Df*	Mean Square (MS)	Calculated F-value	Tabulated F-value	p-value
Model	1085.81	14	77.56	112.74	2.637	$1.64x10^{-10}$
Residual	8.26	12	0.688			
Lack of Fit	7.86	10	0.7863	4.01	19.396	0.2162
Pure Error	0.3925	2	0.1962			
Cor Total	1094.07	26				

*Df = Degrees of freedom

Another way to evaluate the model is by checking the lack of fit. As in the regression fit, the lack of fit should be evaluated by comparing the F-value calculated to the tabulated one. In this case, the degrees of freedom of the lack of fit and the pure error must be taken into account. The F distribution appoints that for a $F_{10,2,0.05}$, the value is 19.396, while the calculated F-value is 4.01, meaning that the lack of fit *is not significant.* This is the expected response for the lack of fit. It means that the model errors are due to random and inherent errors of the system rather than a problem with the data fit. Random errors are not related to model quality, while lack of fit is.

The p-value is related to the F-value and is defined as the probability that the data would be at least as extreme as those observed [55]. In other words, it is related to the strength of evidence against the null hypothesis. Low p-values allow rejecting the null hypothesis, which in this case would be that the model is not relevant or that the factors don't influence the response. If the null hypothesis is rejected, then the alternative hypothesis must be true, which would mean that the model and the factors are relevant. Treatments that result in p-values lower than a pre-determined significance level, which in this case is 0.05, are considered statistically significant. Therefore, the current model is statistically relevant, and the lack of fit is not.

5.2.1.2 Another tools to assess the model fit

The quality of the fit was also assessed by other statistical tools. The regression coefficient was estimated as R^2=0.9925, indicating that the observed and predicted values are close and that the model can be used to predict responses. To assess the viability and accuracy of the model, some facts must be checked. First, the residuals of the runs should be normally distributed. Second, the mean of the residuals should be close to 0 and third, the residuals should be unrelated to the levels of any known variables [56]. Residuals are estimates of the errors done by subtracting the observed response, or the experimental response, from the predicted response. The normality of the residuals can be assessed by verifying the normal plot of residuals, displayed on Figure 13. The expectations is that the data is normally distributed when all the runs fall within a straight diagonal line, without any residuals occurring too far from the line neither any tendency to form a specific pattern, such as a curve in form of an “s”. Figure 13 shows a set of data that is normally distributed.

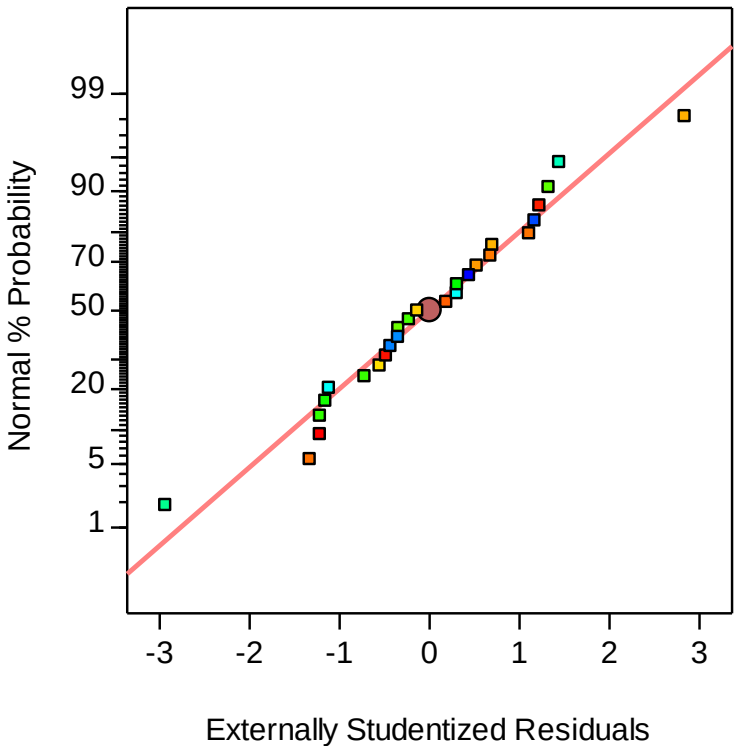

Figure 13 - Normal plot of residuals.

The residuals versus predicted plotted on Figure 14 helps to verify if the residuals are close to 0 and if the residuals are unrelated to the level of the variables. Both conditions are satisfied, as the residuals fall close to the black line indicating a 0 mean, and that no specific pattern, such a funnel like appearance, is formed as the predict response increases.

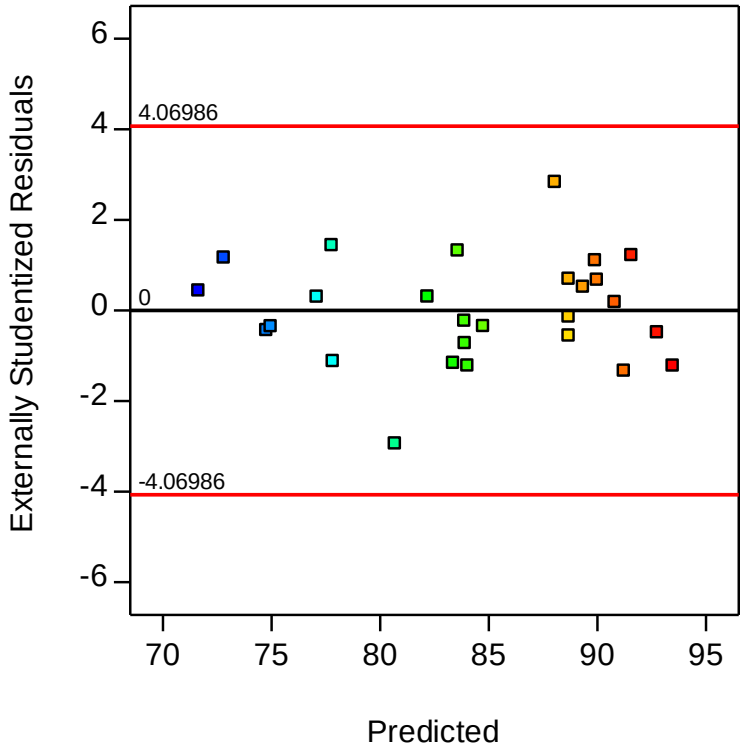

Figure 14 - Residuals versus predicted values.

Also, the residual versus predicted plot helps to identify outliers, which are runs with very large residuals that must be discarded from the statistical evaluation. Any value outside the red line on Figure 14 should be considered an outlier and the experiment or measurements of the responses should be repeated. It is important to note that those are only tools to help to identify problems with the model, so it is important to check for values that are really far apart from the objective and not that every value falls in the black line that indicates a deviation of 0.

5.2.1.3 Factors effect on the conversion

There are several ways to evaluate the influence of the factors on the response. One way is by applying the same logic when the model regression was evaluated, taking into consideration the degrees of freedom of each factor and the degree of freedom of the residual. The ANOVA table can also be built to analyze the influence of each factor, as well as the interactions between them and their quadratic effect on the response. As it can be seen on Table 16, the calculated F-value is higher than the tabulated one for the following parameters: A (time); C (molar ratio); D (catalyst dosage); C^2; D^2; CD; A^2; BC, BD and AC. The remaining terms are not significant, including, in this list, the reaction temperature. Besides helping understanding whether the factor is statistically significant, the ANOVA helps to interpret how significant each one is. This can be assessed by the *p-value*. The lowest it is, the highest the influence on the response. In this way, the order of importance is C (molar ratio MeOH/OA) > D (catalyst dosage) > A (time) ≈ C^2 > D^2 > CD > A^2 > BC > BD > AC.

Table 16 - ANOVA analysis for the parameters influencing the Conversion.

Source	Sum of squares (SS)	Df*	Mean Square (MS)	Calculated F-value	Tabulated F-value	p-value
A-Time	126.82	1	126.82	184.34	4.965	$1.216x10^{-08}$
B-Temperature	0.5208	1	0.5208	0.7571	4.965	0.4013
C-Molar ratio MeOH/OA	601.80	1	601.80	874.77	4.965	$1.4x10^{-12}$
D-Catalyst dosage	144.84	1	144.84	210.53	4.965	$5.68x10^{-09}$
AB	0.1600	1	0.1600	0.2326	4.965	0.6383
AC	4.95	1	4.95	7.20	4.965	0.0199
AD	0.4900	1	0.4900	0.7123	4.965	0.4152
BC	7.00	1	7.00	10.17	4.965	0.0078
BD	5.13	1	5.13	7.46	4.965	0.0182
CD	13.10	1	13.10	19.05	4.965	0.0009
A^2	11.12	1	11.12	16.17	4.965	0.0017
B^2	0.0486	1	0.0486	0.0706	4.965	0.7950
C^2	144.65	1	144.65	210.27	4.965	$5.71x10^{-09}$
D^2	50.81	1	50.81	73.86	4.965	$1.8x10^{-06}$

*Df = Degrees of freedom

Figures 15 through 20 display the response surface for several pairs of variables and the interaction plots of those same variables and their influence on the conversion, in coded values. Any variable that is not on display on each plot was set to its intermediate value (0).

Figure 15 displays the response surface regarding the influence of variables time and temperature and the interaction plot of those two variables. The response surface indicates that the temperature variable is negligible for the conversion. By establishing a fixed value for the time, for instance -1, and moving along the temperature axis, no change in the response is noticed, therefore, its influence is irrelevant. On the other hand, by doing the same analysis for the time variable, it is possible to verify that the response alters as we move to upper values for the variable time.

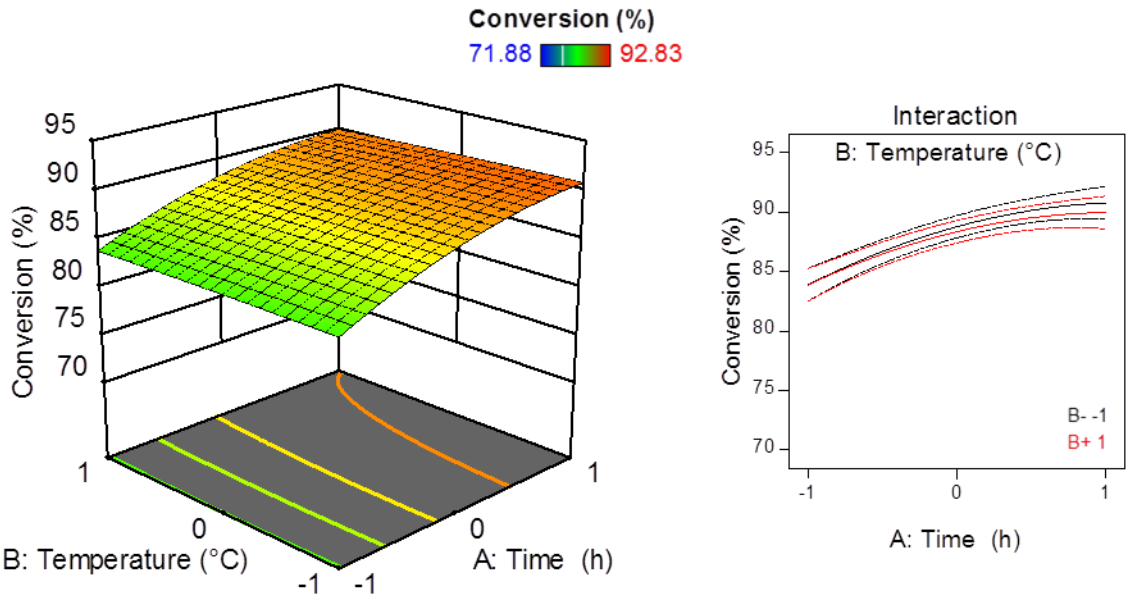

Figure 15 - Response surface for the conversion being influenced by time (A) and temperature (B) and the interaction plot of those variables (Molar ratio = 0; Catalyst dosage = 0).

The interaction plot on Figure 15 permits to evaluate if the variables influence one another. If the interaction plot displays two parallel lines, the conclusion is that the effect of one factor does not depends on the level of the other factor. If the lines are

not parallel, it means that the effect displayed by one factor depends on the level of the other factor. In other words, it means that one factor not only influences the response by itself, but it also influences the other variable, changing the effect of this second variable on the response. As displayed on Figure 15, it is clear that the variables do not affect each other.

Figure 16 displays the response surface for the variables time and molar ratio and their interaction plot. Both variables influence positively the response. By combining them in their bottom value (-1), the conversion is estimated as 72%, while for their upper bound (+1) the conversion is estimated as above 90%. Also, it is clear that the molar ratio has a stronger influence on the response. The interaction plot displays two slight non-parallel lines, meaning that these variables influence each other. This is in agreement with the *p-value* of 0.0199 found for the interaction of those factors.

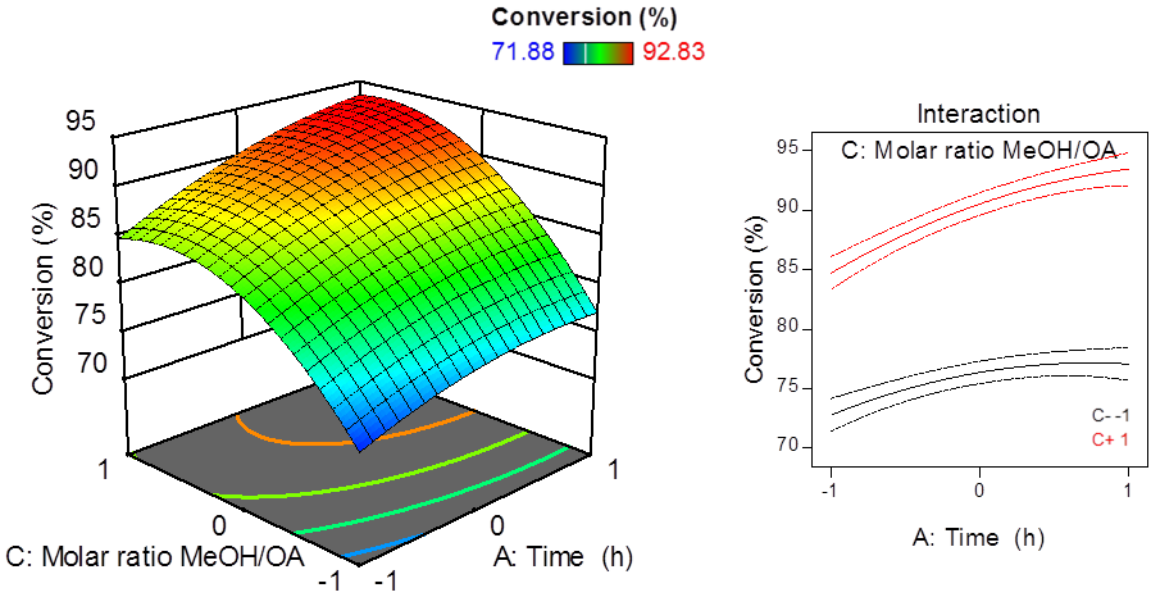

Figure 16 - Response surface for the conversion being influenced by time (A) and molar ratio between methanol and oleic acid (C) and the interaction plot of those variables (Temperature = 0; Catalyst dosage = 0).

Figure 17 displays the response surface for the variables time and catalyst dosage and their respective interaction plot. The behavior of both variables is very similar, and significant to the response. This restates the *p-values* found for the individual

factors of 1.216×10^{-8} for time and 5.68×10^{-9} for the catalyst dosage. The values mean that the factors are statistically relevant for the response and they are somewhat close, therefore justifying the similar behavior displayed. The interaction plot displays two parallel lines, indicating that there is no influence of one factor on the other, in agreement with the *p-value* of 0.4152.

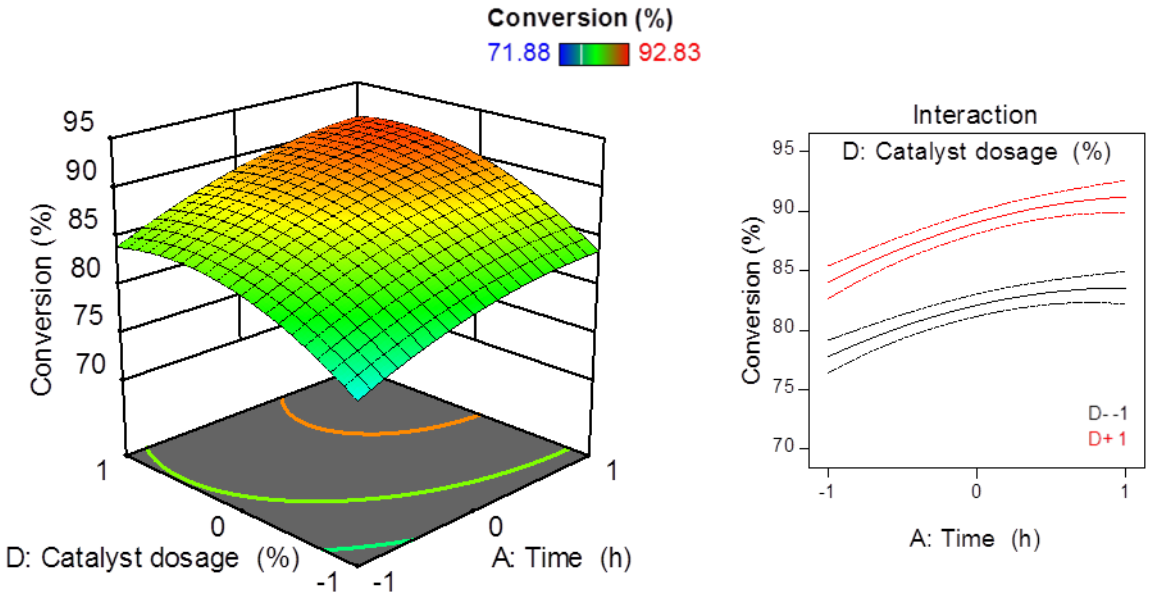

Figure 17 - Response surface for the conversion being influenced by time (A) and catalyst dosage (D) and the interaction plot of those variables (Temperature = 0; molar ratio = 0).

Figure 18 shows the surface response for the variables temperature and molar ratio between methanol and oleic acid and their interaction plot. The surface clearly indicates that the variable temperature is not relevant, while the molar ratio is. The interaction plot shows two non-parallel lines, indicating that the variables have influence on one another. For this case, the interaction can be easily justified. Even though the reaction is carried under methanol reflux, the rise in temperature leads to an elevation on the rate of methanol that is evaporating. Therefore, it also influences the amount of methanol that is present at every moment during the reaction. This influence is mainly felt when the molar ratio is in its lower value (-1), as displayed on the interaction plot on Figure 18.

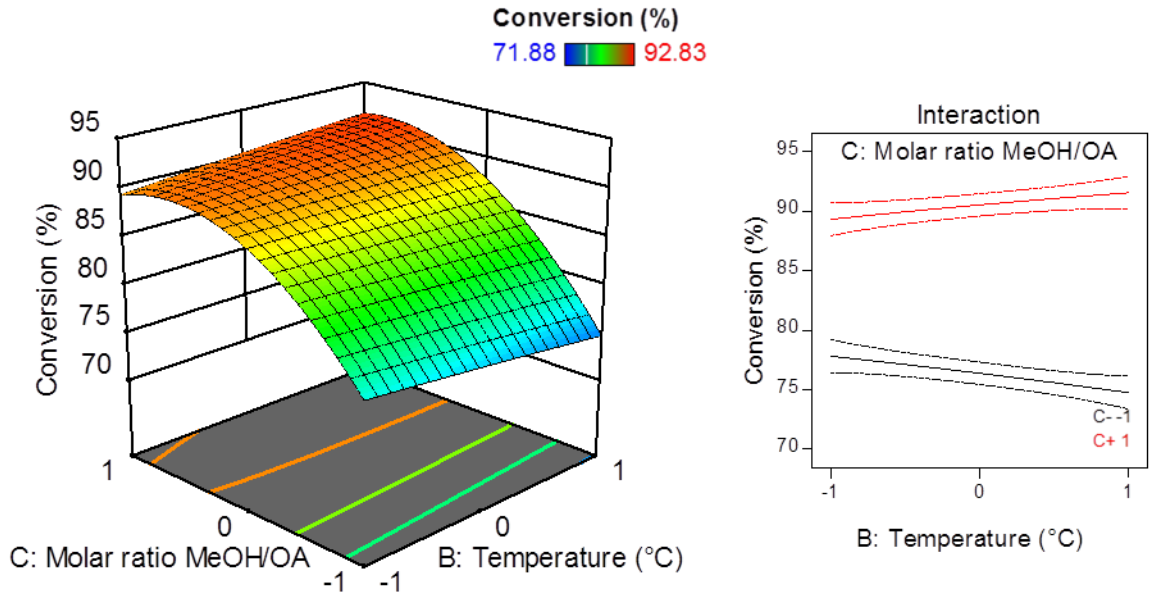

Figure 18 - Response surface for the conversion being influenced by temperature (B) and molar ratio between methanol and oleic acid (C) and the interaction plot of those variables (time = 0; catalyst dosage = 0).

Figure 19 shows the response surface for the temperature and catalyst dosage variables.

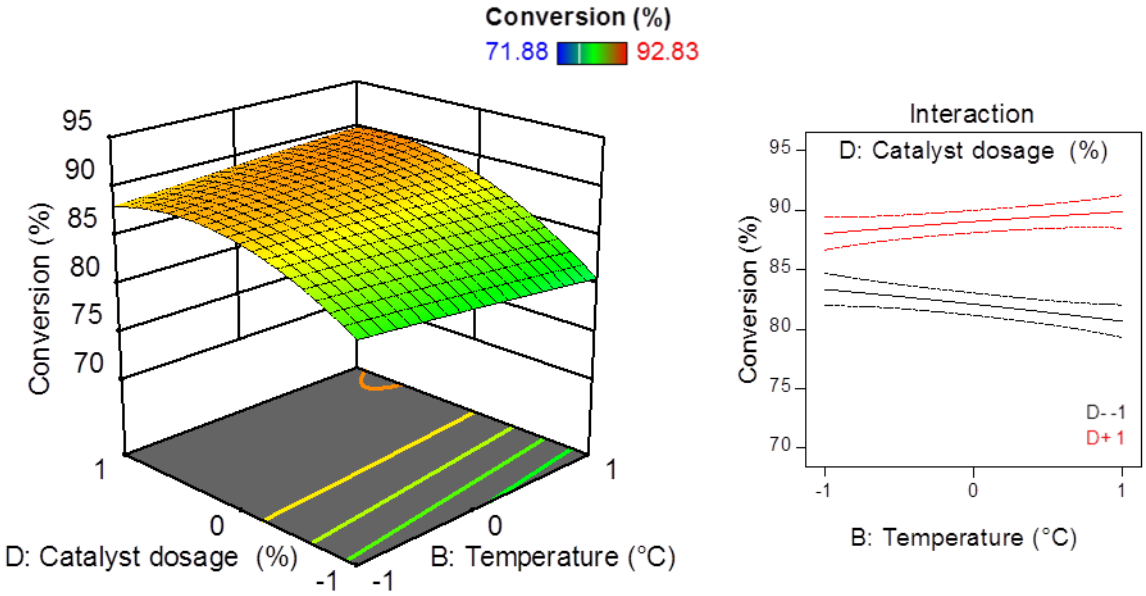

Figure 19 - Response surface for the conversion being influenced by temperature (B) and catalyst dosage (D) and the interaction plot of those variables (time = 0; molar ratio = 0).

Again, in Figure 19, the temperature does not show any great alteration on the response, while the catalyst dosage does. The interaction plot shows two non-parallel lines, indicating that there is influence of the parameters on each other.

Figure 20 displays the response surface for the catalyst dosage and molar ratio variables and their interaction plot. Both the variables have a great influence on the response, although it is possible to identify that the molar ratio variable is much more relevant. The interaction plot indicates that the variables have influence on each other, as the lines displayed are not parallel. The interaction of those two variables is the most relevant interaction, with a *p-value* of 0.009.

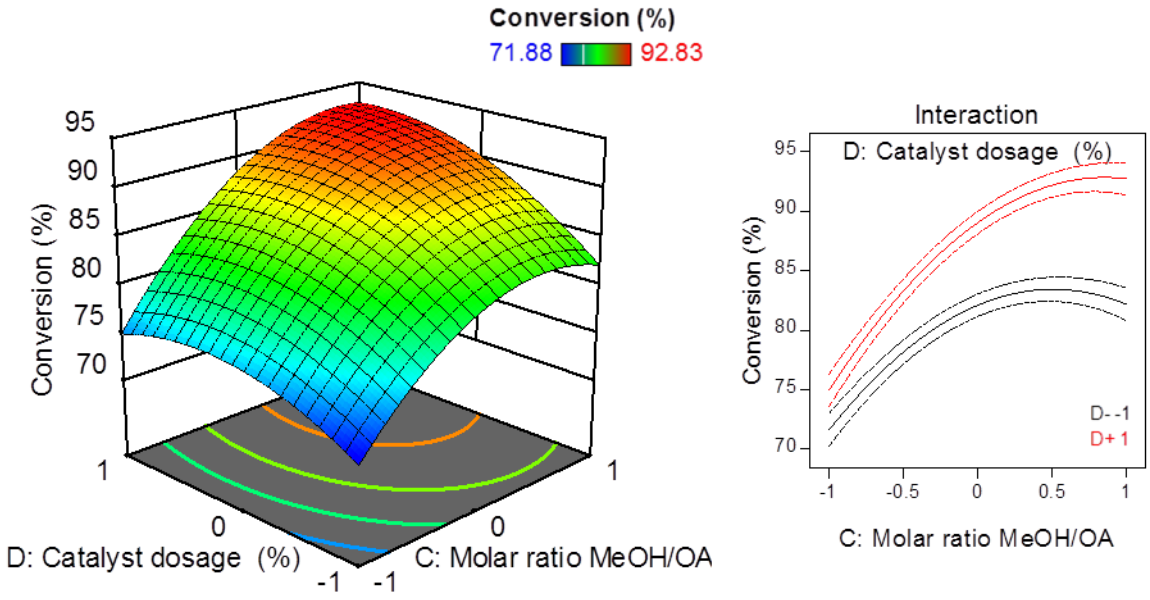

Figure 20 - Response surface for the conversion being influenced by molar ratio between methanol and oleic acid (C) and catalyst dosage (D) and the interaction plot of those variables (time =0; temperature = 0).

5.2.1.4 Optimal conditions estimation

One of the advantages of applying a Response Surface Methodology, such as the Box-Behnken Design, is that it allows the construction of a quadratic equation in the form of equation (4) presented in section 4.6, and as a consequence, allows us to determine the optimum combination of a set of parameters [57] .

$$Y = \beta_0 + \sum_{i=1}^{4} \beta_i X_i + \sum_{i=1}^{4} \beta_{ii} X_i^2 + \sum_{j<i} \beta_{ji} X_j X_i \quad (4)$$

Where Y is the response, β_0 is the intercept coefficient, β_i are the linear terms, β_{ii} the quadratic terms, $\beta_{ji}$the interaction terms and X_i and X_j are the independent factors. Table 17 displays the coefficients determined by regression of the data set. Using the information of the coefficients, it is possible to construct the equation that best fits the region studied, as displayed by equation (6). The equation is constructed using coded values.

Table 17 - Coefficients for the quadratic equation.

Coded Factor	Coefficient
Intercept	88.68
A	3.25
B	-0.2083
C	7.08
D	3.47
A^2	-1.44
B^2	-0.0954
C^2	-5.21
D^2	-3.09
AB	-0.2000
AC	1.11
AD	0.3500
BC	1.32
BD	1.13
CD	1.81

$$Y = 88.68 + 3.25\,A - 0.21\,B + 7.08\,C + 3.47\,D - 1.44\,A^2 - 0.1\,B^2 - 5.21\,C^2 - 3.1\,D^2 - 0.20\,AB + 1.11\,AC + 0.35\,AD + 1.32\,BC + 1.13\,BD + 1.81\,CD \quad (6)$$

By maximizing equation (6), it is possible to determine which values for the set of parameters studied would lead to the highest conversion of oleic acid, which is displayed on Table 18, both in coded values and in real values. It is important to understand that the optimal values found are strongly related to the region studied. If the real values for the molar ratio were changed, for instance, possibly the optimum combination of the parameters would be different.

Table 18 - Optimal values for the conversion of oleic acid.

Factor	Factor Name	Coded Value	Real Value
A	Time	1.00	8h
B	Temperature	1.00	110°C
C	Molar Ratio MeOH/OA	1.00	15:1
D	Catalyst Dosage	0.99	15%

Even though the evaluation of the influence of the parameters indicated that the temperature does not significantly influences the response, the values obtained for the optimal conditions do not reflect only the individual influence of each factor, but also the interaction that they have amongst each other. That is the reason why even not being statistically significant, the optimal conditions are obtained with the temperature at its highest value (+1).

After estimating the optimal conditions, new runs were carried out with the purpose of confirming the predicted results and consequently, the model. Three experiments were run and the results obtained are displayed in Figure 21.

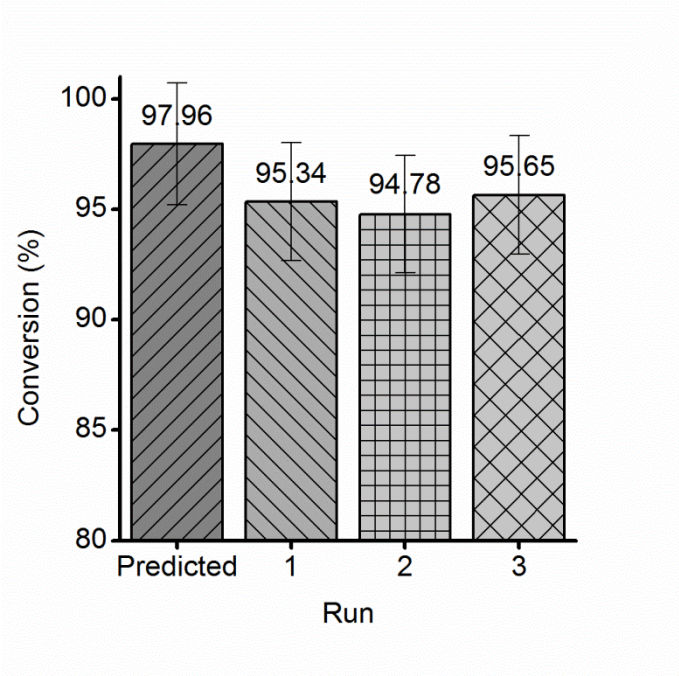

Figure 21 - Predicted results and confirmation runs for the conversion of oleic acid.

The average of the conversion is 95.25, which is within the range predicted by the model, with a 95% confidence level (range for conversion: 95.21 -100.73%). This confirms that the model is suitable for predicting the behavior of the system.

5.2.2 Analysis for the FAME content

5.2.2.1 ANOVA table

The ANOVA table was built in the same way as it was built for the conversion. The ANOVA for the FAME content evaluation displayed on Table 19 indicates that the model is significant, with a calculated F-value higher than the tabulated one. Also, the lack of fit is not significant (calculated F-value lower than the tabulated one).

Table 19 - ANOVA table for the FAME content.

Source	Sum of squares	Df	Mean Square	Calculated F-value	Tabulated F-value	p-value
Model	1319.90	14	94.28	72.92	2.637	$2.14x10^{-09}$
Residual	15.52	12	1.29			
Lack of Fit	15.12	10	1.51	7.63	19.396	0.1213
Pure Error	0.3961	2	0.1980			
Total	1335.41	26				

5.2.2.2 Another tools to assess the model fit

The regression coefficient was estimated as R^2= 0.9884, indicating a good regression. The normal plot of residuals distributed along the straight diagonal line displayed on Figure 22 indicates a reliable model, satisfying the condition that residuals should be normally distributed. Figure 23 allows verifying that the residuals are independent of the level of the known variables and that they fall close to the 0 line, since the residuals are distributed within the red lines and more or less close to the 0 line.

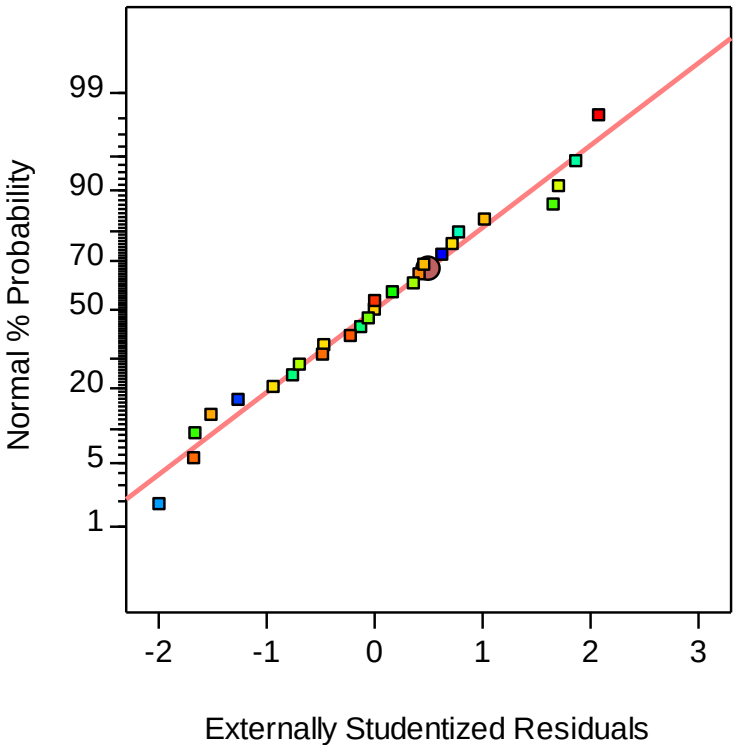

Figure 22 - Normal plot of residuals for the FAME content.

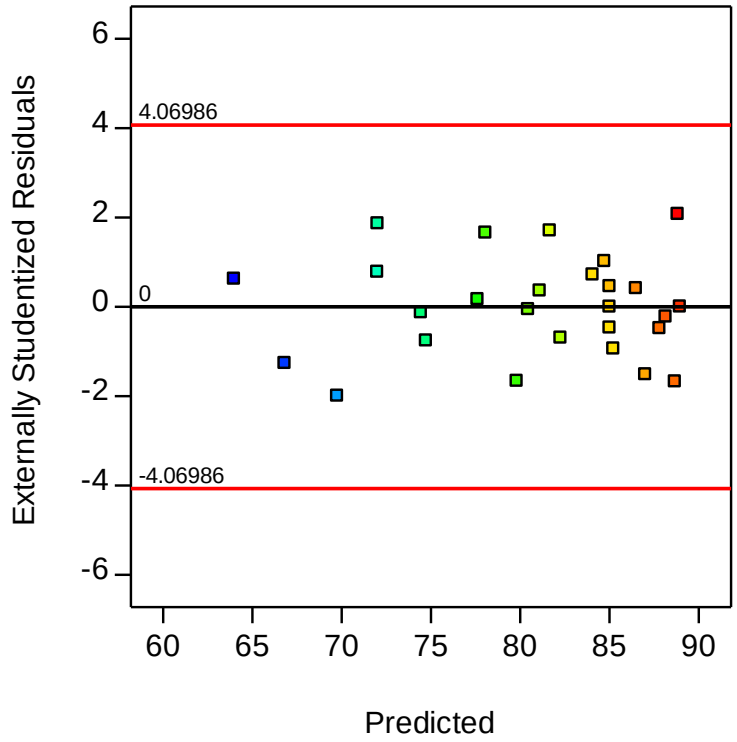

Figure 23 - Residual versus predicted for the FAME content.

5.2.2.3 Parameters effect

The information displayed in the ANOVA table, in Table 20, appoints that the relevant factors are C (molar ratio between methanol and oleic acid) > D (catalyst dosage) ≈ C^2 > A (time) > D^2 >> BC, in order of relevance. As observed for the conversion, the temperature is not a relevant factor in the FAME content. Figures 24 to 29 displays the response surface for variables and their influence on the FAME content along with the interaction plot of the variables.

Table 20 - ANOVA table for the influence of the parameters on the FAME content.

Source	Sum of squares	Df	Mean Square	Calculated F-value	Tabulated F-value	p-value
A-Time	115.38	1	115.38	89.24	4.965	$6.6x10^{-07}$
B-Temperature	2.18	1	2.18	1.69	4.965	0.2181
C-Molar ratio MeOH/OA	750.34	1	750.34	580.34	4.965	$1.6x10^{-11}$
D-Catalyst dosage	192.96	1	192.96	149.24	4.965	$3.9x10^{-08}$
AB	0.0841	1	0.0841	0.0650	4.965	0.8030
AC	2.07	1	2.07	1.60	4.965	0.2294
AD	0.2352	1	0.2352	0.1819	4.965	0.6773
BC	9.61	1	9.61	7.43	4.965	0.0184
BD	0.1681	1	0.1681	0.1300	4.965	0.7247
CD	0.0006	1	0.0006	0.0005	4.965	0.9828
A^2	0.8129	1	0.8129	0.6287	4.965	0.4432
B^2	0.1070	1	0.1070	0.0828	4.965	0.7785
C^2	197.51	1	197.51	152.76	4.965	$3.5x10^{-08}$
D^2	48.78	1	48.78	37.73	4.965	$5.0x10^{-05}$

The response surfaces and the interaction plots allow verifying the conclusions inferred in the ANOVA table. The most relevant variable is the molar ratio, and it is very easy to conclude that by looking at Figure 25, Figure 27 and Figure 29. For any of the mentioned plots, increasing the level of the molar ratio has a strong and clear effect in the response observed. The leas relevant variable is the temperature, and by checking Figure 24, Figure 27 and Figure 28 it is easy to arrive at this conclusion. Changing the level of the temperature does not cause any visible alteration on the FAME content.

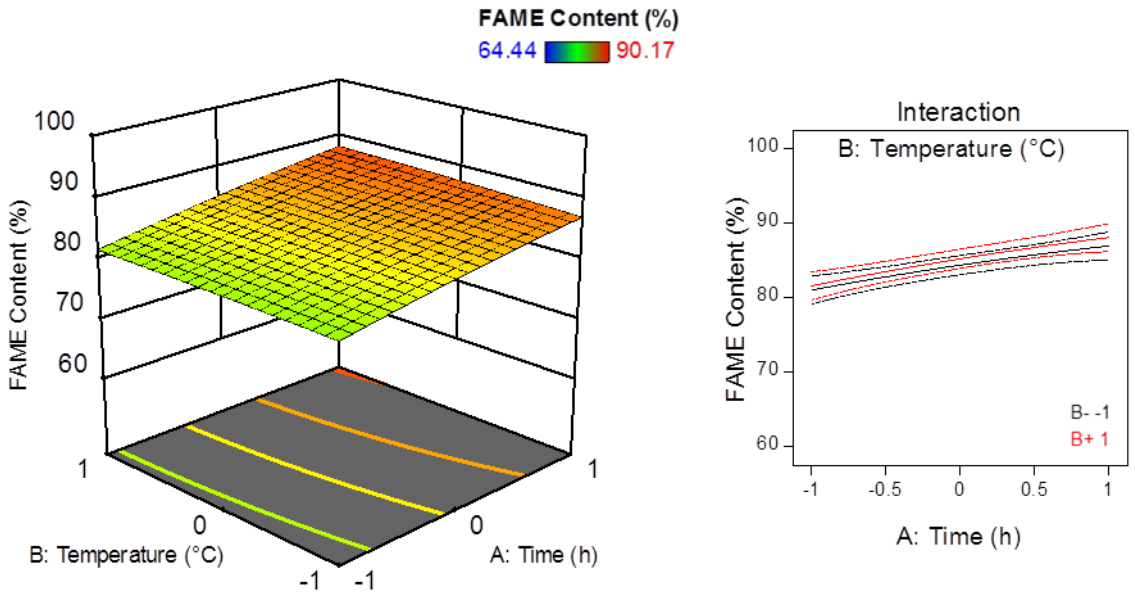

Figure 24 - Response surface regarding the influence of time (A) and temperature (B) on the FAME content and the interaction plot of those variables (C = 0; D = 0).

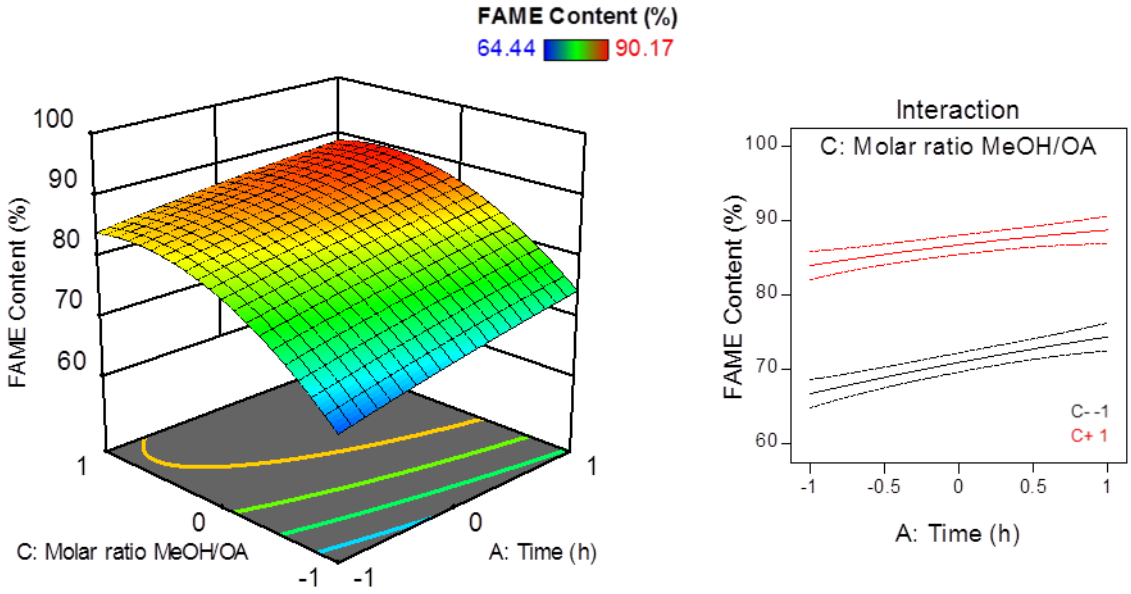

Figure 25 - Response surface regarding the influence of time (A) and molar ratio between methanol and oleic acid (C) on the FAME content and the interaction plot of those variables (B = 0; D = 0).

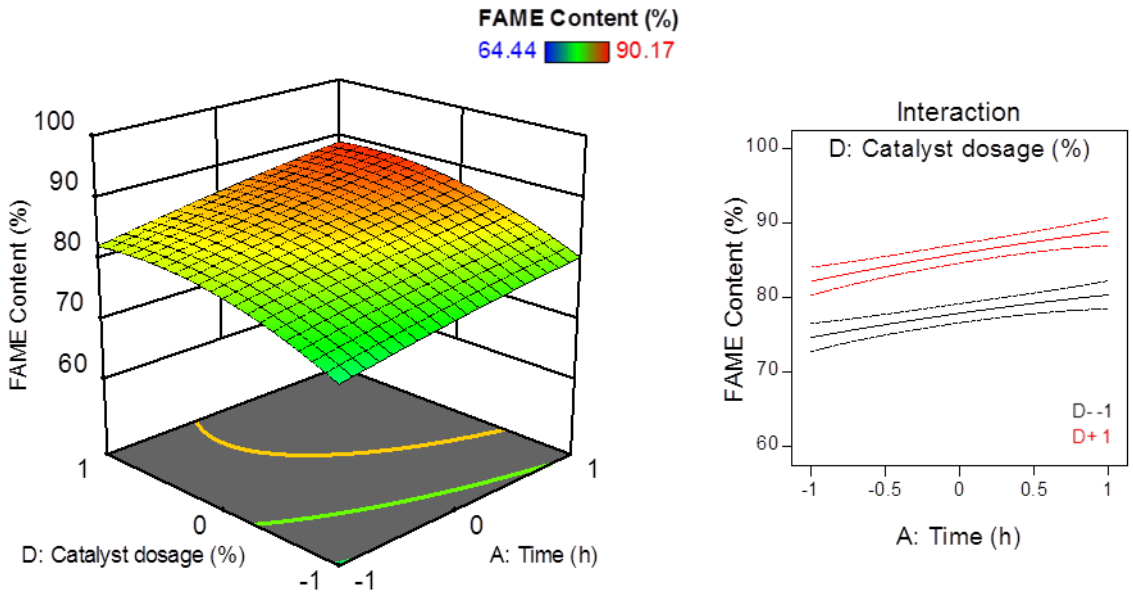

Figure 26 - Response surface regarding the influence of time (A) and catalyst dosage (D) on the FAME content and the interaction plot of those variables (B = 0; C = 0).

Also, the only relevant interaction between factors, according to the ANOVA, is between variables temperature and molar ratio, displayed on Figure 27.

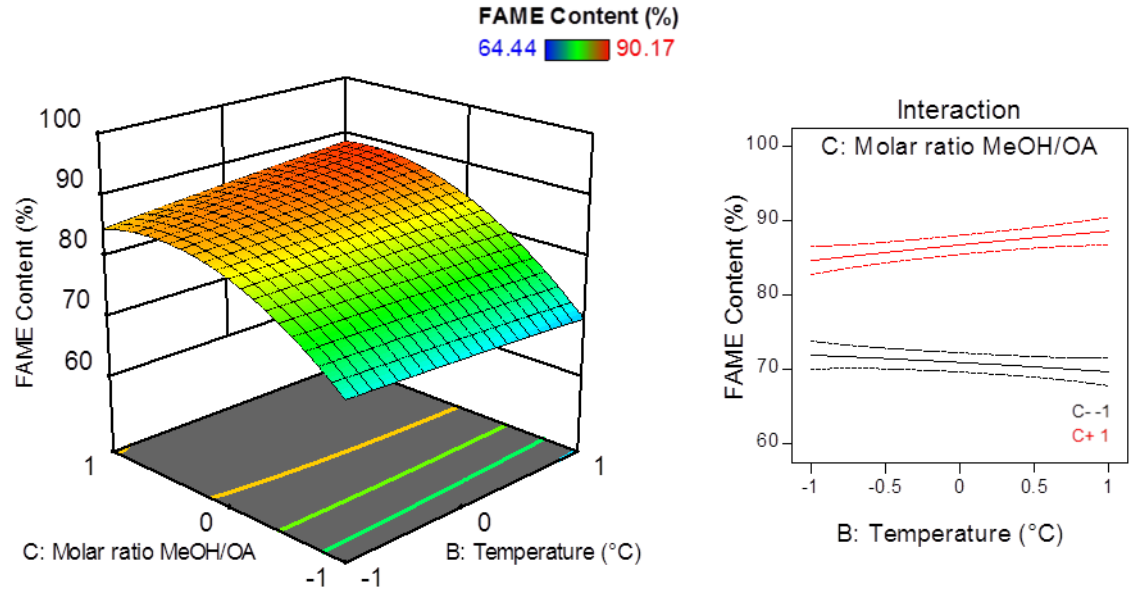

Figure 27 - Response surface regarding the influence of temperature (B) and molar ratio between methanol and oleic acid (C) on the FAME content and the interaction plot of those variables (A = 0; D =0).

The interaction plot displays non-parallel lines, confirming the information given by the ANOVA. The interaction plots for all other interactions display only parallel lines.

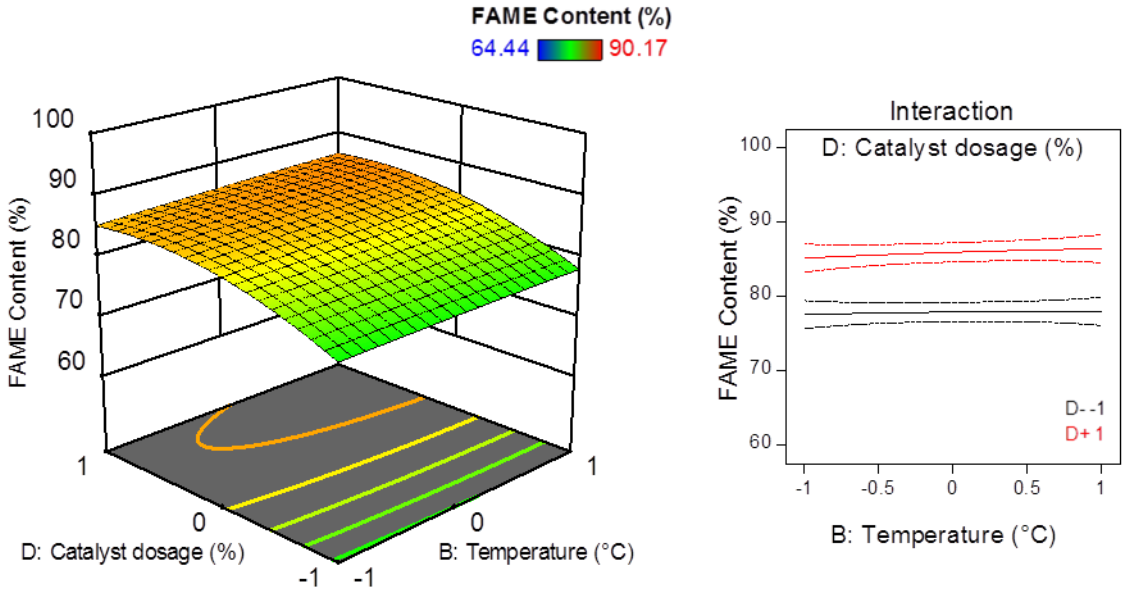

Figure 28 - Response surface regarding the influence of temperature (B) and the catalyst dosage (D) on the FAME content and the interaction plot of those variables (A = 0; C = 0).

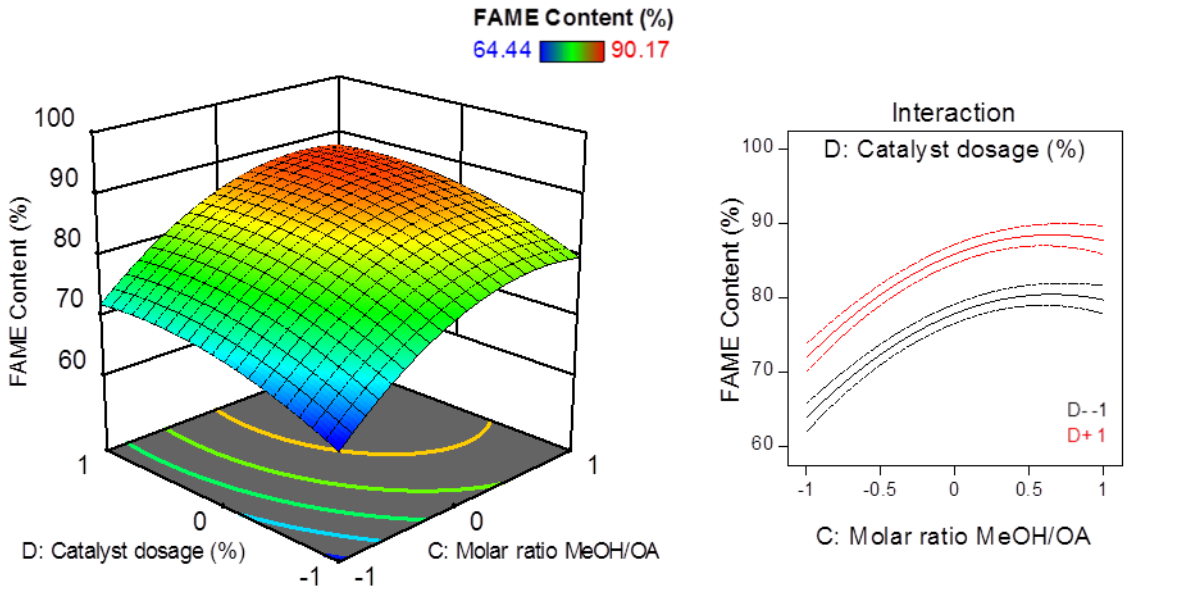

Figure 29 - Response surface regarding the influence of molar ratio between methanol and oleic acid (C) and catalyst dosage (D) on the FAME content and the interaction plot of those variables (A = 0; B = 0).

5.2.2.4 Optimal conditions estimation

Multiple linear regression of the observed data led to coefficients displayed on Table 21. Equation (7) displays the actual form of the model, in coded values.

Table 21 - Coefficients for FAME content.

Coded factor	Coefficient
Intercept	85.01
A	3.10
B	0.4267
C	7.91
D	4.01
A^2	-0.3904
B^2	-0.1417
C^2	-6.09
D^2	-3.02
AB	0.1450
AC	-0.7200
AD	0.2425
BC	1.55
BD	0.2050
CD	-0.0125

$$Y = 85.01 + 3.10\,A + 0.43\,B + 7.91\,C + 4.01\,D - 0.40\,A^2 - 0.14\,B^2 - 6.09\,C^2 - 3.02\,D^2 + 0.145\,AB - 0.72\,AC + 0.24\,AD + 1.55\,BC + 0.21\,BD - 0.0125\,CD \quad (7)$$

Maximizing equation (7) leads to the values displayed in Table 22. Three confirmation runs were performed which are displayed in Figure 30. The average obtained for the three runs is 90.55%. This value is within the range estimated by the model, indicating it is well fitted and accurate (range for FAME content: 89.62 – 96.12%).

Table 22 - Optimal values for FAME content.

Factor	Factor Name	Coded Value	Real Value
A	Time	1.00	8h
B	Temperature	1.00	110°C
C	Molar Ratio MeOH/OA	0.72	13.6:1
D	Catalyst Dosage	0.74	13.5wt%

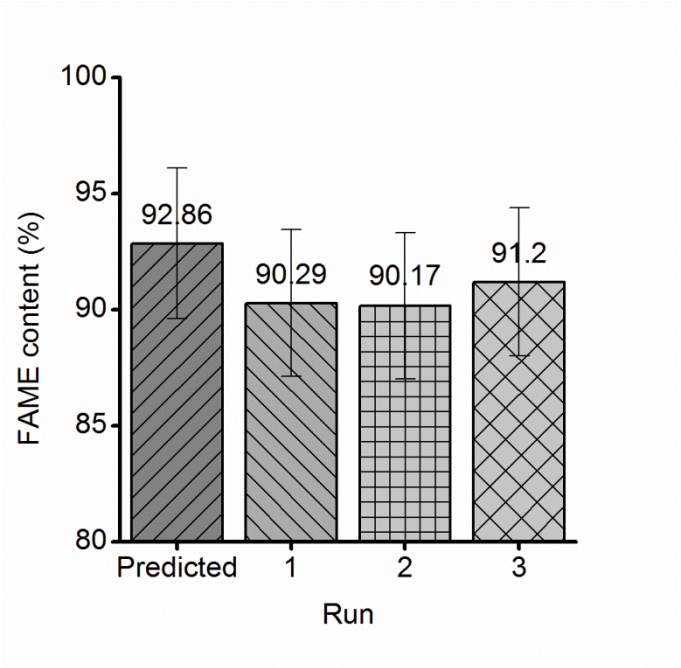

Figure 30 - Predicted value and confirmation runs for the FAME content.

5.2.3 Comparison of results with the literature

Table 23 summarizes the optimal conditions estimated both for the conversion and for the FAME content.

Table 23 - Summary of optimum conditions for conversion and FAME content.

Parameters	Conversion	FAME content	
A – Time (h)	8	8	
B – Temperature (°C)	110	110	Least significant
C – Molar ratio MeOH/OA	15:1	14:1	Most significant
D – Catalyst dosage (wt%)	15	13.5%	
Predicted response (%)	97.96	92.86	
Real response (%)	95.26	90.55	

There are two studies on the literature that apply the same catalyst for biodiesel production. The first is the investigation performed by Xu et al. (2015) [33] regarding the transesterification reaction of castor oil and methanol. The response evaluated was for the FAME content and the optimal conditions were determined as molar ratio of 6:1, 4h reaction time, 77°C and a catalyst dosage 12wt%. The temperature was the most relevant factor, while the time was the least important and it was not

investigated by the response surface methodology. The FAME content under these conditions was 89.82%. They have arrived at a very different conclusion regarding the influence of the temperature on the FAME content. This can be related to the region chosen for the investigation: they studied the influence of the temperature on the range 65 – 85°C. Our study was performed on the range 80 – 110°C. The same can be appointed for the molar ratio: Xu et al. investigated the molar ratio varying from 5:1 – 7:1, and we have studied from 5:1 – 15:1. This difference in the regions chosen leads to a different combination of optimal conditions, and therefore explains the contrasting conclusion.

The second study was an esterification reaction of oleic acid performed by Sun et al. (2015) [37]. The response evaluated was the conversion, and under the optimal conditions (molar ratio 4:1, reaction time 6h and catalyst dosage 3.5 mL) the conversion was 92.5%. The temperature was not mentioned and there is no information regarding on the influence of each factor. There is also no information regarding the regions studied. The results obtained are moreover similar to ours, although the optimal conditions are distinct.

The two most relevant parameters in both responses were the molar ratio and the catalyst dosage. Some authors reached a comparable conclusion. Ding et al.(2018) [38] also concluded that those variables were the most influential for the transesterification reaction of palm oil using [HSO_3-BMIM][HSO_4], although the order of influence was inverse. Zhang et al. (2017) [58] also concluded that the molar ratio is the most important variable in the esterification reaction of oleic acid using [BSMIM]CF_3SO_3.

On the other hand, temperature was the least relevant factor. A similar conclusion was drawn by Jansri et al. (2011) [45] when studying biodiesel production from a high acidic oil using an esterification reaction catalyzed by sulfuric acid as a treatment step followed by a transesterification reaction with sodium hydroxide. They studied the kinetics of both the esterification and the transesterification reaction, and after

testing three different temperatures (55 - 65°C) they concluded that there was no increase in the reaction rate due to temperature and they established that a 60°C was sufficient for biodiesel production in the two-stage process.

5.3 Kinetic study

The esterification reaction of the oleic acid with methanol is an equilibrium reaction that can be described by equation (8). The reaction rate can be described by equation (9), where OA stands for oleic acid, *a* stands for the order related to the oleic acid, MeOH stands for methanol, *b* for the order related to methanol, OAME stands for the oleic acid methyl ester (biodiesel), *c* for the order related to the oleic acid methyl ester (biodiesel) and *d* to the order related to water. k_1 is the reaction rate constant for the direct reaction while k_{-1} is the reaction rate constant for the inverse reaction.

$$C_{18}H_{34}O_2 + CH_3OH \rightleftharpoons C_{19}H_{36}O_2 + H_2O \quad (8)$$

$$-r_{OA} = k_1 {C_{OA}}^a \ {C_{MeOH}}^b - k_{-1} {C_{OAME}}^c \ {C_{H_2O}}^d \quad (9)$$

The reaction rate can be simplified by assuming that the methanol is used in excess in the reaction, therefore supposing that the term ${C_{MeOH}}^b$ is approximately constant during the reaction. Also, since the methanol is in excess, the reaction is shifted towards product formation, and therefore the rate of the direct reaction is much greater than the rate of the inverse reaction in the beginning of the reaction (when approaching the equilibrium, the rate of inverse reaction tends to the rate of the direct reaction). This turns equation (9) into equation (10), where only the concentration of oleic acid is relevant to the rate of reaction.

$$-r_{OA} = \frac{dC_{OA}}{dt} = k'_1 {C_{OA}}^a \quad (10)$$

To determine the order of the reaction in relation to the oleic acid a set of experiments were carried out under the optimum conditions determined by the experimental design: 15 wt% catalyst dosage, 15:1 methanol/oleic acid molar ratio and 8-hour reaction time. Those conditions remained fixed throughout all experiments. The temperature, in its turn, was varied in each experiment: 110, 100, 90, 80 and 70°C. A sample of 1 mL was retrieved from the reaction throughout the reaction, at pre-determined times (0, 15, 30, 60, 90, 120, 180, 240, 300, 360, 420 and 480 min). The acid value of each sample was determined following the EN 14104 [49] and the conversion was estimated by comparing the initial and final acid value, according to equations (1) and (2). It was considered that the initial acid value is the acid value of the point at 0 min.

Figure 31 displays the data obtained from each reaction for the acid value and Figure 32 displays the conversion of oleic acid versus time.

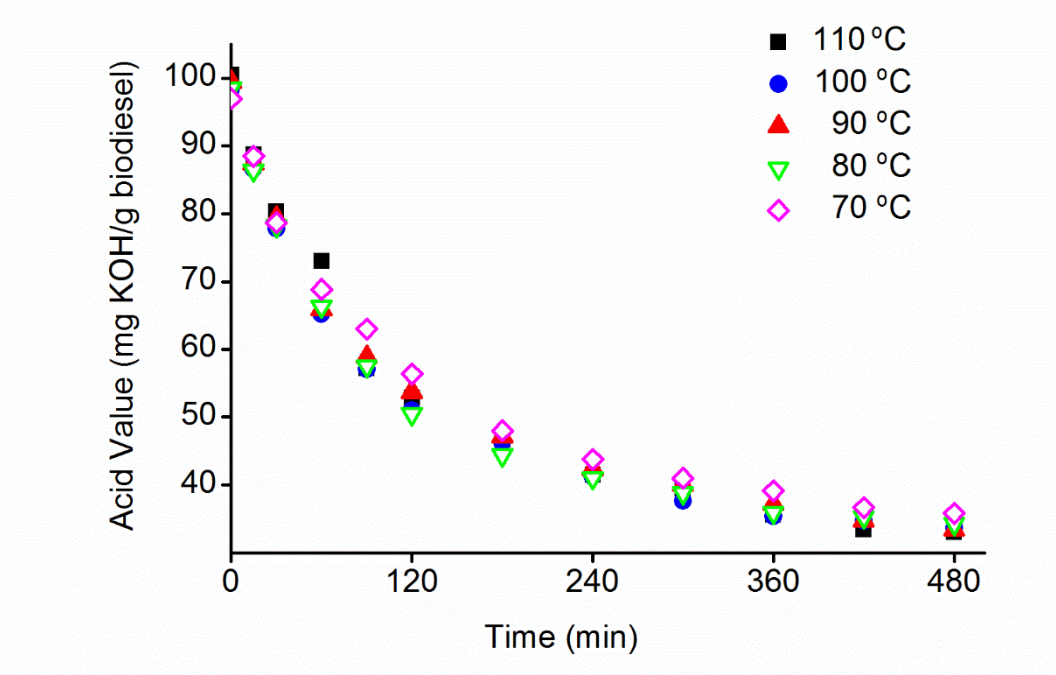

Figure 31 - Acid value versus reaction time for different temperatures.

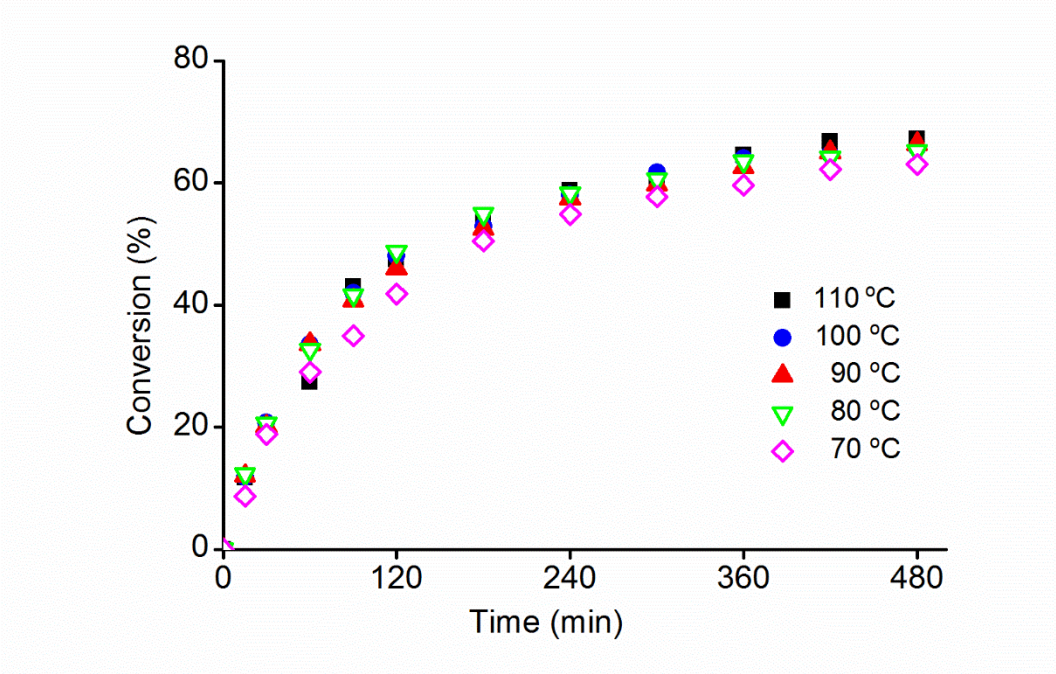

Figure 32 - Conversion versus reaction time for different temperatures.

From this data, it was possible to determine the apparent order of the reaction in relation to the oleic acid. For this purpose, the integral method was applied for the 0th, 1st, 2nd and 3rd order, for all temperatures. Equation (10) was integrated with *a* varying from 0 to 3, giving origin to equations (11) to (14).

0th order $$C_{OA} = C_{OA;0} - k'_1 t \quad (11)$$

1st order $$\ln C_{OA} = \ln C_{OA;0} - k'_1 t \quad (12)$$

2nd order $$\frac{1}{C_{OA}} = \frac{1}{C_{OA;0}} + k'_1 t \quad (13)$$

3rd order $$\frac{1}{{C_{OA}}^2} = \frac{1}{{C_{OA;0}}^2} + 2k'_1 t \quad (14)$$

The data was then plotted for each reaction order, and it was expected that the data would be distributed in a straight line. Then, to determine the order of the reaction, the coefficient of determination (R^2) of each experiment was compared. The order

that resulted in a highest coefficient was understood as the apparent order of the reaction. The coefficients of determination for each temperature and each trial are displayed on Table 24. The highest coefficient was obtained for the 3rd order for all temperatures.

Table 24 - Coefficient of determination obtained applying the integral method for several reaction orders.

	R^2			
Temperature (°C)	0th order	1st order	2nd order	3rd order
110	0.79104	0.89321	0.96452	0.99502
100	0.76587	0.87159	0.94736	0.98604
90	0.77845	0.88433	0.95906	0.99457
80	0.75418	0.85525	0.93169	0.97686
70	0.81139	0.89896	0.95992	0.99089

The integrated form of the reaction rate for a 3rd order reaction is represented by equation (14). It is possible to retrieve a value of k'_1 for each temperature, which is appointed on Table 25.

Table 25 - Kinetic constants for each temperature.

Temperature (°C)	k'_1 (L^2.mol^{-2}.min^{-1})
110	0.00914
100	0.00829
90	0.00805
80	0.00760
70	0.00700

The kinetics constant k'_1 is related to the temperature by the Arrhenius equation and it is given in the form of equation (15).

$$k'_1 = k_0 exp^{\frac{-Ea}{RT}} \quad (15)$$

Where k'_1 is the kinetics constant at a determined temperature, k_0 is the pre-exponential factor, *Ea* is the activation energy, in kJ/mol, *R* is the gas constant, in kJ/mol.K, and *T* is the temperature, in K. The Arrhenius equation establishes that at a given temperature *T,* the fraction of collisions between molecules with the minimum

required energy *Ea* is proportional to $e^{-Ea/RT}$ and therefore, the rate constant is also proportional to that same factor [39]. The Arrhenius equation can be linearized by applying the natural logarithm in both sides of equation (15), leading to equation (16).

$$\ln k'_1 = \ln k_0 - \frac{Ea}{RT} \tag{16}$$

Therefore, by plotting the inverse of the temperature, in K, and the natural logarithm of the kinetics constant at each temperature, it is possible to estimate the activation energy for the reaction. The Arrhenius plot is displayed on Figure 33. A coefficient of determination of R^2=0.9181 was obtained. The pre-exponential factor (k_0) was estimated as 0.0765 $L^2.mol^{-2}.min^{-1}$ and the activation energy (E_a) as 6.8 kJ/mol. The low activation energy indicates a certain independency to the temperature. As mentioned earlier, reactions with small activation energies have rates that only increase slightly with the temperature. This result agrees with the conclusion achieved through the RSM for the conversion that the temperature is not statistically relevant.

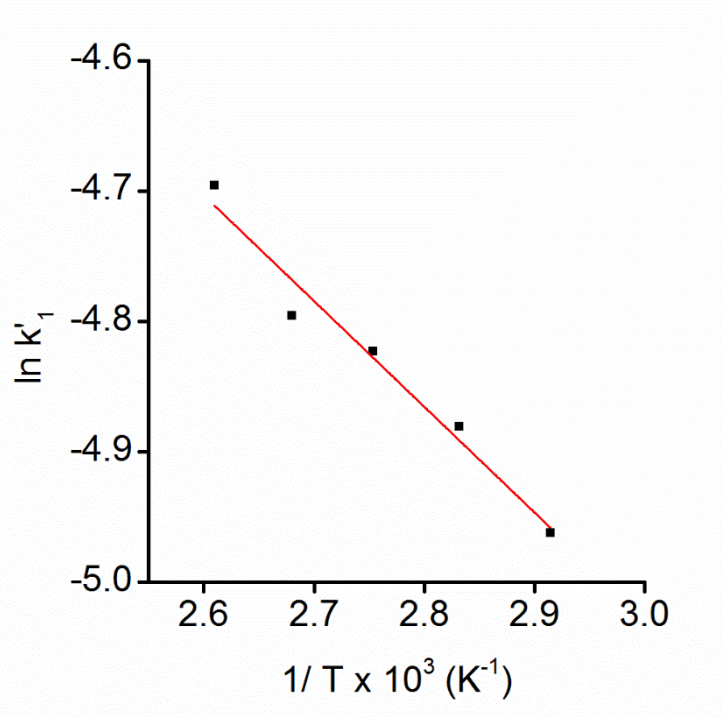

Figure 33 - Arrhenius plot for the experimental data.

Aranda et al. (2008) [44] arrived at similar results for the activation energy. They studied the esterification reaction applying sulfuric acid and methanesulfonic acid and arrived at the activation energies of 6.53 kJ/mol and 3.78 kJ/mol, respectively. Even though the values are very similar to the ones observed in our study, the ionic liquid presents the advantage of being environmentally friendly and also safer in terms of handling. Other authors reported activation energies for the esterification using sulfuric acid that are higher than the one observed in this paper [42,43,45].

Activation energies for the esterification reaction using various ionic liquids as catalysts were also reported. Fauzi et al. (2014) [41] reported a value of 17.97 kJ/mol for the ionic liquid *1-butyl-3-methylimidazolium tetrachloroferrite*. Ullah et al. (2017) [46] obtained a value of 19.24 kJ/mol for the ionic liquid *3-methyl-1-(4-sulfobutyl)-benzimidazolium trifluoromethanesulfonate*. Both reported values are higher than the one observed in this study, reinforcing the suitability of the ionic liquid *1-methylimidazolium hydrogen sulfate* as catalyst for the esterification reaction of FFAs.

5.4 Transesterification study

A set of experiments was done in order to evaluate the ionic liquid as a suitable catalyst for promoting the transesterification reaction of triglycerides as well. As the purpose of the current work is to replace conventional catalysts by alternatives that could be applied to low quality feedstock, the available oil sample was replaced by a mixture of oil and oleic acid, which was varied in different mass proportions. The FAME content was evaluated for each sample. The reaction was carried out under the optimum conditions determined for the conversion of oleic acid: 8h, 110°C and 15wt% catalyst dosage. The mole ratio of methanol was increased to 20:1 and it was calculated assuming that the total mass for each run was of triolein.

Table 26 presents the conditions for each run and the FAME content obtained and Figure 34 shows the observed relationship between the amount, in relation to the total mass, of oleic acid added to the mixture and the obtained FAME content. The

results indicate that probably only the FFAs present in the oleic acid were synthesized to esters, which means that the catalyst was only able to promote the esterification reaction. Moreover, more investigation should be done in order to evaluate if this apparent conclusion really applies. Anyhow, the ionic liquid seems suitable to be used as treatment step for acidic oils.

Table 26 - Conditions and FAME content for transesterification reactions.

Run	Ionic liquid mass (g)	Oil mass (g)	Oleic Acid mass (g)	Oleic acid (wt%)	Total mass (g)	Methanol volume (mL)	Temp. (°C)	Time (h)	FAME content (%)
T1	3.0050	4.0229	16.0911	80%	20.1140	18.5	110	8	71.36
T2	3.0929	8.0110	12.0716	60%	20.0826	18.5	110	8	53.26
T3.1	3.0014	10.0048	10.0084	50%	20.0132	18.5	110	8	45.69
T3.2	3.0103	10.0084	10.2600	51%	20.2684	18.5	110	8	44.71
T4	3.0557	12.0164	8.0026	40%	20.0190	18.5	110	8	37.93
T5	3.0138	15.9998	4.0199	20%	20.0197	18.5	110	8	19.89

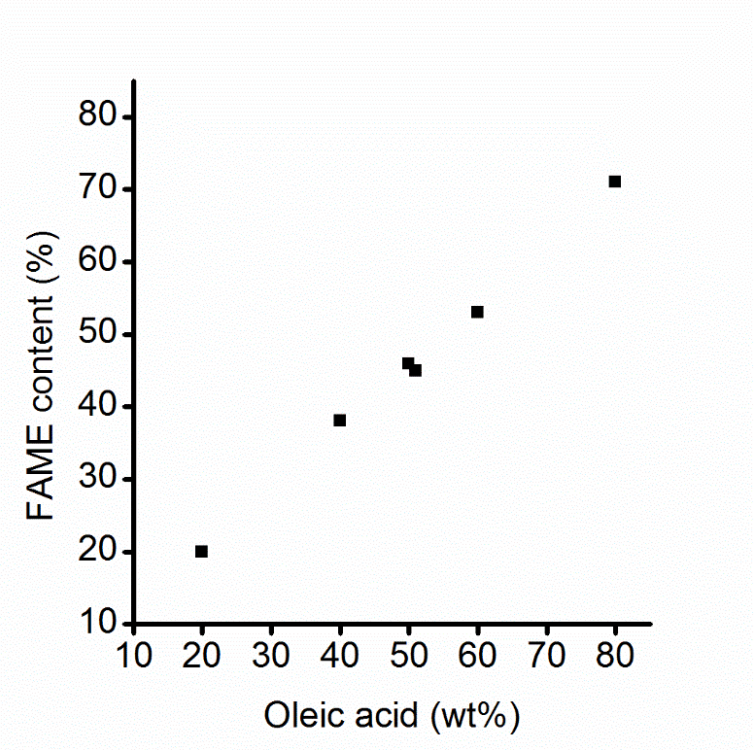

Figure 34 - Relationship between the amount of oleic acid added and FAME content.

5.5 FT-IR analysis

FT-IR was used to characterize several samples, including the starting materials and the products. FT-IR helps to understand if the reaction is actually accomplishing the objective of converting the FFAs into FAMEs. Figure 35 displays the oleic acid sample. The broad band from 3300 to 2500 cm^{-1} and centered at 3000 cm^{-1} is a characteristic absorption attributed to acidic and strongly bounded hydrogen, such as those of carboxylic acids. The bands at 2650 and 2550 cm^{-1} are also in this overtone region and are a characteristic pattern for a COOH group. The bands at 2924 and 2855 cm^{-1} that overlap with the broad band corresponding to the O-H bond are associated with the asymmetric and symmetric stretching of aliphatic C-H bonds, respectively. The most strong and sharp that is visible at 1705 cm^{-1} is ascribed to the C=O stretching of a dimer in the carboxylic acid, such as the oleic acid. The band at 1458 cm^{-1} is associated with the asymmetrical CH_3 deformation and the band at 1410 cm^{-1} is related to the CH_2 bend. The multiple weak bands at 1288 and 1242 cm^{-1} are related to wagging vibrations from CH_2 in normal hydrocarbon chains. Both 1288 cm^{-1} and 1242 cm^{-1} bands are related with the stretch and bend in the COOH group. They result from combination of O-C-O asymmetric stretch and OH bend. The band at 933 cm^{-1} is characteristic of the dimeric oleic acid and results from an angular deformation outside the plan of O-H bond. The band at 725 cm^{-1} is ascribed to the concerted rocking of all CH_2 groups in the chain of four or more carbons [59,60].

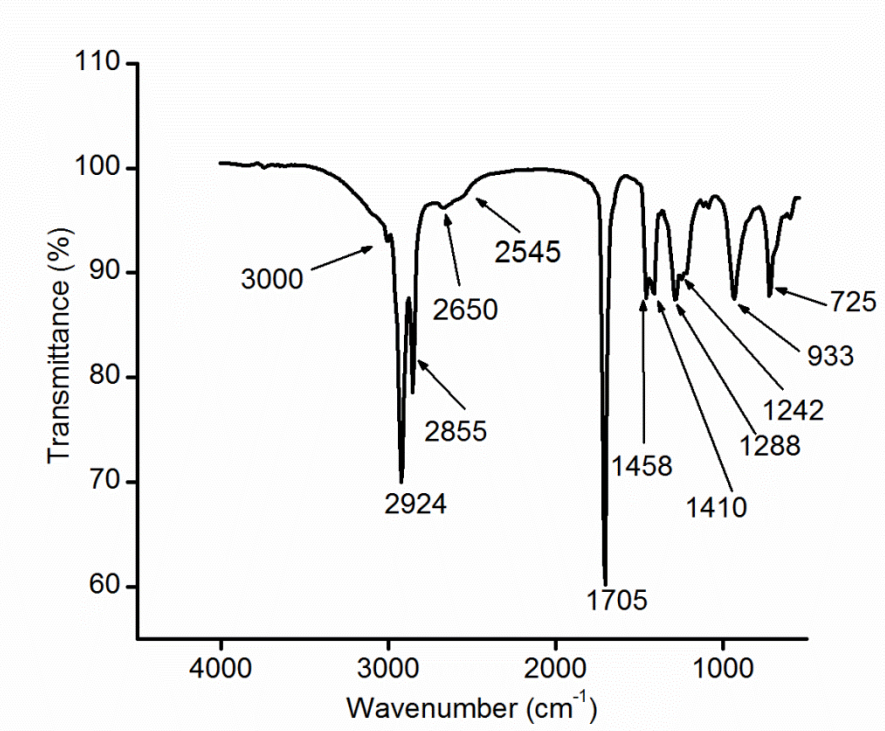

Figure 35 - FT-IR spectrum of oleic acid ($CH_3(CH_2)_7CH=CH(CH_2)_7COOH$).

The FT-IR spectrum of the biodiesel sample was very similar to the spectrum of the oleic acid, as displayed on Figure 36. The biodiesel sample analyzed was obtained through esterification under the optimum conditions (8h, 110°C, 15:1 mole ratio, 15wt% catalyst dosage). The bands at 2924 and 2855 cm^{-1} are also associated with the asymmetric and symmetric stretching of aliphatic C-H bonds, respectively. The bands at 1458 and 1373 cm^{-1} are related to the CH_3 asymmetric and symmetric deformation, respectively, in methyl groups close to the carbonyl group. The band at 717 cm^{-1} is associated with the rocking motion of four or more CH_2 groups in an open chain [60]. The differences are related to the disappearance of the broad band centered at 3000 cm^{-1} and the shifting in the absorption of the C=O bond, now at 1744 cm^{-1}, which is a characteristic absorption of the C=O bond in esters. Also, two or more bands related to the C-O stretching vibration are present in the spectrum, in the region from 1300 – 1000 cm^{-1}. The C-O stretch that is attached to the carbonyl group appears in the region 1300 to 1150 cm^{-1} while the other band, that is usually weaker than the first, appears in the region 1150 – 1000 cm^{-1} [60]. Therefore, the

bands at 1172 cm^{-1} and 1018 cm^{-1} are ascribed to the absorption of the C-O stretching. Those differences appointed are a confirmation that the FFAs were successfully converted into FAMEs.

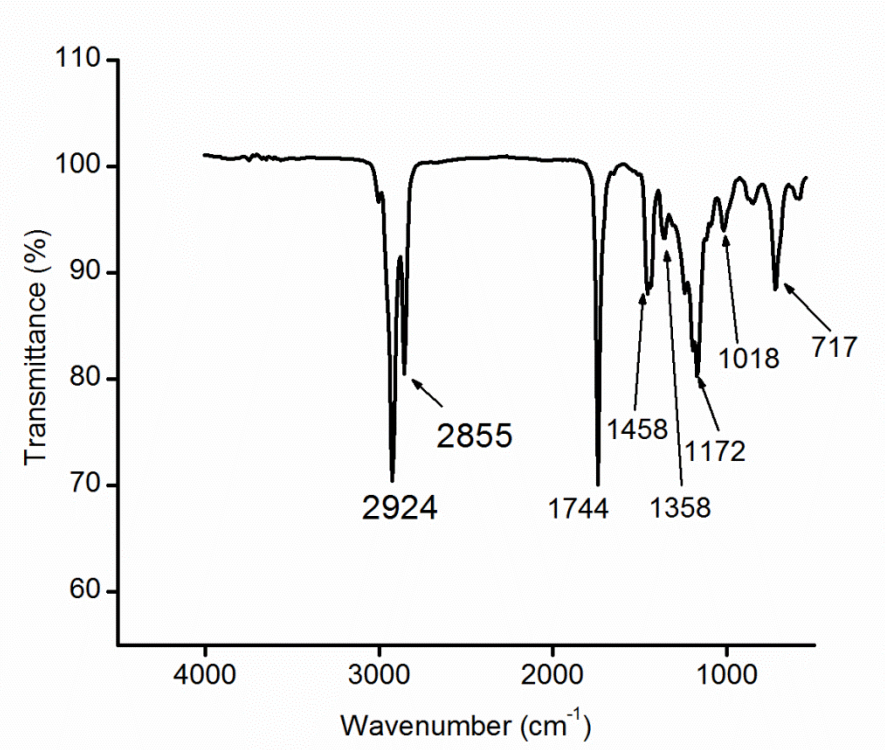

Figure 36 - FT-IR spectrum of biodiesel (FAMEs) sample ($CH_3(CH_3)_nCOOCH_3$).

The same analysis was done to verify the structure of the methanol, the ionic liquid and the waste oil. Figure 37 displays the FT-IR for the methanol. The most characteristics IR absorption bands for alcohols are in the range of 3650 – 3200 cm^{-1}, related to the stretching vibration of the -OH and the region from 1260 – 970 cm^{-1}, associated to the stretching vibration of the CO bond [61]. Therefore, the broad band centered at 3325 cm^{-1} is ascribed to the OH stretching and the sharp and strong band at 1026 cm^{-1} to the C-O bond. The bands at 2985, 2947, 2893 and 2831 cm^{-1} are related to aliphatic CH stretching. The band at 1450 cm^{-1} is related to the symmetric CH_3 umbrella deformation, which is overlapped by the out of plane C-OH deformation at 1396 cm^{-1}. The out-of-plane C-OH deformation gives rises to a second broad band, which is identified as the one at 655 cm^{-1}.

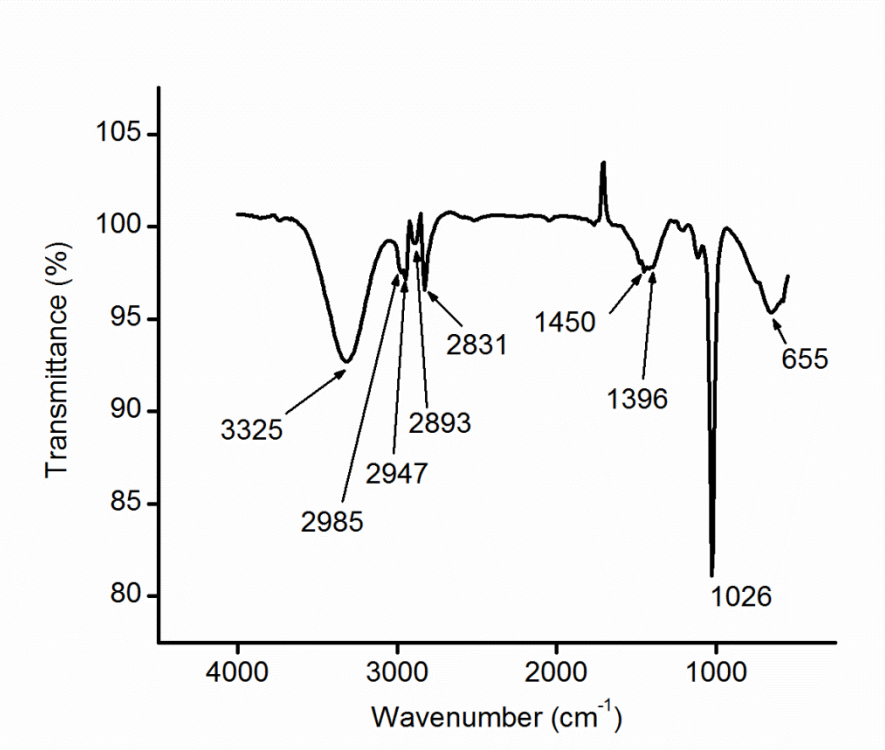

Figure 37 - FT-IR spectrum of methanol (CH_3OH).

Figure 38 presents the FT-IR obtained for the ionic liquid, which structure is displayed in Figure 12. Heterocyclic compounds with two double bonds in a five-membered ring usually show three ring vibrations near 1590, 1490 and 1400 cm^{-1}. The CH stretch for heteroaromatic rings containing nitrogen falls in the region 3180 – 3090 cm^{-1} [59]. Therefore, the bonds at 1590, 1550 and 1450 cm^{-1} are related to the ring in the imidazolium cation while the band at 3140 cm^{-1} can be ascribed to the stretching vibration of the CH bonds in the cation. Also, most of five-membered rings containing a CH=CH unsubstituted group have strong hydrogen wag absorption in the region 900 – 700 cm^{-1} [59], and therefore the bands at 840 and 756 cm^{-1} can be associated with this vibration. The band at 2970 cm^{-1} is attributed to the out-of-phase CH_3 stretch and the band at 2877 cm^{-1} to the in-phase CH_3 stretch [59]. The group HSO_4^{-1} has two absorption bands: one from 1190 – 1160 cm^{-1} related to the asymmetric SO_3^{-1} stretch and at 1080 – 1015 cm^{-1} related to the symmetric SO_3^{-1} stretch [59], consequently bands 1158 and 1018 cm^{-1} can be ascribed to the anion.

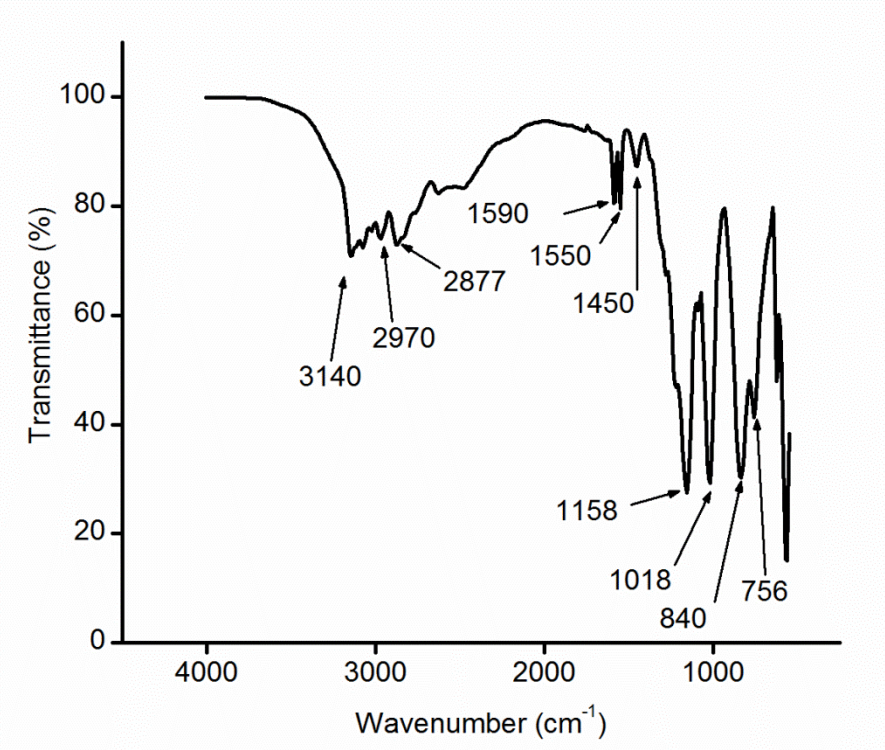

Figure 38 - FT-IR spectrum of ionic liquid.

Figure 39 displays the FT-IR for the waste cooking oil. The oil is mainly composed by triglycerides, which are esters. The characteristics absorptions of ester are a strong absorption near 1740 cm $^{-1}$ associated to the C=O stretching and the strong band near 1200 cm^{-1} related to the asymmetric stretching of C-O bond [61]. Thus, the strong and sharp bond at 1745 cm^{-1} is ascribed to the C=O bond and the band at 1157 cm^{-1} is attributed to the C-O bond. The bands at 2924 and 2855 cm^{-1} are again ascribed to the stretching of aliphatic C-H bonds. The bands at 1458 and 1373 cm^{-1} are related to the CH_3 asymmetric and symmetric deformation, respectively, in methyl groups close to the carbonyl group. The band at 972 cm^{-1} is attributed to the wag vibration of the CH_2. The band at 718 cm^{-1} is ascribed to the concerted rocking vibration of four or more CH_2 groups in an open chain.

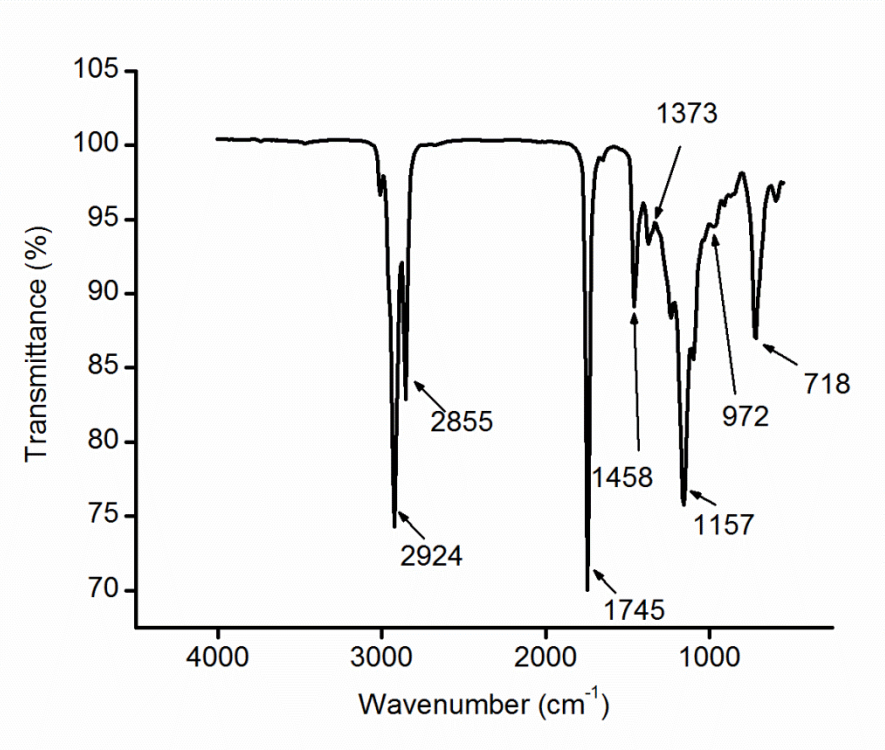

Figure 39 - FT-IR spectrum of the waste oil.

6. CONCLUSIONS

Ionic liquids as catalysts for biodiesel production seem like a viable alternative to common acidic catalysts. From the 5 tested ionic liquids, 3 displayed good catalytic activity and resulted in a conversion higher than 77%. The chosen ionic liquid, *1-methylimidazolium hydrogen sulfate* resulted in the highest conversion in the screening step of this work. The experimental design applied allowed to understand how each factor (time, temperature, molar ratio between methanol and oleic acid and catalyst dosage) influences both the conversion of the oleic acid and the FAME content of the obtained biodiesel samples when *[HMIM][HSO_4]* was used as catalyst.

The most relevant factors were the molar ratio between oleic acid and methanol and the catalyst dosage, for both responses (conversion of oleic acid and FAME content). It was possible to set the optimum conditions that lead to the highest possible conversion and highest possible FAME content. The optimal condition for the conversion was estimated as 8h, 110°C, 15:1 molar ratio and 15wt% catalyst dosage, leading to a conversion of 95%. The optimum condition, that lead to a 90% FAME content, was estimated as 8h, 110°C, 14:1 molar ratio and 13.5wt% catalyst dosage. These results indicate that this catalyst has a high potential in biodiesel production: not only it achieved high conversions of the reactant, but it also lead to a product with a high content of fatty acid methyl esters.

The preliminary transesterification experiments indicated that the catalyst is not very suitable for the transesterification reaction. A very low FAME content was obtained for the transesterification experiments and a more comprehensive study is required for more adequate conclusions.

The kinetic study allowed to estimate the activation energy of the esterification reaction catalyzed by the ionic liquid *1-methylimidazolium hydrogen sulfate*, achieving a very low value of 6.8 kJ/mol. Low activation energy is beneficial, as it means that the reaction requires small energy in order to occur, which leads to a cheaper process. This low activation energy also helped reinforcing a conclusion

drawn based on the experimental design: that the temperature is not a very important parameter for the studied system. The experimental design indicated that the change in temperature does not affects significantly the reaction and low activation energy is an indication that with the change in temperature, the rate constant does not vary greatly, and therefore the reaction rate does not change greatly as well.

In conclusion, the use of ionic liquids as catalyst in biodiesel production presents several advantages. The catalyst chosen for this study led to very good results, putting it as a suitable replacement for the traditional catalysts. The experimental design allied to the kinetic study indicated that the catalyst permits a reaction that does not require high temperature, meaning a more economic process.

7. SUGGESTIONS FOR FUTURE WORK

Some studies are still necessary in order to fully evaluate the suitability of the ionic liquid *1-methylimidazolium hydrogen sulfate* for biodiesel production. The suggestions for future work are:

- A multi-objective optimization of both responses (conversion and FAME content) to determine the optimum condition that would lead simultaneously to the highest conversion and FAME content.
- A wider study comprehending the use of the ionic liquid *1-methylimidazolium hydrogen sulfate* as a possible catalyst for simultaneously promoting the esterification reaction of FFAs and the transesterification reaction of triglycerides for low quality feedstock.
- Test of the ionic liquid as a treatment step for low quality oils, by previous esterification of FFAs, followed by a transesterification reaction with a classical alkali catalyst.
- A more complete study of the kinetics of the esterification reaction, by varying the proportions between methanol and oleic acid and the amount of ionic liquid;
- A recovery study for the ionic liquid *[HMIM][HSO_4],* in order to assess the number of reaction cycles in which high conversions and high FAME content could be attained.
- A more extensive study using the other ionic liquids (*1-methylimidazolium hydrogen sulfate* and *1-methylimidazolium methyl sulfate)* that displayed adequate results to determine their applicability in biodiesel production.
- Phase equilibrium study for the mixture methanol-water-biodiesel-oleic acid.

REFERENCES

[1] Talebian-Kiakalaieh A, Amin NAS. Single and Two-Step Homogeneous Catalyzed Transesterification of Waste Cooking Oil: Optimization by Response Surface Methodology. International Journal of Green Energy 2015;12:888–99.

[2] Lotero E, Liu Y, Lopez DE, Suwannakarn K, Bruce DA, Goodwin JG. Synthesis of Biodiesel via Acid Catalysis. Industrial & Engineering Chemistry Research 2005;44:5353–63.

[3] International Energy Agency. WORLD ENERGY BALANCES: AN OVERVIEW. 2017.

[4] U.S. Energy Information Administration. International Energy Outlook 2016: Transportation sector energy consumption by fuel. 2016.

[5] Demirbas A. Importance of biodiesel as transportation fuel. Energy Policy 2007;35:4661–70.

[6] Avinash A, Subramaniam D, Murugesan A. Bio-diesel—A global scenario. Renewable and Sustainable Energy Reviews 2014;29:517–27.

[7] Atabani AE, Silitonga AS, Badruddin IA, Mahlia TMI, Masjuki HH, Mekhilef S. A comprehensive review on biodiesel as an alternative energy resource and its characteristics. Renewable and Sustainable Energy Reviews 2012;16:2070–93.

[8] Fukuda H, Kond A, Noda H. Biodiesel Fuel Production by Transesterification of Oils. Journal of Bioscience and Bioengineering 2001;92:405–16.

[9] Nurfitri I, Maniam GP, Hindryawati N, Yusoff MM, Ganesan S. Potential of feedstock and catalysts from waste in biodiesel preparation: A review. Energy Conversion Management 2013;74:395–402.

[10] Demirbas A. Biodiesel. London: Springer London; 2008.

[11] Verma P, Sharma MP. Review of process parameters for biodiesel production from different feedstocks. Renewable and Sustainable Energy Reviews 2016;62:1063–71.

[12] Ambat I, Srivastava V, Sillanpää M. Recent advancement in biodiesel production methodologies using various feedstock: A review. Renewable and Sustainable Energy Reviews 2018;90:356–69.

[13] Devi BLAP, Reddy TVK, Yusoff MFM. Chapter 12 - Ionic Liquids in the Production of Biodiesel and Other Oleochemicals. Ionic Liquids in Lipid Processing and Analysis, Elsevier; 2016, p. 373–401.

[14] Sun Y, Cooke P, Reddy HK, Muppaneni T, Wang J, Zeng Z, et al. 1-Butyl-3-methylimidazolium hydrogen sulfate catalyzed in-situ transesterification of Nannochloropsis to fatty acid methyl esters. Energy Conversion Management 2017;132:213–20.

[15] Knothe G, Razon LF. Biodiesel fuels. Progress in Energy and Combustion Science 2017;58:36–59.

[16] Fang Z. Biodiesel - Feedstocks, Production and Applications. InTech; 2012.

[17] Andreani L, Rocha JD. Use of Ionic Liquids in Biodiesel Production: a review. Brazilian Journal of Chemical Engineering 2012;29:1–13.

[18] Smith MB, March J. March's advanced organic chemistry: reactions, mechanisms, and structure. 6th ed. Hoboken, NJ, USA: John Wiley & Sons, Inc.; 2007.

[19] Zeng Z, Cui L, Xue W, Chen J, Che Y. Chapter 12 - Recent Developments on the Mechanism and Kinetics of Esterification Reaction Promoted by Various Catalysts. In: Patel V, editor. Chemical Kinetics, InTech; 2012, p. 255–82.

[20] Leung DYC, Wu X, Leung M. A review on biodiesel production using catalyzed transesterification. Applied Energy 2010;87:1083–95.

[21] Ishak ZI, Sairi NA, Alias Y, Aroua MKT, Yusoff R. A review of ionic liquids as catalysts for transesterification reactions of biodiesel and glycerol carbonate production. Catalysis Reviews 2017;59:44–93.

[22] Ramos LP, Silva FR da, Mangrich AS, Cordeiro CS. Tecnologias de Produção de Biodiesel. Revista Virtual de Química 2011;3:385–405.

[23] Coman SM, Parvulescu VI. Chapter 4 - Heterogeneous Catalysis for Biodiesel Production. The Role of Catalysis for the Sustainable Production of Bio-fuels Bio-chemicals, Elsevier; 2013, p. 93–136.

[24] Muhammad N, Elsheikh YA, Mutalib MIA, Bazmi AA, Khan RA, Khan H, et al. An overview of the role of ionic liquids in biodiesel reactions. Journal of Industrial and Engineering Chemistry 2015;21:1–10.

[25] Helwani Z, Othman MR, Aziz N, Fernando WJN, Kim J. Technologies for production of biodiesel focusing on green catalytic techniques: A review. Fuel Processing Technology 2009;90:1502–14.

[26] Troter DZ, Todorović ZB, Đokić-Stojanović DR, Stamenković OS, Veljković VB. Application of ionic liquids and deep eutectic solvents in biodiesel production: A review. Renewable and Sustainable Energy Reviews 2016;61:473–500.

[27] Han BY, Zhang W Di, Chen YB, Yin F, Liu SQ, Zhao XL. A Review on Biodiesel Synthesis Using Catalyzed Transesterification Base Ionic Liquids as Catalyst. Advanced Materials Research 2013;772:303–8.

[28] Amarasekara AS. Acidic Ionic Liquids. Chemical Reviews 2016;116:6133–83.

[29] Hajipour AR, Rafiee F. Basic Ionic Liquids. A Short Review. Journal of the Iranian Chemical Society 2009;6:647–78.

[30] Mai NL, Ahn K, Koo Y-M. Methods for recovery of ionic liquids—A review. Process Biochemistry 2014;49:872–81.

[31] Elsheikh YA, Man Z, Bustam MA, Yusup S, Wilfred CD. Brønsted imidazolium ionic liquids: Synthesis and comparison of their catalytic activities as pre-catalyst for biodiesel production through two stage process. Energy Conversion Management 2011;52:804–9.

[32] Li Y, Hu S, Cheng J, Lou W. Acidic ionic liquid-catalyzed esterification of oleic acid for biodiesel synthesis. Chinese Journal of Catalysis 2014;35:396–406.

[33] Xu W, Ge X, Yan X, Shao R. Optimization of methyl ricinoleate synthesis with

ionic liquids as catalysts using the response surface methodology. Chemical Engineering Journal 2015;275:63–70.

[34] Fauzi AHM, Amin NAS. Optimization of oleic acid esterification catalyzed by ionic liquid for green biodiesel synthesis. Energy Conversion Management 2013;76:818–27.

[35] Liu S, Wang Z, Yu S, Xie C. Transesterification of waste oil to biodiesel using Brønsted acid ionic liquid as catalyst. Bulletin of the Chemical Society of Ethiopia 2013;27:289–94.

[36] Ullah Z, Bustam MA, Man Z. Biodiesel production from waste cooking oil by acidic ionic liquid as a catalyst. Renewable Energy 2015;77:521–6.

[37] Sun Y, Liang L, Ren T, Qiao Q, Liu Q. Synthesis of methyl oleate catalyzed by acidic ionic liquid [Hmim]HSO4. Zhongguo Youzhi 2015;40:68–71.

[38] Ding H, Ye W, Wang Y, Wang X, Li L, Liu D, et al. Process intensification of transesterification for biodiesel production from palm oil: Microwave irradiation on transesterification reaction catalyzed by acidic imidazolium ionic liquids. Energy 2018;144:957–67.

[39] Atkins PW, Jones L. Chemistry: molecules, matter, and change. 3rd ed. New York: W.H. Freemand and Company; 1997.

[40] Morrison RT, Boyd RN. Química Orgânica. 6th ed. Lisboa: Fundaçäo Calouste Gulbekian; 1992.

[41] Fauzi AHM, Amin NAS, Mat R. Esterification of oleic acid to biodiesel using magnetic ionic liquid: Multi-objective optimization and kinetic study. Applied Energy 2014;114:809–18.

[42] Kostić MD, Veličković A V., Joković NM, Stamenković OS, Veljković VB. Optimization and kinetic modeling of esterification of the oil obtained from waste plum stones as a pretreatment step in biodiesel production. Waste Management 2016;48:619–29.

[43] Neumann K, Werth K, Martín A, Górak A. Biodiesel production from waste cooking oils through esterification: Catalyst screening, chemical equilibrium and reaction kinetics. Chemical Engineering Research and Design 2016;107:52–62.

[44] Aranda DAG, Santos RTP, Tapanes NCO, Ramos ALD, Antunes OAC. Acid-Catalyzed Homogeneous Esterification Reaction for Biodiesel Production from Palm Fatty Acids. Catalysis Letters 2008;122:20–5.

[45] Jansri S, Ratanawilai SB, Allen ML, Prateepchaikul G. Kinetics of methyl ester production from mixed crude palm oil by using acid-alkali catalyst. Fuel Processing Technology 2011;92:1543–8.

[46] Ullah Z, Bustam MA, Man Z, Khan AS, Muhammad N, Sarwono A. Preparation and kinetics study of biodiesel production from waste cooking oil using new functionalized ionic liquids as catalysts. Renewable Energy 2017;114:755–65.

[47] National Institute of Standards and Technology. NIST Chemistry WebBook, NIST Standard Reference Database. Gaithersburg MD: 2018.

[48] The Merck Index: An Encyclopedia of Chemicals, Drugs, and Biologicals, 14th ed. Edited by Maryadele J. O'Neil (Editor), Patricia E. Heckelman (Senior Associate Editor), Cherie B. Koch (Associate Editor), and Kristin J. Roman (Assistant Editor). Merck and. vol. 129. American Chemical Society; 2006.

[49] European Commitee for Standardization. EN 14104: Fat and oil derivatives - Fatty Acid Methyl Esters (FAME) - Determination of acid value 2003;3:1–14.

[50] European Committee for Standardization. EN-14103: Fat and oil derivatives - Fatty Acid Methyl Esters (FAME) - Determination of ester and linolenic acid methyl ester contents 2003:1–11.

[51] David F, Sandra P, Vickers AK. Column Selection for the Analysis of Fatty Acid Methyl Esters. 2005.

[52] Box GEP, Behnken DW. Some New Three Level Designs for the Study of Quantitative Variables. Technometrics 1960;2:455–75.

[53] Alimova I. Production of biodiesel through esterification catalysed by Ionic liquids. Master thesis, 66p, Instituto Politécnico de Bragança, Bragança, 2016.

[54] Bezerra MA, Santelli RE, Oliveira EP, Villar LS, Escaleira LA. Response surface methodology (RSM) as a tool for optimization in analytical chemistry. Talanta 2008;76:965–77.

[55] Wasserstein RL, Lazar NA. The ASA's Statement on p -Values: Context, Process, and Purpose.The American Statician 2016;70:129–33.

[56] Box GEP, Hunter WG, Hunter JS. Statistics for experimenters. 1978.

[57] Oehlert GW. A First Course in Design and Analysis of Experiments. New York: Freeman; 2000.

[58] Zhang H, Yuqi Li B, Zexiang Lu B, Mei Wu B, Shi R, Lihui Chen B, et al. Highly efficient synthesis of biodiesel catalyzed by CF 3 SO 3 H-functionalized ionic liquids: experimental design and study with response surface methodology. Reaction Kinetics Mechanisms and Catalysis 2017;121:579–92.

[59] Colthup NB, Daly LH, Wiberley SE. Introduction to infrared and raman spectroscopy. 3rd ed. San Diego: Academi Press; 1990.

[60] Pavia DL, Lampman GM, Kriz GS. Introduction to Spectroscopy. 2nd Editio. Orlando: Saunders College Publishing; 1979.

[61] Pretsch E, Clerc T, Seibl J, Simon W. Spectral data for structure determination of organic compounds. Berlin: Springer-Verlag; 1989.

APPENDIX A – Conferences

Figure A.1 – Encontro Galego-Portugués de Química, Ferrol, nov. 2017.

Ionic Liquid Catalyzed Reaction for Biodiesel Production

Fernanda F. Roman[1,*], Ana Queiroz[1], António E. Ribeiro[1], Eduardo S. Chaves[2], Paulo Brito[1]

[1] Polytechnic Institute of Bragança, Department of Chemical and Biological Technology, School of Technology and Management, Bragança, Portugal

[2] Federal University of Technology - Paraná, Department of Chemical Engineering, Ponta Grossa, Brasil

*fontanarfr@gmail.com

Biodiesel is a promising energy source that could replace petro-diesel [1]. The biodiesel production with the currently employed catalysts presents drawbacks, linked to cost, environmental issues, reaction time, among others [2,3]. Many researches have been shifted towards finding catalysts that are environmentally benign, allow good conversions, permit the use of low cost feedstock and lead to high quality biodiesel. Ionic Liquids (IL) are a class of catalysts that have been considered for biodiesel production, due to the fact that they may surpass some of the downsides of classical catalysts [3]. Thus, the goal of this study is to optimize the conversion of the esterification reaction of oleic acid with methanol, by estimating the optimum conditions, using the IL *1-methylimidazolium hydrogen sulfate* as catalyst, and applying a Response Surface Methodology (RSM).

The experiments were delineated using the Box-Behnken Design (BBD) [4], with 4 factors in 3 levels, which are displayed in Table 1, leading to 27 experiments. IL, oleic acid and methanol were charged to the reactor and reaction was performed with reflux, under the determined conditions. After the reaction, the mixture was kept under refrigeration until the phases were able to be separated. The oleic acid conversion was estimated by comparing the initial acidity of the oleic acid sample and the final acidity of the biodiesel phase, according to a procedure adapted from EN 14104.

The p-value obtained for the regression is smaller than 0.05 and the lack of fit is estimated as 0.265, both acquired through the Analysis of Variance (ANOVA). The regression fit was determined as R^2=0.986, placing the model as reasonable and statistically reliable. The quadratic model that best fits the experimental results is as follows:

$$Y = 38.77 + 3.36A - 0.11B + 7.07C + 3.76D - 1.43A^2 - 0.044B^2 - 5.05C^2 - 3.37D^2 - 0.39AB + 1.13AC + 0.13AD + 1.29BC + 0.04BD + 1.70CD \quad (1)$$

In general, increasing the value of the factor also increases the response. The order of importance is: C > D > C^2 > A > D^2 > C*D > A^2 > B*C > A*C. The reaction temperature (B) did not greatly influence the response, being statistically irrelevant to this investigation. Fig. 1 displays the influence of the molar ratio and catalyst dosage over the response. The greater value for conversion is obtained when both parameters are set to +1. Similar analysis can be made to all interactions between factors. The best result was obtained when all 4 factors were set to their maximum value, achieving a conversion of 94.8%.

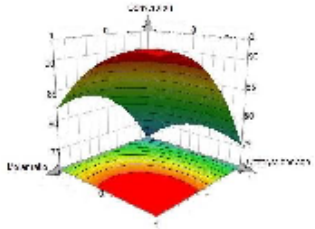

Fig. 1. Influence of molar ratio and catalyst dosage in the conversion.

Table 1. Selected factors and respective values.

Factor	Coded	-1	0	+1
Reaction time (h)	A	4	6	8
Reaction temperature (°C)	B	80	95	110
Molar ratio(MeOH/OA)*	C	5:1	10:1	15:1
Catalyst dosage (%wt)	D	5	10	15

*OA – oleic acid; MeOH– methanol

References

[1] A. Atabani, A. Silitonga, I. Braduddin *et al*, Renewable and Sustainable Energy Reviews, 16 (2012) 2070.
[2] Z. Ishak, N. Sairi, Y. Alias, A. Taieb, Y. Rozita, Catalysis Review, 59 (2017) 44.
[3] L. Andreani, J.D. Rocha, Brazilian Journal of Chemical Engineering, 29 (2012) 1.
[4] G. Box, D. Behnken, Technometrics, 2 (1960) 455.

XXIII ENCONTRO

GALEGO PORTUGUÉS DE QUÍMICA

Centro de Innovaciones y Servicios. C.I.S.
15 al 17 de noviembre de 2017
Ferrol - España

Dña. Fernanda Fontana Román ha participado en el ***XXIII Encontro Galego-Portugués de Química,*** celebrado en el Centro de Innovaciones y Servicios C.I.S. de Ferrol (España), del 15 al 17 de noviembre de 2017. Presentando la comunicación en formato ORAL

"Ionic Liquid Catalyzed Reaction for Biodiesel Production"

Para que conste y a los efectos oportunos, se expide el presente documento.

En Vigo, a 15 de Noviembre de 2017

Comisión Organizadora.

Colegio Oficial de Químicos de Galicia

SOCIEDADE PORTUGUESA DE QUÍMICA

ASOCIACIÓN DE QUÍMICOS DE GALICIA

Figure A.2 – Encontro de Jovens Investigadores, Bragança, nov. 2017.

Produção de biodiesel através de catálise ácida aplicando líquidos iónicos

Fernanda F. Roman [1]; Ana M. Queiróz[2]; António E. Ribeiro[3]; Eduardo Chaves[4], Paulo Brito[5]

[1] fontanarfr@gmail.com, Instituto Politécnico de Bragança, ESTIG, Bragança, Portugal
[2] amqueiroz@ipb.pt, Instituto Politécnico de Bragança, ESTIG, Bragança, Portugal
[3] aribeiro@ipb.pt, Instituto Politécnico de Bragança, Laboratory of Separation and Reaction Engineering (LSRE), Portugal
[4] eschaves@utfpr.edu.br, Universidade Tecnológica Federal do Paraná, Ponta Grossa, Brasil
[5] paulo@ipb.pt, Instituto Politécnico de Bragança, ESTIG, Bragança, Portugal

Resumo

O biodiesel é uma fonte energética promissora, que pode substituir completamente o diesel proveniente do petróleo. O atual método de produção do biodiesel apresenta inconvenientes, relacionados com custo de produção, problemas ambientais, tempo de produção e processos de separação e purificação. A maior parte das pesquisas tem procurado catalisadores que permitam superar os problemas associados aos processos tradicionais. Os líquidos iónicos (ILs) são uma classe de catalisadores que têm sido considerados para a produção de biodiesel. Assim, o objetivo deste trabalho foi estudar a reação de produção de biodiesel aplicando o líquido iónico *1-metilimidazólio hidrogenossulfato* como catalisador. A primeira etapa da investigação foi o estudo da reação de esterificação entre o ácido oleico e o metanol, otimizando os principais parâmetros da reação (tempo, temperatura, razão molar metanol/ácido oleico e a quantidade de catalisador) através de uma Metodologia de Superfície de Resposta (RSM) conhecida por Box-Behnken Design (BBD). Esta metodologia permite variar os fatores em três níveis (-1, 0 e +1), de forma a ajustar os dados obtidos experimentalmente a uma curva que os represente, permitindo a determinação do valor ótimo para os fatores em estudo. O valor máximo para a conversão de ácido oleico (94,8%) foi obtido quando todos os fatores estavam no seu nível máximo (temperatura 110 °C, tempo de reação 8 h, razão molar metanol/ácido oleico 15:1 e uma quantidade de catalisador 15%, em relação à massa de ácido oleico). A próxima etapa será a aplicação deste mesmo catalisador à reação de transesterificação de um óleo usado com metanol.

Palavras-Chave: biodiesel; líquidos iónicos; esterificação; transesterificação.

V encontro de jovens investigadores

29 de novembro de 2017

Certificado de comunicação

Certifica-se que no **V Encontro de Jovens Investigadores**, que decorreu em Bragança, Portugal, no dia 29 de novembro de 2017, foi apresentada por **Fernanda Fontana Roman** a comunicação oral **Biodiesel production through acidic catalysis by applying ionic liquids**, tendo como autores:
F. Roman, A.M. Queiróz, A. Ribeiro, E. Chaves, P. Brito

Bragança, 29 de novembro de 2017

A Comissão de Organização,

João Sobrinho Teixeira
Presidente do Instituto Politécnico de Bragança

ipb INSTITUTO POLITÉCNICO DE BRAGANÇA

Figure A.3 – Encontro Nacional de Cromatografia, Bragança, dec. 2017.

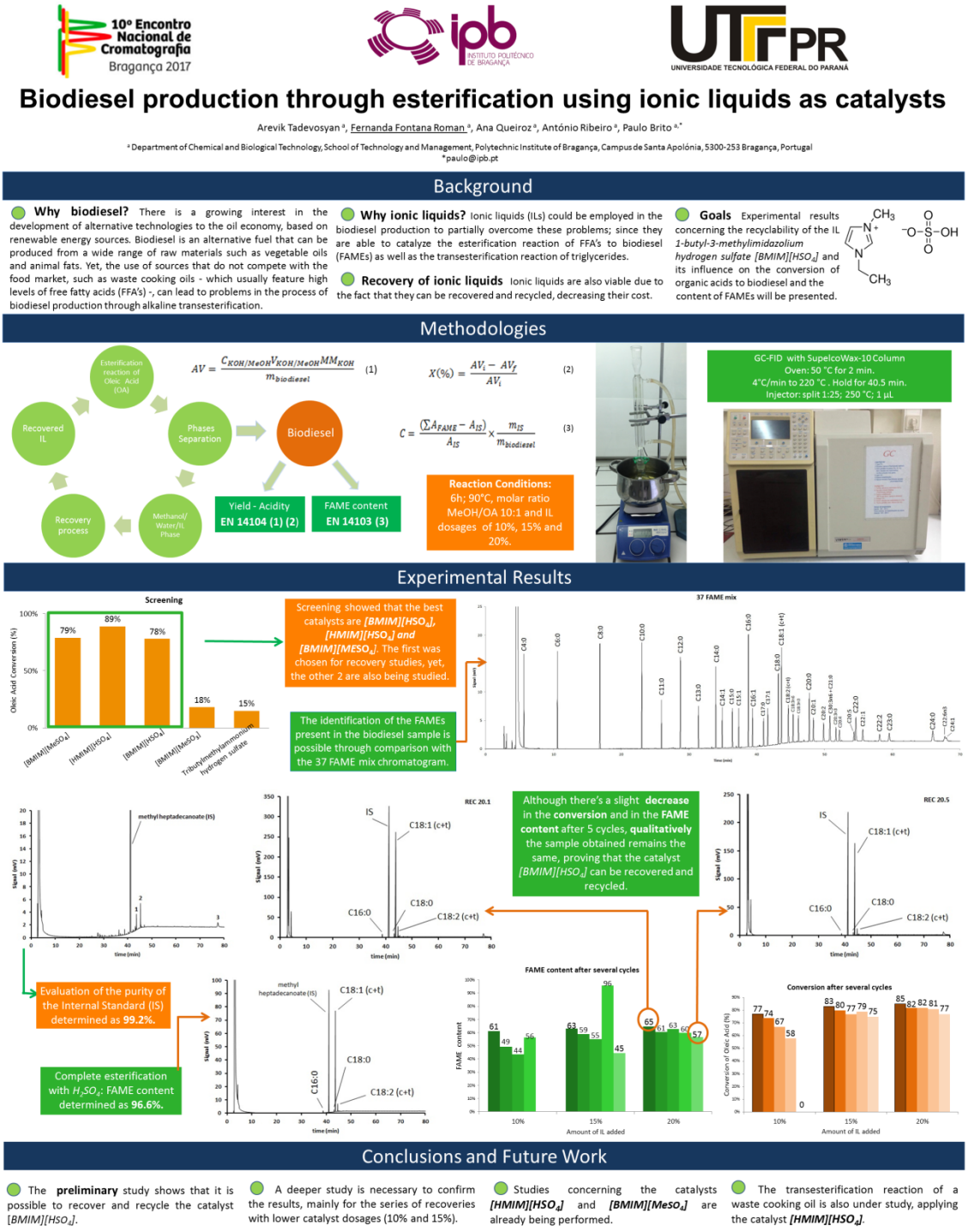

10º Encontro Nacional de Cromatografia
Bragança 2017

CERTIFICADO

Certifica-se que o(a) Senhor(a) **Fernanda Fontana Roman (Fernanda Fontana Roman)**

apresentou o(a) Comunicação em Painel com título

Biodiesel production through esterification using ionic liquids as catalysts

no(a) 10º Encontro Nacional de Cromatografia - 10ENC em Bragança, Portugal, de 04/12/2017 a 06/12/2017

Pel´A Comissão Organizadora

Bragança, Portugal,
06 de Dezembro de 2017

Isabel C.F.R. Ferreira

APPENDIX B - Design matrix with experimental conditions applied.

Table B.1 – Design matrix and experimental conditions applied.

Run	Coded Factors				Factors				Real Conditions				
	A	B	C	D	A - Time (h)	B - Temp (C)	C - Molar ratio MeOH/AO	D - Cat dosage (%wt)	IL mass (g)	OA mass (g)	MeOH (mL)	T (°C)	t (h)
1	-1	1	0	0	4	110	10	10	0.5705	5.7076	8.1	110	4
2	-1	0	0	-1	4	95	10	5	0.2869	5.6557	8.2	95	4
3	0	0	0	0	6	95	10	10	0.5669	5.6728	8.2	95	6
4	-1	0	-1	0	4	95	5	10	0.5648	5.6557	4.1	95	4
5	0	-1	1	0	6	80	15	10	0.5632	5.6306	12.2	80	6
6	0	1	0	1	6	110	10	15	0.8435	5.6582	8.1	110	6
7	0	1	1	0	6	110	15	10	0.5645	5.6807	12.2	110	6
8	0	1	0	-1	6	110	10	5	0.2816	5.7664	8.1	110	6
9	0	-1	-1	0	6	80	5	10	0.5664	5.7209	4.1	80	6
10	1	1	0	0	8	110	10	10	0.5628	5.6364	8.1	110	8
11	1	0	-1	0	8	95	5	10	0.5615	5.6243	4.1	95	8
12	-1	0	1	0	4	95	15	10	0.5614	5.6133	12.2	95	4
13	0	-1	0	-1	6	80	10	5	0.2814	5.6627	8	80	6
14	0	0	1	1	6	95	15	15	0.8474	5.6612	12.2	95	6
15	0	0	1	-1	6	95	15	5	0.2834	5.6746	12.2	95	6
16	1	0	0	-1	8	95	10	5	0.2821	5.6551	8.1	95	8
17	1	-1	0	0	8	80	10	10	0.5663	5.6673	8.1	80	8
18	0	1	-1	0	6	110	5	10	0.5608	5.6096	4.1	110	6
19	0	0	0	0	6	95	10	10	0.5645	5.6548	8.1	95	6
20	-1	-1	0	0	4	80	10	10	0.5615	5.6583	8.1	80	4
21	0	0	0	0	6	95	10	10	0.5624	5.6308	8.2	95	6
22	-1	0	0	1	4	95	10	15	0.8444	5.6547	8.1	95	4
23	1	0	0	1	8	95	10	15	0.8464	5.664	8.2	95	8
24	1	0	1	0	8	95	15	10	0.5692	5.7295	12.3	95	8
25	0	-1	0	1	6	80	10	15	0.8503	5.6638	8.1	80	6
26	0	0	-1	1	6	95	5	15	0.8485	5.7147	4.1	95	6
27	0	0	-1	-1	6	95	5	5	0.2859	5.6506	4.1	95	6

APPENDIX C – Measured masses of layers after separation.

Table C.1 – Experimental measured masses of layers.

Run	Coded Factors				Experimental measured masses of layers (g)	
	A	B	C	D	Aqueous Layers (Contains water, unreacted methanol and ionic liquid)	Organic layer (contains biodiesel and unreacted oleic acid)
1	-1	1	0	0	4.9924	6.7392
2	-1	0	0	-1	3.9963	6.1595
3	0	0	0	0	5.3074	6.4161
4	-1	0	-1	0	2.1915	6.6163
5	0	-1	1	0	8.7911	5.9822
6	0	1	0	1	5.1939	6.5246
7	0	1	1	0	7.7233	6.1694
8	0	1	0	-1	3.9062	7.1817
9	0	-1	-1	0	2.0636	6.3933
10	1	1	0	0	5.0249	6.3268
11	1	0	-1	0	1.9470	6.5081
12	-1	0	1	0	8.0747	6.3393
13	0	-1	0	-1	4.4625	6.8144
14	0	0	1	1	8.4882	6.3645
15	0	0	1	-1	10.9731	6.2398
16	1	0	0	-1	4.6049	6.5538
17	1	-1	0	0	5.9733	6.2543
18	0	1	-1	0	0.6385	5.7862
19	0	0	0	0	5.2212	6.4282
20	-1	-1	0	0	5.0238	5.8120
21	0	0	0	0	5.6152	6.3540
22	-1	0	0	1	4.1327	6.6007
23	1	0	0	1	4.3158	6.4060
24	1	0	1	0	9.074	6.1001
25	0	-1	0	1	5.2829	6.5782
26	0	0	-1	1	1.3710	6.3509
27	0	0	-1	-1	2.0597	5.8228

APPENDIX D - Determination of the acid value.

Table D.1 – Titration of biodiesel samples acid value determination.

Run	Biodiesel mass (g)			V_{KOH} (mL)			C_{KOH} (mol/L)	Acid value (mg KOH/ g biodiesel)			
	1	2	3	1	2	3		1	2	3	Average
Oleic Acid	0.4967	0.5040	-	20.70	21.10	-	0.0786	183.24	184.08	-	183.66
1	0.5764	0.6932	-	4.00	4.70	-	0.0786	30.16	29.53	-	29.85
2	0.6826	0.6773	-	6.47	6.51	-	0.0744	39.19	39.75	-	39.47
3	0.6615	0.6728	-	3.39	3.43	-	0.0744	21.02	20.92	-	20.97
4	0.6345	0.6173	-	7.40	7.30	-	0.0744	48.28	48.95	-	48.61
5	0.6727	0.4520	-	3.13	2.12	-	0.0744	19.06	19.04	-	19.05
6	0.6561	0.5771	-	2.80	2.48	-	0.0744	17.44	17.52	-	17.48
7	0.5598	0.6558	0.6548	1.99	2.27	2.32	0.0744	14.41	14.08	14.42	14.30
8	0.5962	0.6654	0.6772	5.50	6.10	6.10	0.0744	38.09	37.89	37.23	37.73
9	0.6610	0.6743	-	6.70	6.80	-	0.0744	41.93	41.72	-	41.82
10	0.5694	0.6105	0.6503	2.45	2.64	2.86	0.0744	17.53	17.65	17.98	17.72
11	0.6880	0.6151	0.6864	7.00	6.20	6.90	0.0744	42.10	41.66	41.59	41.78
12	0.5804	0.6934	0.6857	4.00	4.80	4.70	0.0744	28.34	28.54	28.25	28.38
13	0.5906	0.6986	0.7175	4.60	5.30	5.50	0.0744	32.08	31.31	31.65	31.68
14	0.6837	0.6863	-	2.32	2.33	-	0.0744	13.81	13.82	-	13.81
15	0.5388	0.6158	0.6261	4.30	4.80	4.90	0.0744	32.85	32.13	32.27	32.42
16	0.5700	0.6760	0.6488	4.00	4.70	4.60	0.0744	28.86	28.65	29.21	28.91
17	0.5349	0.6218	0.5604	2.20	2.60	2.30	0.0744	16.72	17.06	16.70	16.83
18	0.6785	0.6753	-	7.70	7.60	-	0.0744	46.99	46.60	-	46.80
19	0.6552	0.5560	0.5729	3.22	2.70	2.80	0.0744	20.14	19.83	19.98	19.98
20	0.6771	0.6703	-	5.00	4.90	-	0.0744	30.46	30.14	-	30.30
21	0.5882	0.6758	0.6527	3.10	3.56	3.39	0.0744	21.58	21.63	21.30	21.50
22	0.5918	0.6862	0.6650	4.70	5.10	4.90	0.0744	30.66	30.38	-	30.52
23	0.6194	0.6801	0.6908	2.62	2.85	3.00	0.0744	17.26	17.13	17.77	17.39
24	0.6024	0.6564	0.6659	1.90	2.11	2.18	0.0744	12.77	13.05	13.30	13.04
25	0.5392	0.6198	-	2.60	3.00	-	0.0744	19.68	19.81	-	19.74
26	0.6082	0.6649	-	6.80	7.60	-	0.0744	46.24	47.33	-	46.78
27	0.6149	0.6968	0.6858	7.70	8.70	8.50	0.0744	51.84	51.74	51.36	51.65

APPENDIX E - Initial and final acid value of esterification samples.

Table E.1 – Initial and final acid value to conversion determination.

Run	Coded Factors				Acid value		Conversion (%)
	A	B	C	D	Initial Acid value (mg KOH/g oleic acid)	Final Acid value (mg KOH/ g biodiesel)	
1	-1	1	0	0	183.661	29.85	83.75
2	-1	0	0	-1	183.661	39.47	78.51
3	0	0	0	0	183.661	20.97	88.58
4	-1	0	-1	0	183.661	48.61	73.53
5	0	-1	1	0	183.661	19.05	89.63
6	0	1	0	1	183.661	17.48	90.48
7	0	1	1	0	183.661	14.30	92.21
8	0	1	0	-1	183.661	37.73	79.45
9	0	-1	-1	0	183.661	41.82	77.23
10	1	1	0	0	183.661	17.72	90.35
11	1	0	-1	0	183.661	41.78	77.25
12	-1	0	1	0	183.661	28.38	84.55
13	0	-1	0	-1	183.661	31.68	82.74
14	0	0	1	1	183.661	13.81	92.48
15	0	0	1	-1	183.661	32.42	82.35
16	1	0	0	-1	183.661	28.91	84.26
17	1	-1	0	0	183.661	16.83	90.90
18	0	1	-1	0	183.661	46.80	74.52
19	0	0	0	0	183.661	19.98	89.16
20	-1	-1	0	0	183.661	30.30	83.50
21	0	0	0	0	183.661	21.50	88.29
22	-1	0	0	1	183.661	30.52	83.38
23	1	0	0	1	183.661	17.39	90.53
24	1	0	1	0	183.661	13.04	92.83
25	0	-1	0	1	183.661	19.74	89.25
26	0	0	-1	1	183.661	46.78	74.60
27	0	0	-1	-1	183.661	51.65	71.87

APPENDIX F - Biodiesel mass, concentration of internal standard and FAME content obtained for each injection.

Table F.1 – Conditions used in the determination of the FAME content

Run	Biodiesel mass (mg)	C_{IS} (mg/mL)	FAME content (%)		Average (%)
			1	2	
1	254.3	9.916	82.54	83.10	82.8
2	269.4	9.916	73.94	74.37	74.2
3	261.5	9.916	84.58	85.44	85.0
4	256.4	10.003	65.55	66.25	65.9
5	300.3	9.916	85.65	85.26	85.5
6	253.7	9.916	87.05	86.54	86.8
7	254.8	10.001	87.07	87.96	87.5
8	259.5	10.001	77.87	78.03	78.0
9	250.5	10.001	72.42	72.73	72.6
10	252.4	9.916	87.94	88.02	88.0
11	258.6	10.001	73.68	75.02	74.4
12	252.5	10.001	84.50	84.70	84.6
13	289.6	10.003	76.94	78.53	77.7
14	255.9	10.001	87.99	86.89	87.4
15	255.1	10.001	78.54	78.79	78.7
16	251.9	10.001	80.70	80.09	80.4
17	249.2	10.001	86.58	85.31	85.9
18	251	10.001	68.53	68.35	68.4
19	252.1	10.001	84.72	84.40	84.6
20	254.8	10.001	81.25	81.49	81.4
21	267.4	10.001	85.87	85.03	85.5
22	258.5	10.001	81.76	81.71	81.7
23	288.2	10.001	86.87	87.03	87.0
24	260.9	10.001	90.29	90.05	90.2
25	292.2	10.001	84.68	84.37	84.5
26	266.1	10.003	73.82	72.70	73.3
27	250.7	9.916	64.77	64.10	64.4

APPENDIX G - Confirmation runs for conversion and FAME content.

Table G.1 - Real conditions applied

Sample	Time (h)	Temperature (°C)	MeOH/OA Ratio	Cat dosage (wt%)	IL mass (g)	OA mass (g)	V MeOH (mL)
CO1	8	110	15	15	0.8445	5.6553	12.5
CO2	8	110	15	15	0.8415	5.6657	12.5
CO3	8	110	15	15	0.8479	5.612	12.5
CO1_FAME	8	110	14	13.5	0.5716	4.2461	8.5
CO2_FAME	8	110	14	13.5	0.5714	4.237	8.5
CO3_FAME	8	110	14	13.5	0.5742	4.2426	8.5

Table G.2 - Titration of samples for determination of acid value and conversion

Sample	Biodiesel mass (g)			Volume KOH (mL)			C KOH (mol/L)	Acid value (mg KOH/g biodiesel)		
	1	2	3	1	2	3		1	2	3
CO1	0.6135	0.6512	0.4980	1.19	1.23	0.96	0.0744	7.71	7.52	7.57
CO2	0.5497	0.6125	0.5724	1.24	1.44	1.32	0.0679	8.20	8.61	8.41
CO3	0.5414	0.5738	0.6056	1.15	1.20	1.25	0.0679	7.69	7.59	7.51
CO1_FAME	0.2917	0.3643		0.86	1.10		0.0746	11.53	11.99	
CO2_FAME	0.2820	0.3604		0.86	1.07		0.0746	11.93	11.77	
CO3_FAME	0.1962	0.1850		0.64	0.63		0.0746	12.44	12.98	

Table G.3 - Biodiesel mass, internal standard concentration and FAME content obtained.

Sample	Biodiesel mass (mg)	C_{IS} (mg/mL)	FAME content (%)		
			1	2	Average
CO1	289.0	10.003	91.74	91.43	91.6
CO2	248.6	10.003	88.83	88.08	88.5
CO3	259.0	10.003	90.68	90.48	90.6
CO1_FAME	252.2	10.018	90.71	89.86	90.3
CO2_FAME	252.5	10.018	90.08	90.25	90.2
CO3_FAME	258.0	10.018	90.89	91.51	91.2

APPENDIX H - Real conditions applied for the transesterification reactions and fame content obtained.

Table H.1 – Experimental conditions applied for the transesterification reaction.

Run	IL mass (g)	Oil mass (g)	Oleic acid mass (g)	OA (%)	Total mass (g)	MeOH V (mL)
T1	3.0050	4.0229	16.0911	80.00	20.1140	18.5
T2	3.0929	8.0110	12.0716	60.11	20.0826	18.5
T3.1	3.0014	10.0048	10.0084	50.01	20.0132	18.5
T3.2	3.0103	10.0084	10.2600	50.62	20.2684	18.5
T4	3.0557	12.0164	8.0026	39.98	20.0190	18.5
T5	3.0138	15.9998	4.0199	20.08	20.0197	18.5

Table H.2 – Conditions used for determination of FAME content.

Run	Biodiesel mass (mg)	Concentration Internal standard (mg/mL)	FAME Content (%)		
			1	2	Average
T1	256.9	10.003	71.84	70.87	71.14
T2	260.4	10.003	53.20	53.31	53.25
T3.1	250.9	10.003	45.38	45.99	45.68
T3.2	266.2	10.003	44.88	44.54	44.71
T4	281.6	10.003	37.82	38.03	37.92
T5	270.2	10.003	19.88	19.90	19.89

APPENDIX I - Kinetic study at 110°C

Table I.1 - Conditions applied in the esterification reaction.

Conditions				
IL mass (g)	OA mass (g)	MeOH V (mL)	Temperature (°C)	Ca0 (mol/L)
3.3286	22.1746	50	110	1.0193

Table I.2 - Acid value for each sample removed from the vessel

	Time (min)	Biodiesel mass (g)			KOH/MeOH V (mL)			Acid value (mg KOH/mg sample)			
		1	2	3	1	2	3	1	2	3	Average
t0	0	0.1738	0.1892		4.19	4.52		100.96	100.05		100.51
t1	15	0.1772	0.1873		3.79	3.93		89.57	87.87		88.72
t2	30	0.1764	0.1892		3.40	3.61		80.72	79.91		80.31
t3	50	0.1717	0.1886		3.01	3.27		73.42	72.61		73.01
t4	90	0.1763	0.1921		2.43	2.6		57.72	56.68		57.20
t5	120	0.1775	0.1870		2.23	2.37		52.61	53.08		52.84
t6	180	0.1676	0.1238	0.1898	1.85	1.41	2.09	46.23	47.70	46.12	46.68
t7	240	0.1784	0.1881		1.75	1.88		41.08	41.86		41.47
t8	300	0.1714	0.1530		1.64	1.42		40.07	38.87		39.47
t9	360	0.1803	0.1862		1.5	1.62		34.84	36.44		35.64
t10	420	0.1875	0.1855		1.51	1.47		33.73	33.19		33.46
t11	480	0.1751	0.1882		1.32	1.55		31.57	34.49		33.03

Table I.3 – Experimental and calculated data used for the reaction order determination

Time	Acidity	Conversion	0^{th} order	1^{st} Order	2^{nd} Order	3^{rd} Order
			Ca	Ln Ca	1/Ca	$1/Ca^2$
0	100.50506	0	1.01926	0.01908	0.9811	0.96256
15	88.72127	0.11725	0.89976	-0.10563	1.11141	1.23524
30	80.31218	0.20091	0.81448	-0.20521	1.22778	1.50745
50	73.01304	0.27354	0.74045	-0.30049	1.35052	1.82392
90	57.20193	0.43086	0.58011	-0.54454	1.72382	2.97156
120	52.84495	0.47421	0.53592	-0.62377	1.86595	3.48176
180	46.6795	0.53555	0.47339	-0.74783	2.1124	4.46224
240	41.46845	0.5874	0.42055	-0.8662	2.37785	5.65418
300	39.46918	0.60729	0.40027	-0.91561	2.4983	6.24151
360	35.63829	0.64541	0.36142	-1.01771	2.76685	7.65547
420	33.45656	0.66712	0.3393	-1.08088	2.94728	8.68646
480	33.03067	0.67135	0.33498	-1.09369	2.98528	8.91191

Table I.4 - Statistics to the linear fitting for each order

	0^{th} order	1^{st} order	2^{nd} order	3^{rd} order
Number of points	11	11	11	11
Degrees of freedom	9	9	9	9
Residual sum of squares	0.10322	0.14137	0.15109	0.3246
Pearson's r	-0.90107	-0.95073	0.9839	0.99776
Adj.R square	0.79104	0.89321	0.96452	0.99502

Table I.5 - Linear equations adjusted to the experimental data

	Intercept (b)	Slope (a)	Adj.R square
0^{th} order	0.83435	-0.00144	0.79104
1^{st} order	-0.17364	-0.00248	0.89321
2^{nd} order	1.15002	0.00461	0.96452
3^{rd} order	1.06414	0.01827	0.99502

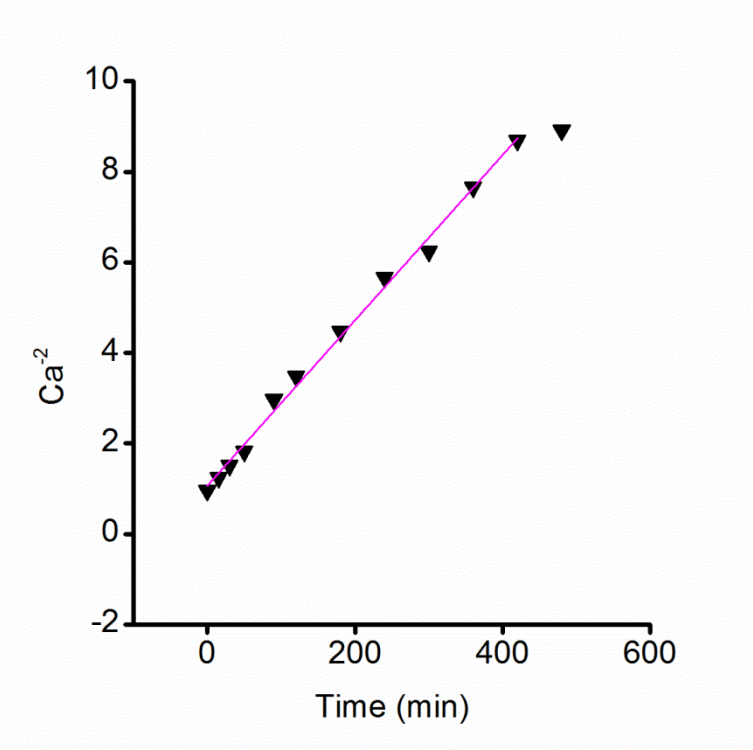

Figure 40 – 3^{rd} order equation adjusted to experimental data at 110 °C.

APPENDIX J - Kinetic study at 100°C

Table J.1 - Conditions applied in the esterification reaction.

Conditions				
IL mass (g)	OA mass (g)	MeOH V (mL)	Temperature (°C)	Ca0 (mol/L)
3.3502	22.5111	50	100	1.0294

Table J.2 - Acid value for each sample removed from the vessel

	Time (min)	Biodiesel mass (g)		KOH/MeOH V (mL)		Acid value (mg KOH/mg sample)		
		1	2	1	2	1	2	Average
t0	0	0.1790	0.1890	4.23	4.40	98.96	97.50	98.23
t1	15	0.1681	0.1881	3.52	3.84	87.69	85.49	86.59
t2	30	0.1811	0.1837	3.31	3.47	76.54	79.11	77.82
t3	50	0.1725	0.1893	2.70	2.93	65.55	64.82	65.18
t4	90	0.1699	0.1865	2.34	2.51	57.68	56.36	57.02
t5	120	0.1862	0.1893	2.23	2.34	50.16	51.77	50.96
t6	180	0.1789	0.1875	1.96	2.09	45.88	46.68	46.28
t7	240	0.1804	0.1844	1.75	1.84	40.63	41.79	41.21
t10	420	0.1924	0.1864	1.55	1.54	33.74	34.60	34.17
t11	480	0.1783	0.1847	1.41	1.51	33.12	34.24	33.68

Table J.3 - Experimental and calculated data used for the reaction order determination

Time	Acidity (mg KOH/g sample)	Conversion (%)	0^{th} order	1^{st} order	2^{nd} order	3^{rd} order
			Ca (mol/L)	Ln Ca	1/Ca	$1/Ca^2$
0	98.22995	0	1.02951	0.02908	0.97134	0.9435
15	86.59372	0.11846	0.90755	-0.097	1.10186	1.2141
30	77.82454	0.20773	0.81565	-0.20377	1.22602	1.50313
60	65.18464	0.33641	0.68317	-0.38101	1.46376	2.14259
90	57.0204	0.41952	0.59761	-0.51482	1.67334	2.80007
120	50.9615	0.4812	0.53411	-0.62716	1.87229	3.50546
180	46.28116	0.52885	0.48505	-0.7235	2.06163	4.25031
240	41.20644	0.58051	0.43187	-0.83964	2.31552	5.36165
420	34.17282	0.6522	0.35811	-1.02692	2.79246	7.79782
480	33.7	0.6572	0.35296	-1.0414	2.83317	8.02686

Table J.4 - Statistics to the linear fitting for each order

	0^{th} order	1^{st} order	2^{nd} order	3^{rd} order
Number of points	9	9	9	9
Degrees of freedom	7	7	7	7
Residual sum of squares	0.10744	0.14819	0.17214	0.42307
Pearson's r	-0.8609	-0.92311	0.96986	0.99472
Adj.R square	0.70417	0.831	0.93214	0.98796

Table J.5 - Linear equations adjusted to the experimental data

	Intercept	Slope	Adj.R square
0^{th} order	0.83585	-0.00145	0.70417
1^{st} order	-0.17619	-0.00242	0.831
2^{nd} order	1.16402	0.00433	0.93214
3^{rd} order	1.1587	0.01653	0.98796

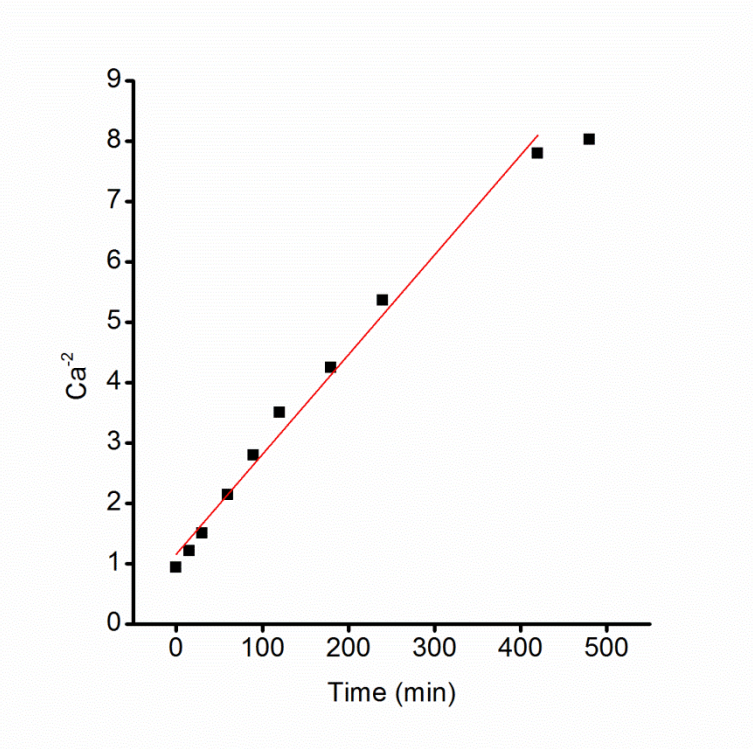

Figure 41 – 3^{rd} order equation adjusted to experimental data at 100 °C.

APPENDIX K - Kinetic study at 90°C

Table K.1 - Conditions applied in the esterification reaction.

Conditions				
IL mass (g)	OA mass (g)	MeOH V (mL)	Temperature (°C)	Ca0 (mol/L)
3.3891	22.3762	50	90	1.0250

Table K.2 - Acid value for each sample removed from the vessel

	Time (min)	Biodiesel mass (g)		KOH/MeOH V (mL)		Acid value (mg KOH/mg sample)		
		1	2	1	2	1	2	Average
t0	0	0.1827	0.1807	4.33	4.30	99.25	99.66	99.45
t1	15	0.1836	0.1851	3.77	3.93	85.99	88.92	87.45
t2	30	0.1719	0.1784	3.30	3.34	80.40	78.41	79.40
t3	50	0.1800	0.1897	2.85	2.97	66.31	65.57	65.94
t4	90	0.1773	0.1869	2.49	2.63	58.81	58.93	58.87
t5	120	0.1818	0.1879	2.35	2.39	54.13	53.27	53.70
t6	180	0.1804	0.1880	2.05	2.1	47.59	46.78	47.18
t7	240	0.1763	0.1827	1.76	1.87	41.81	42.86	42.34
t8	300	0.1811	0.1799	1.74	1.71	40.24	39.81	40.02
t9	360	0.1805	0.183	1.59	1.64	36.89	37.53	37.21
t10	420	0.1825	0.1871	1.51	1.56	34.65	34.92	34.78
t11	480	0.1798	0.1848	1.42	1.49	33.07	33.77	33.42

Table K.3 - Experimental and calculated data used for the reaction order determination

Time	Acidity (mg KOH/g sample)	Conversion (%)	0^{th} order	1^{st} order	2^{nd} order	3^{rd} order
			Ca (mol/L)	Ln Ca	1/Ca	$1/Ca^2$
0	99.45426	0	1.02499	0.02468	0.97562	0.95184
15	87.45421	0.12066	0.90131	-0.1039	1.10949	1.23097
30	79.4002	0.20164	0.81831	-0.20052	1.22203	1.49337
60	65.93717	0.33701	0.67956	-0.38632	1.47155	2.16546
90	58.87236	0.40805	0.60675	-0.49965	1.64814	2.71636
120	53.70062	0.46005	0.55344	-0.59159	1.80687	3.26476
180	47.18436	0.52557	0.48629	-0.72096	2.0564	4.22877
240	42.33584	0.57432	0.43632	-0.82938	2.29191	5.25284
300	40.02182	0.59759	0.41247	-0.88559	2.42442	5.87783
360	37.21046	0.62585	0.3835	-0.95843	2.60759	6.79955
420	34.7839	0.65025	0.35849	-1.02586	2.7895	7.78133
480	33.42007	0.66397	0.34443	-1.06586	2.90334	8.42938

Table K.4 - Statistics to the linear fitting for each order

	0th order	1st order	2nd order	3rd order
Number of points	11	11	11	11
Degrees of freedom	9	9	9	9
Residual sum of squares	0.10116	0.13472	0.14434	0.27176
Pearson's r	-0.89477	-0.94652	0.9814	0.99755
Adj.R square	0.77845	0.88433	0.95906	0.99457

Table K.5 - Linear equations adjusted to the experimental data

	Intercept	Slope	Adj.R square
0th order	0.83304	-0.00138	0.77845
1st order	-0.17731	-0.00233	0.88433
2nd order	1.16165	0.0042	0.95906
3rd order	1.14141	0.01609	0.99457

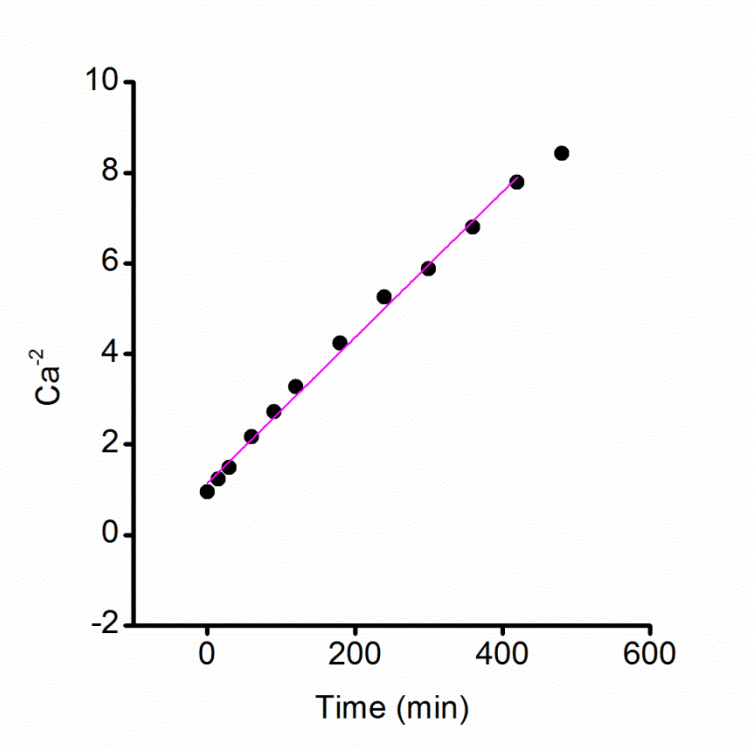

Figure 42 – 3rd order equation adjusted to experimental data at 90 °C.

APPENDIX L - Kinetic study at 80°C

Table L.1 - Conditions applied in the esterification reaction.

Conditions				
IL mass (g)	OA mass (g)	MeOH V (mL)	Temperature (°C)	Ca0 (mol/L)
3.3354	22.2654	50	80	1.0221

Table L.2 - Acid value for each sample removed from the vessel

	Time (min)	Biodiesel mass (g)		KOH/MeOH V (mL)		Acid value (mg KOH/mg sample)		
		1	2	1	2	1	2	Average
t0	0	0.1813	0.1855	4.26	4.37	98.40	98.66	98.53
t1	15	0.1818	0.1875	3.77	3.85	86.84	85.99	86.42
t2	30	0.1807	0.1872	3.36	3.51	77.87	78.52	78.20
t3	50	0.1492	0.1867	2.37	2.95	66.52	66.17	66.35
t4	90	0.1822	0.1907	2.48	2.64	57.00	57.98	57.49
t5	120	0.1851	0.1958	2.21	2.38	50.00	50.90	50.45
t6	180	0.1763	0.1888	1.89	1.98	44.90	43.92	44.41
t7	240	0.1818	0.1272	1.79	1.24	41.23	40.83	41.03
t8	300	0.1803	0.1907	1.64	1.8	38.09	39.53	38.81
t9	360	0.1775	0.1899	1.53	1.62	36.10	35.73	35.91
t10	420	0.1798	0.1874	1.51	1.58	35.17	35.31	35.24
t11	480	0.1891	0.1848	1.52	1.54	33.66	34.90	34.28

Table L.3 - Experimental and calculated data used for the reaction order determination

Time	Acidity (mg KOH/g sample)	Conversion (%)	0^{th} order	1^{st} order	2^{nd} order	3^{rd} order
			Ca (mol/L)	Ln Ca	1/Ca	$1/Ca^2$
0	98.52982	0	1.02203	0.02179	0.97845	0.95736
15	86.41745	0.12293	0.89639	-0.10938	1.11559	1.24454
30	78.19656	0.20637	0.81111	-0.20935	1.23287	1.51997
60	66.34723	0.32663	0.6882	-0.37367	1.45306	2.11137
90	57.48923	0.41653	0.59632	-0.51697	1.67695	2.81215
120	50.45279	0.48794	0.52334	-0.64753	1.91082	3.65124
180	44.40739	0.5493	0.46063	-0.77517	2.17095	4.71303
240	41.02938	0.58358	0.42559	-0.85428	2.34969	5.52104
300	38.81075	0.6061	0.40257	-0.90987	2.48401	6.17031
360	35.91204	0.63552	0.37251	-0.9875	2.68451	7.2066
420	35.23959	0.64235	0.36553	-1.0064	2.73574	7.48426
480	34.28062	0.65208	0.35558	-1.03399	2.81227	7.90885

Table L.4 - Statistics to the linear fitting for each order

	0^{th} order	1^{st} order	2^{nd} order	3^{rd} order
Number of points	12	12	12	12
Degrees of freedom	10	10	10	10
Residual sum of squares	0.13873	0.22564	0.36089	2.09073
Pearson's r	-0.87055	-0.92342	0.96222	0.98546
Adj.R square	0.73365	0.83798	0.91845	0.96825

Table L.5 - Linear equations adjusted to the experimental data

	Intercept	Slope	Adj.R square
0^{th} order	0.80495	-0.00119	0.73365
1^{st} order	-0.22087	-0.00207	0.83798
2^{nd} order	1.23152	0.00385	0.91845
3^{rd} order	1.36938	0.01519	0.96825

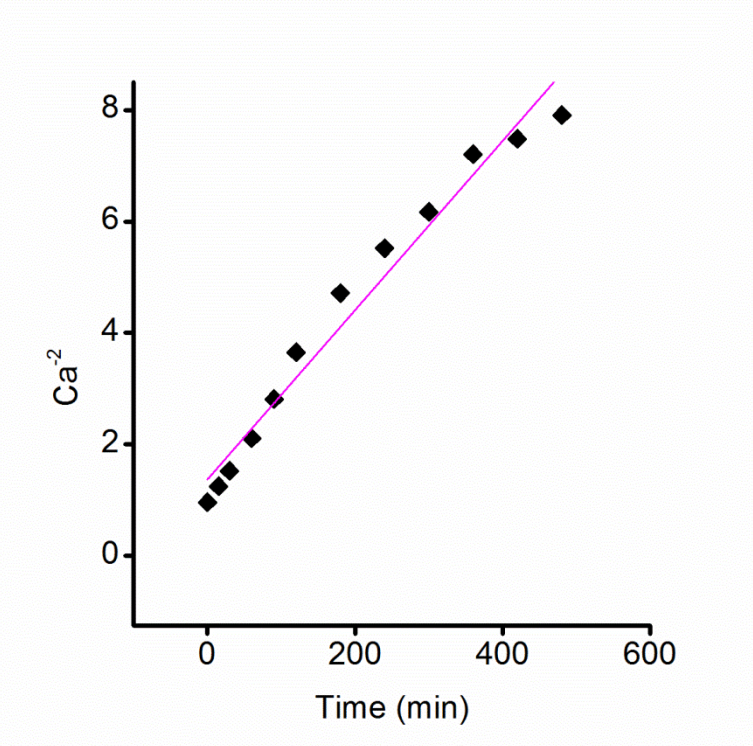

Figure 43 – 3^{rd} order equation adjusted to experimental data at 80 °C.

APPENDIX M - Kinetic study at 70°C

Table M.1 - Conditions applied in the esterification reaction.

Conditions				
IL mass (g)	OA mass (g)	MeOH V (mL)	Temperature (°C)	Ca0 (mol/L)
3.3259	22.1094	50	70	1.0172

Table M.2 - Acid value for each sample removed from the vessel

	Time (min)	Biodiesel mass (g)		KOH/MeOH V (mL)		Acid value (mg KOH/mg sample)		
		1	2	1	2	1	2	Average
t0	0	0.1827	0.1914	4.25	4.41	97.42	96.49	96.96
t1	15	0.1814	0.1867	3.80	3.98	87.73	89.28	88.50
t2	30	0.1536	0.1904	2.91	3.55	79.34	78.08	78.71
t3	50	0.1822	0.1882	2.98	3.11	68.50	69.20	68.85
t4	90	0.1808	0.1893	2.69	2.88	62.31	63.71	63.01
t5	120	0.1849	0.1882	2.47	2.55	55.94	56.74	56.34
t6	180	0.1865	0.1879	2.12	2.17	47.60	48.36	47.98
t7	240	0.1746	0.1930	1.84	2	44.13	43.40	43.77
t8	300	0.1849	0.1924	1.81	1.88	41.00	40.92	40.96
t9	360	0.1899	0.1889	1.78	1.76	39.25	39.02	39.14
t10	420	0.1871	0.1797	1.62	1.59	36.26	37.05	36.66
t11	480	0.1806	0.191	1.54	1.64	35.71	35.96	35.83

Table M.3 - Experimental and calculated data used for the reaction order determination

Time	Acidity (mg KOH/g sample)	Conversion (%)	0^{th} order	1^{st} order	2^{nd} order	3^{rd} order
			Ca (mol/L)	Ln Ca	1/Ca	$1/Ca^2$
0	96.95521	0	1.01725	0.0171	0.98304	0.96637
15	88.50174	0.08719	0.92856	-0.07412	1.07694	1.1598
30	78.71149	0.18817	0.82584	-0.19136	1.21089	1.46626
60	68.84981	0.28988	0.72237	-0.32522	1.38433	1.91638
90	63.01117	0.3501	0.66111	-0.41383	1.51261	2.28798
120	56.34351	0.41887	0.59115	-0.52568	1.69161	2.86154
180	47.98453	0.50509	0.50345	-0.68627	1.98629	3.94534
240	43.76542	0.5486	0.45918	-0.7783	2.17777	4.74269
300	40.95813	0.57756	0.42973	-0.8446	2.32704	5.41511
360	39.13655	0.59634	0.41062	-0.89009	2.43535	5.93092
420	36.65754	0.62191	0.38461	-0.95553	2.60004	6.76022
480	35.83455	0.6304	0.37597	-0.97823	2.65975	7.0743

Table M.4 - Statistics to the linear fitting for each order

	0th order	1st order	2nd order	3rd order
Number of points	11	11	11	11
Degrees of freedom	9	9	9	9
Residual sum of squares	0.08184	0.10646	0.1186	0.34642
Pearson's r	-0.91118	-0.95345	0.9818	0.99589
Adj.R square	0.81139	0.89896	0.95992	0.99089

Table M.5 - Linear equations adjusted to the experimental data

	Intercept	Slope	Adj.R square
0th order	0.85614	-0.00137	0.81139
1st order	-0.1471	-0.00223	0.89896
2nd order	1.12702	0.00385	0.95992
3rd order	1.09413	0.014	0.99089

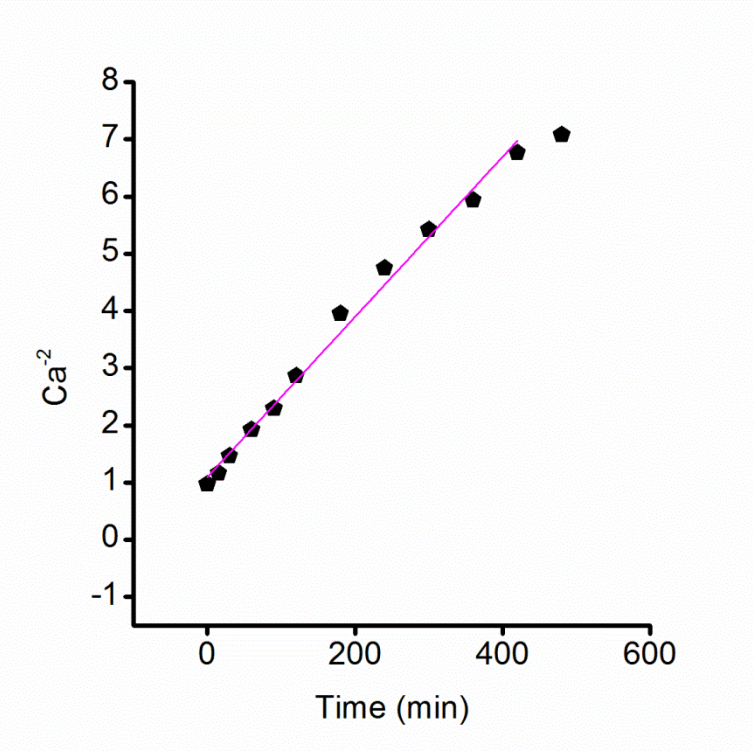

Figure 44 – 3rd order equation adjusted to experimental data at 70 °C.